

**Fundamental Study on Transient Bubble (Slug)
Behavior by Characterizing Transient Forces
of Solid Particles in Fluidized Beds**

1990 Annual Report

H.O. Kono

January 1991

Work Performed Under Contract No.: DE-FC21-87MC24207

For
U.S. Department of Energy
Office of Fossil Energy
Morgantown Energy Technology Center
Morgantown, West Virginia

By
West Virginia University
Chemical Engineering Department
Morgantown, West Virginia

MASTER

EP

DISTRIBUTION AND USE AGREEMENT

DISCLAIMER

This report was prepared as an account of work sponsored by an agency of the United States Government. Neither the United States Government nor any agency thereof, nor any of their employees makes any warranty, express or implied, or assumes any legal liability or responsibility for the accuracy, completeness or usefulness of any information, apparatus, product, or process disclosed, or represents that its use would not infringe privately owned rights. Reference herein to any specific commercial product, process, or service by trade name, trademark, manufacturer, or otherwise, does not necessarily constitute or imply its endorsement, recommendation, or favoring by the United States Government or any agency thereof. The views and opinions of authors expressed herein do not necessarily state or reflect those of the United States Government or any agency thereof.

This report has been reproduced directly from the best available copy.

Available to DOE and DOE contractors from the Office of Scientific and Technical Information, P.O. Box 62, Oak Ridge, TN 37831; prices available from (615)576-8401, FTS 626-8401.

Available to the public from the National Technical Information Service, U.S. Department of Commerce, 5285 Port Royal Rd., Springfield, VA 22161.

**Fundamental Study on Transient Bubble (Slug)
Behavior by Characterizing Transient Forces
of Solid Particles in Fluidized Beds**

1990 Annual Report

H.O. Kono

Work Performed Under Contract No.: DE-FC21-87MC24207

**For
U.S. Department of Energy
Office of Fossil Energy
Morgantown Energy Technology Center
P.O. Box 880
Morgantown, West Virginia 26507-0880**

**By
West Virginia University
Chemical Engineering Department
Morgantown, West Virginia 26506**

January 1991

ABSTRACT

The objective of this work is to recognize and interpret the signals of transient motion of bubbles (slugs) in fluidized beds by measuring and utilizing the signals of transient motion of solid particles.

The two signals were measured simultaneously and also synchronized by using the TTL signal technique in the same fluidized beds. Also, a simultaneous study of video bubble image, transient force and pressure signals was initiated in a two dimensional fluidized bed. we successfully synchronized three signals so that the relationship of bubble behavior and force pressure signals can be identified and characterized.

It has been found that bubble image can well be correlated to the transient force signal of solid particles under certain conditions in three dimensional fluidized beds. Accordingly, it seems that the transient force signals can significantly help understanding the transient motion of bubbles (slugs), which is important to design the fluidized beds.

TABLE OF CONTENTS

Section No.	Page No.
1. EXECUTIVE SUMMARY	1
2. TECHNICAL BACKGROUND	2
3. EXPERIMENTAL METHODOLOGY	3
4. EXPERIMENTAL RESULTS AND DISCUSSIONS	5
4.1. Gas Pressure Fluctuation (ΔAP) in the Same Sized Fluidized Bed as METC's for Bubble Image Analysis	5
4.2. Comparisons of Experimental Data on Peaks of Prevailing Force in Fluidized Beds by Using Three Different Measurement Methods	5
4.3. Experimental Data of Transient Solid Particle Force Synchronized with METC's Image Analysis	16
4.4. Consideration on the Data Processing Approach to Intensity Distribution of Gas Phase Pressure Fluctuation	16
4.5. Correlation Analysis on Synchronized Bubble Image and Pressure Fluctuation	26

TABLE OF CONTENTS

(Continued)

Section No.	Page No.
5. A NEW APPROACH FOR TRANSIENT GAS BUBBLE IMAGE - FORCE OF SOLID PARTICLES - GAS PRESSURE FLUCTUATION CORRELATION STUDY	91
5.1. Synchronize the Bubble Image with Transient Force of Solid Particles and Gas Pressure Fluctuation Signals	91
5.2. Recognition of Bubble Behavior	91
5.3. Correlation between Transient Bubble Image and Transient Force of Solid Particles - Gas Pressure Fluctuation Measurements	97
6. CONCLUSIONS	103
7. NOMENCLATURE	104
8. BIBLIOGRAPHY	105

LIST OF TABLES

Table	Page No.
Table 1. The Properties of Sample Particles	7
Table 2. Operating Conditions of Four Experiments	21

LIST OF FIGURES

Figure	Page No.
Figure 1. Schematic Diagram of the Experimental Apparatus	6
Figure 2. $U_0/U_{mf}(-)$ versus $\Delta\Delta P$ (Pa) Particles: Nylon $dp=3.175\text{mm}$	8
Figure 3. $U_0/U_{mf}(-)$ versus $\Delta\Delta P$ (Pa) Particles: Plastic $dp=0.7\text{mm}$	9
Figure 4. $U_0/U_{mf}(-)$ versus $\Delta\Delta P$ (Pa) Particles: Glass beads $dp=1\text{mm}$	10
Figure 5. $U_0/U_{mf}(-)$ versus $\Delta\Delta P$ (Pa) Particles: Nylon, Plastic and glass beads	11
Figure 6. $U_0/U_{mf}(-)$ versus $F_p(N)$ Particles: Glass beads $dp=1\text{mm}$	12
Figure 7. $U_0/U_{mf}(-)$ versus $F_t(N)$ Particles: Glass beads $dp=1\text{mm}$	13
Figure 8. Dimensionless Numbers Correlation, F_t/Mg versus $\Delta\Delta P \cdot d_p^2/Mg$	14
Figure 9. F_p versus F_t , Comparison of Force Measured by Piezo-electric and Fracture Sensitive Methods	15
Figure 10. Pressure Fluctuation ($U_0=.259\text{ m/s}$)	17
Figure 11. Pressure Fluctuation ($U_0=.316\text{ m/s}$)	18
Figure 12. Pressure Fluctuation ($U_0=.361\text{ m/s}$)	19
Figure 13. Pressure Fluctuation ($U_0=.220\text{ m/s}$)	20
Figure 14. Intensity Distribution of Gas Phase Pressure Fluctuation (Run 1, 5 seconds)	22
Figure 15. Intensity Distribution of Gas Phase Pressure Fluctuation (Run 2, 5 seconds)	23

LIST OF FIGURES
(Continued)

Figure	Page No.
Figure 16. Intensity Distribution of Gas Phase Pressure Fluctuation (Run 3, 5 seconds)	24
Figure 17. Intensity Distribution of Gas Phase Pressure Fluctuation (Run 4, 5 seconds)	25
Figure 18. Intensity Distribution of Gas Phase Pressure Fluctuation (Run 1, 55 seconds)	27
Figure 19. Intensity Distribution of Gas Phase Pressure Fluctuation (Run 2, 60 seconds)	28
Figure 20. Intensity Distribution of Gas Phase Pressure Fluctuation (Run 3, 60 seconds)	29
Figure 21. Intensity Distribution of Gas Phase Pressure Fluctuation (Run 4, 60 seconds)	30
Figure 22. Intensity Distribution of Gas Phase Pressure Fluctuation (Run 1, 15 seconds)	31
Figure 23. Intensity Distribution of Gas Phase Pressure Fluctuation (Run 2, 15 seconds)	32
Figure 24. Intensity Distribution of Gas Phase Pressure Fluctuation (Run 3, 15 seconds)	33
Figure 25. Intensity Distribution of Gas Phase Pressure Fluctuation (Run 4, 15 seconds)	34
Figure 26. Intensity Distribution of Gas Phase Pressure Fluctuation (Run 1, 30 seconds)	35

LIST OF FIGURES
(Continued)

Figure	Page No.
Figure 27. Intensity Distribution of Gas Phase Pressure Fluctuation (Run 2, 30 seconds)	36
Figure 28. Intensity Distribution of Gas Phase Pressure Fluctuation (Run 3, 30 seconds)	37
Figure 29. Intensity Distribution of Gas Phase Pressure Fluctuation (Run 4, 30 seconds)	38
Figure 30. Pixel Definitions	40
Figure 31. Average Voidage versus Time ($U_0 = .259$, level 1)	41
Figure 32. Average Voidage versus Time ($U_0 = .259$, level 2)	42
Figure 33. Average Voidage versus Time ($U_0 = .259$, level 3)	43
Figure 34. Average Voidage versus Time ($U_0 = .259$, level 4)	44
Figure 35. Average Voidage versus Time ($U_0 = .316$, level 1)	45
Figure 36. Average Voidage versus Time ($U_0 = .316$, level 2)	46
Figure 37. Average Voidage versus Time ($U_0 = .316$, level 3)	47
Figure 38. Average Voidage versus Time ($U_0 = .316$, level 4)	48
Figure 39. Average Voidage versus Time ($U_0 = .361$, level 1)	49
Figure 40. Average Voidage versus Time ($U_0 = .361$, level 2)	50

LIST OF FIGURES
(Continued)

Figure	Page No.
Figure 41. Average Voidage versus Time (U ₀ =.361, level 3)	51
Figure 42. Average Voidage versus Time (U ₀ =.361, level 4)	52
Figure 43. Average Voidage versus Time (U ₀ =.220, level 1)	53
Figure 44. Average Voidage versus Time (U ₀ =.220, level 2)	54
Figure 45. Average Voidage versus Time (U ₀ =.220, level 3)	55
Figure 46. Average Voidage versus Time (U ₀ =.220, level 4)	56
Figure 47. Local Voidage versus Time (U ₀ =.259, cell 1, level 1)	57
Figure 48. Local Voidage versus Time (U ₀ =.259, cell 1, level 2)	58
Figure 49. Local Voidage versus Time (U ₀ =.259, cell 1, level 3)	59
Figure 50. Local Voidage versus Time (U ₀ =.259, cell 1, level 4)	60
Figure 51. Local Voidage versus Time (U ₀ =.316, cell 1, level 1)	61
Figure 52. Local Voidage versus Time (U ₀ =.316, cell 1, level 2)	62
Figure 53. Local Voidage versus Time (U ₀ =.316, cell 1, level 3)	63
Figure 54. Local Voidage versus Time (U ₀ =.316, cell 1, level 4)	64

LIST OF FIGURES

(Continued)

Figure	Page No.
Figure 55. Local Voidage versus Time ($U_0=.361$, cell 1, level 1)	65
Figure 56. Local Voidage versus Time ($U_0=.361$, cell 1, level 2)	66
Figure 57. Local Voidage versus Time ($U_0=.361$, cell 1, level 3)	67
Figure 58. Local Voidage versus Time ($U_0=.361$, cell 1, level 4)	68
Figure 59. Local Voidage versus Time ($U_0=.220$, cell 1, level 1)	69
Figure 60. Local Voidage versus Time ($U_0=.220$, cell 1, level 2)	70
Figure 61. Local Voidage versus Time ($U_0=.220$, cell 1, level 3)	71
Figure 62. Local Voidage versus Time ($U_0=.220$, cell 1, level 4)	72
Figure 63. Local Voidage versus Time ($U_0=.259$, cell 1-33, level 1)	73
Figure 64. Local Voidage versus Time ($U_0=.259$, cell 1-33, level 2)	74
Figure 65. Local Voidage versus Time ($U_0=.259$, cell 1-33, level 3)	75
Figure 66. Local Voidage versus Time ($U_0=.259$, cell 1-33, level 4)	76
Figure 67. Local Voidage versus Time ($U_0=.316$, cell 1-33, level 1)	77
Figure 68. Local Voidage versus Time ($U_0=.316$, cell 1-33, level 2)	78

LIST OF FIGURES

(Continued)

Figure	Page No.
Figure 69. Local Voidage versus Time ($U_0=.316$, cell 1-33, level 3)	79
Figure 70. Local Voidage versus Time ($U_0=.316$, cell 1-33, level 4)	80
Figure 71. Local Voidage versus Time ($U_0=.361$, cell 1-33, level 1)	81
Figure 72. Local Voidage versus Time ($U_0=.361$, cell 1-33, level 2)	82
Figure 73. Local Voidage versus Time ($U_0=.361$, cell 1-33, level 3)	83
Figure 74. Local Voidage versus Time ($U_0=.361$, cell 1-33, level 4)	84
Figure 75. Local Voidage versus Time ($U_0=.220$, cell 1-33, level 1)	85
Figure 76. Local Voidage versus Time ($U_0=.220$, cell 1-33, level 2)	86
Figure 77. Local Voidage versus Time ($U_0=.220$, cell 1-33, level 3)	87
Figure 78. Local Voidage versus Time ($U_0=.220$, cell 1-33, level 4)	88
Figure 79. Pressure Fluctuation versus Voidage ($U_0=.259$ m/s)	89
Figure 80. Schematic Diagram of the Experimental Setting	92
Figure 81 Pressure Fluctuation in Synchronized Experiment	101
Figure 82 Transient Forces in Synchronized Experiment	102

LIST OF PHOTOGRAPHS

Photograph	Page No.
Photograph 1. Video Display at Time 15.44	93
Photograph 2. Video Display at Time 15.47	93
Photograph 3. Video Display at Time 15.50	94
Photograph 4. Video Display at Time 15.54	94
Photograph 5. Video Display at Time 15.57	95
Photograph 6. Video Display at Time 15.60	95
Photograph 7. Video Display at Time 15.64	96
Photograph 8. Video Display at Time 22.93	98
Photograph 9. Video Display at Time 22.97	98
Photograph 10. Video Display at Time 23.00	99
Photograph 11. Video Display at Time 23.04	99
Photograph 12. Video Display at Time 23.07	100

1. EXECUTIVE SUMMARY

The objectives of this work are:

(1) to characterize and recognize the image signals of transient motion of bubble (slug) by measuring the transient forces of solid particles in fluidized beds.

(2) to measure the transient forces of solid particles by synchronizing with the image analysis being accomplished at METC in a fluidized bed.

(3) to measure and analyze the transient forces of solid particles in our laboratory fluidized beds under the similar or corresponding fluidized bed conditions as METC's fluidized beds.

The significance of this approach is to recognize the transient behavior of bubble (slug) in terms of transient forces of solid particles, which can quantitatively and more easily be expressed in a form of digital numbers. In other words, this is a recognition of transient bubble (slug) in terms of transient forces in solid emulsion phase.

The correlation study on these two transient signals was conducted by analyzing the two synchronized transient measurements in the same fluidized bed (6" ID). It has been found that the voidage peak is well correlated to the gas phase pressure fluctuation (energy release) under certain conditions.

In order to systematically study the relationship among bubble behavior, transient forces of solid particles and gas phase pressure fluctuation, a new method was proposed and initiated in a two dimensional fluidized bed. Using this new approach, a detailed study of three synchronized signals can be carried out. Some preliminary data have shown that the new approach will help to understand the fundamental mechanism of bubble motion.

2. TECHNICAL BACKGROUND

Historically the bubble motion and bubble properties (size, shape, cloud, wake, etc.) in fluidized beds have been investigated very intensively by many researchers including famous theoretical, classical works by Davidson et al (1963) and experimental works by Rowe et al (1962). However, these researchers investigated mostly the steady state behavior of the bubble and only a few studies have been conducted for the unsteady transient motion of the bubble.

Rowe et al (1962) pointed out the significance of the transient behavior of bubble's shedding but the experimental results did not follow.

The difficulty of observing transient motion of bubbles is probably due to the fact that the bubble motions are stable in a very thin two dimensional fluidized beds and any impressive, transient motion of bubbles can not be observed under that condition.

In three dimensional fluidized beds the transient motion of bubbles becomes very much enhanced at high gas velocity in coarse particle fluidized beds, in which the observation could have only been accomplished by using X-ray without much success due to its experimental limitation.

Recently Hallow et al (1989) made an experimental break-through by developing an observation method for the transient bubble motion by using a capacitance image method.

To quantify the transient motion image of bubble, the measurement of the transient forces of solid particles has been developed in this project.

3. EXPERIMENTAL METHODOLOGY

The following approaches were developed:

(1). Recognition of Transient Bubble Motions in Three Dimensional Fluidized Beds.

Now the only available method for three dimensional fluidized beds is the capacitance method developed by Hallow et al (1989). When a thin two dimensional fluidized bed is used, the intrinsic transient bubble motion will not be attained due to the enhanced wall effect.

(2). Recognition of Transient Bubble Motions in Two Dimensional Fluidized Beds.

For the systematic study of bubble image, together with transient forces of solid particles and gas pressure fluctuation, two dimensional fluidized bed has its advantages. It is easy to be video taped, and provides the direct, first hand image. Similar bubble image can be collected together with force and pressure signals. The collection of image sample provides reliable information for correlation study.

(3). Recognition of Transient Forces of Solid Particles.

Although the measurement methods of transient forces of solid particles have already been developed, these methods were directed to measure the peaks of the forces. Now a recognition of transient forces of solid particles should be developed to characterize the transient motions of bubbles. The characteristics of transient forces of solid particles may be expressed by peaks, frequencies, intensity distributions, etc.

(4). Experiment at METC's Fluidized Bed.

As the first approach, the transient forces of solid particles were measured by synchronizing the measurement of transient motion of bubbles in METC's fluidized beds (6" I.D.). Since we know the correlation of the transient solid forces obtained from three different kinds of measurement methods, i.e. piezoelectric, fracture sensor and gas pressure fluctuation, the simplest gas pressure fluctuation method was used.

The experimental conditions to attain the most appropriate data processing approach was also investigated.

(4). Experiment at Our Laboratory

By using the identical sized fluidized bed as METC's fluidized bed (for Bubble Image Analysis), transient forces of solid particles were also measured in wide range to support the understanding and characterization of transient forces of solid particles.

4. EXPERIMENTAL RESULTS AND DISCUSSIONS

4.1. Gas Pressure Fluctuation ($\Delta\Delta P$) in the Same Sized Fluidized Bed as METC's for Bubble Image Analysis

The Gas Phase Pressure Fluctuation ($\Delta\Delta P$) was measured in the same sized fluidized bed as METC's and data were obtained and processed by the computer system. The schematic flow diagram of experimental setting is shown in Figure 1. The bed used is identical to the METC's fluidized bed, which is being used for Capacitance Image Tests. The bed materials are: nylon particles of size 3.18mm, glass beads of size 1mm and plastic particles of 0.7mm in diameter. The properties of the sample particles are shown in Table 1.

Figures 2 through 4 show the gas phase pressure fluctuations ($\Delta\Delta P$) under various gas velocities (U_0/U_{mf}) for nylon, plastic particles and glass beads, respectively. The U_0/U_{mf} range is from 1.0 to 3.0 for nylon and plastic particles, and 1.0 to 3.5 for glass beads. The bed diameter D_t is 0.152m and bed aspect ratio H/D_t is 1 for nylon and plastic particles. As for glass beads the bed diameter is 0.152m but H/D_t is 1 and 2.7. For convenience of comparisons, above three Figures are shown on the same picture as Figure 5.

4.2. Comparisons of Experimental Data on Peaks of Prevailing Force in Fluidized Beds by Using Three Different Measurement Methods

Also using the same sized fluidized bed as the one being used by METC's Capacitance Method, the maximum peaks of prevailing forces in fluidized beds were measured by other two different methods, i.e. piezo-electric and fracture sensitive methods. The peaks of prevailing forces measured by piezo-electric sensor (F_p) and by fracture sensitive sensor (F_f) as a function of dimensionless gas velocity are shown in Figure 6 and 7, respectively, to compare with the results of the peaks of gas phase pressure fluctuation shown in Figure 4. The fluidized particle of glass beads is 1mm in diameter, and U_0/U_{mf} range is from 1.0 to 3.8.

Data from past experiments showed that good correlations exist among $\Delta\Delta P$, F_f and F_p (see Figures 8 and 9). Therefore, only one of the above three methods is necessary for the purpose of correlation study between the maximum peaks of prevailing force and bubbling image analysis. Unlike the piezo-electric sensor method and the fracture sensitive sensor method, which are

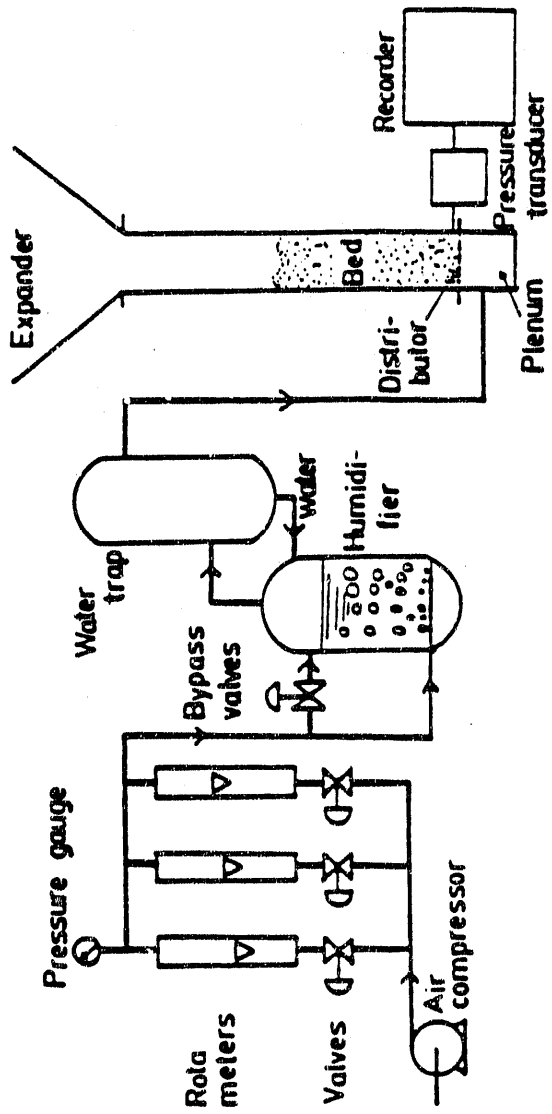


Figure 1. Schematic Diagram of the Experimental Apparatus.

TABLE 1 THE PROPERTIES OF SAMPLE PARTICLES

Material	Weight Average Diameter Microns	Particle Density gm/cc	Bulk Density gm/cc	Packed Voidage	Minimum Fluidization Velocity cm/sec
1/8 inch Nylon spheres	3175	1.12	0.64	0.40	84.1
700-Micron Plastic	704	1.55	0.73	0.53	19.0
Glass Beads	1000	2.49	--	--	46.0

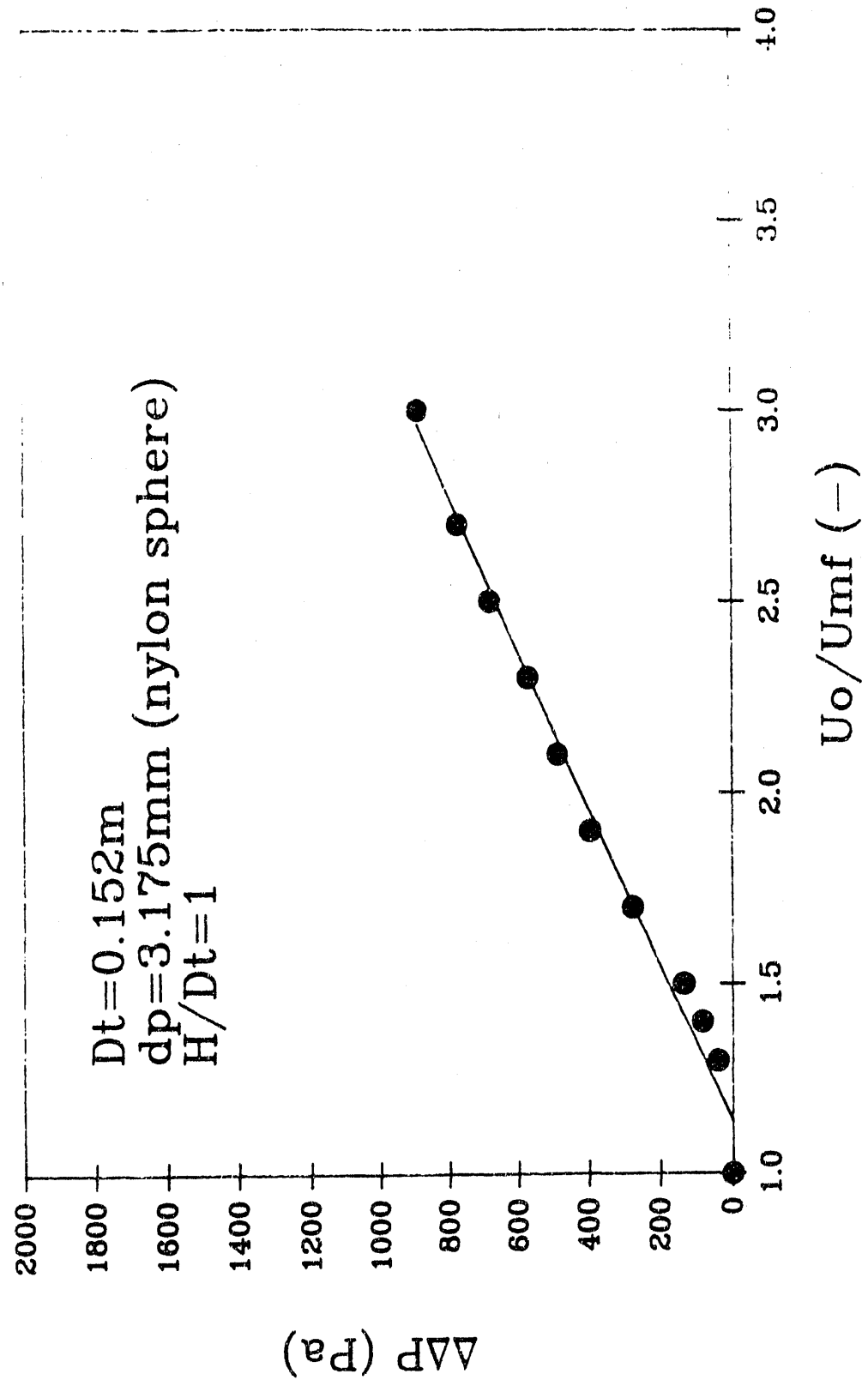


Figure 2. $U_0/U_{mf} (−)$ versus $\Delta\Delta P$ (Pa) Particles: Nylon $d_p = 3.175\text{mm}$

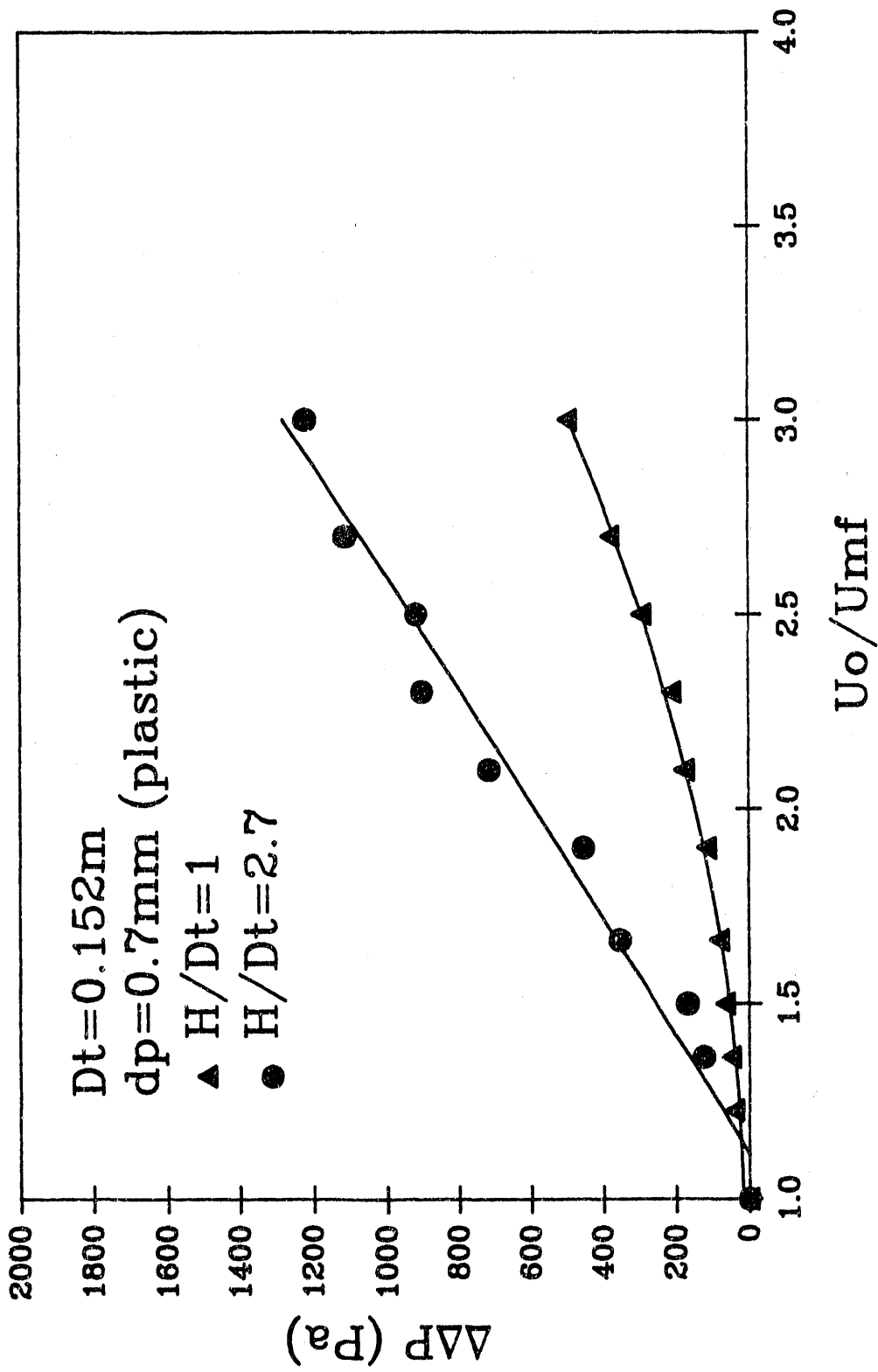


Figure 3. $U_o / U_{mf} (-)$ Versus $\Delta\Delta P$ (Pa) Particles: Plastic $dp = 0.7\text{mm}$

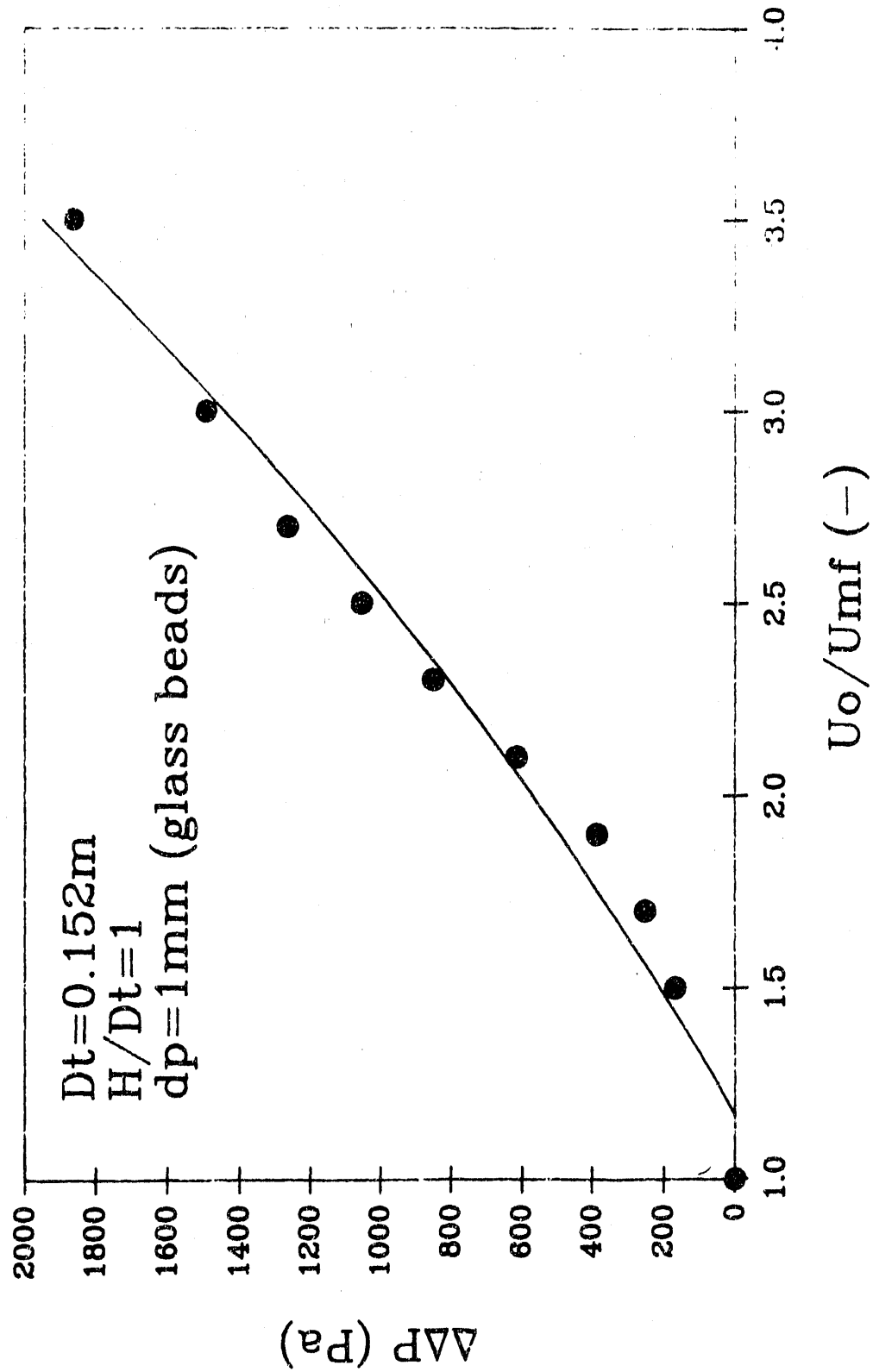


Figure 4. $U_o/U_{mf} (-)$ versus $\Delta \Delta P$ (Pa) Particles: Glass beads $d_p = 1mm$

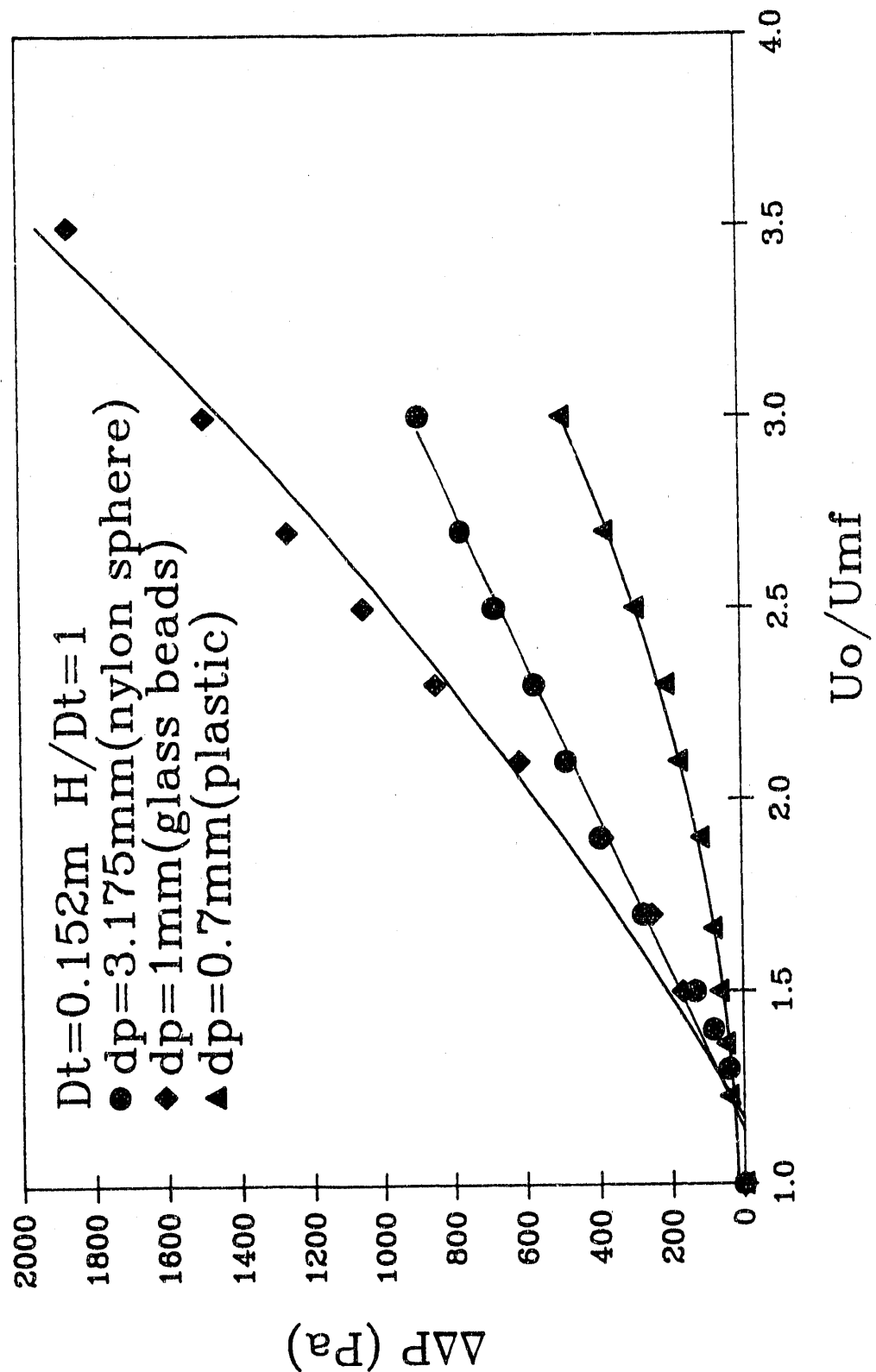


Figure 5. $U_o/U_{mf}(-)$ versus $\Delta\Delta P$ (Pa) Particles: Nylon, Plastic and Glass beads

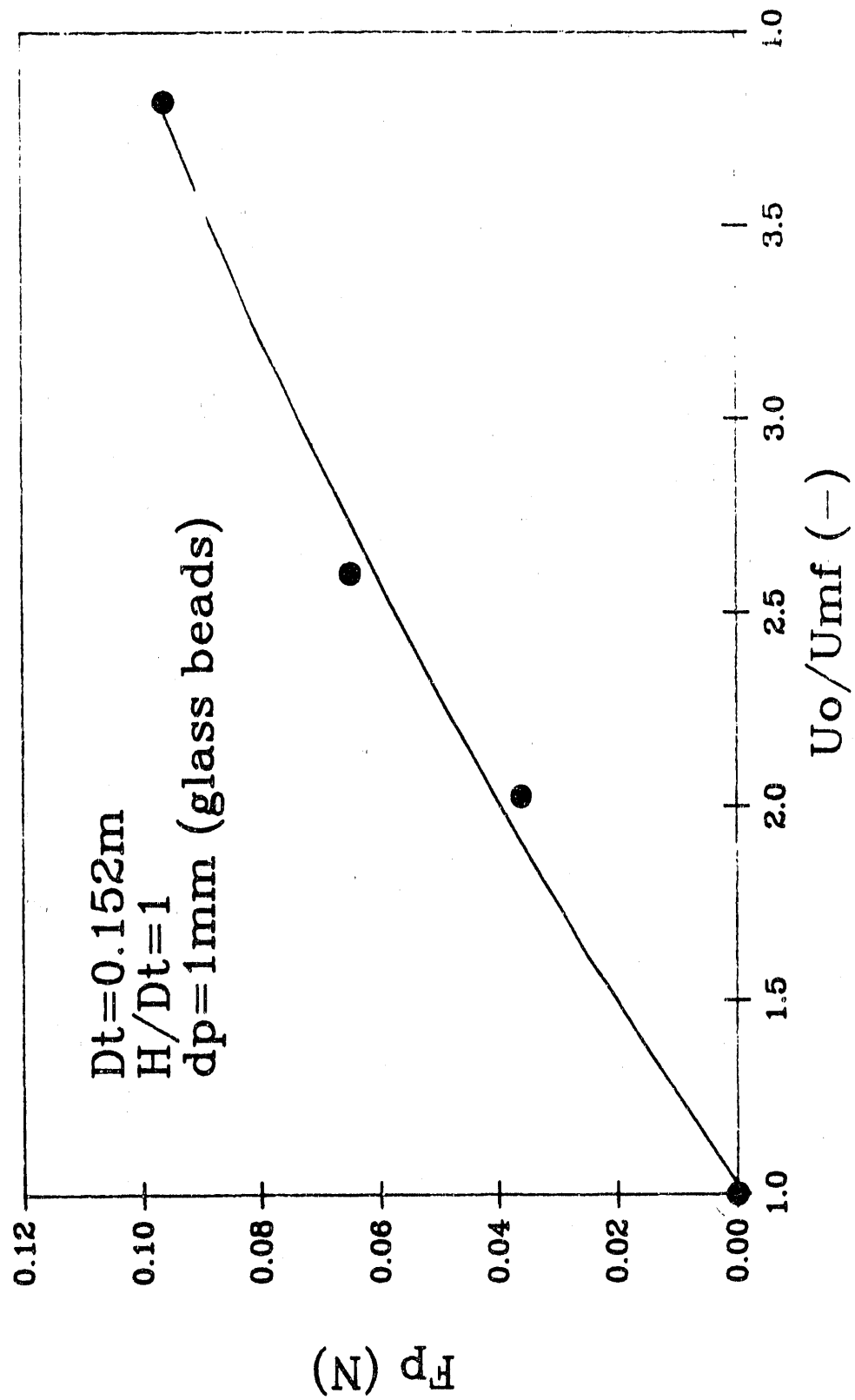


Figure 6. $U_o/U_{mf}(-)$ versus $F_p(N)$ Particles: Glass beads $d_p = 1\text{mm}$

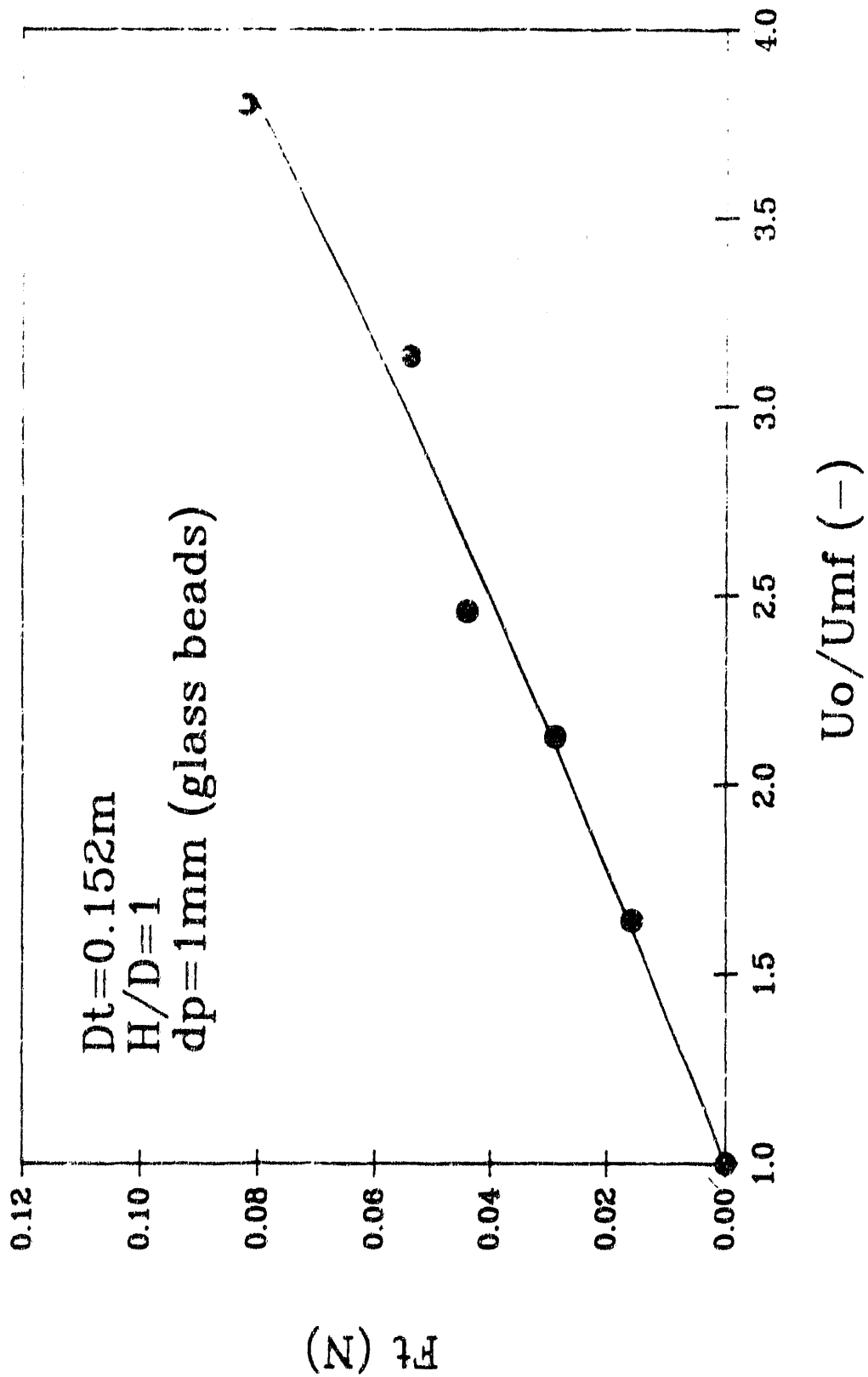


Figure 7. $U_o/U_{mf}(-)$ versus $F_t(N)$ Particles: Glass beads $d_p = 1\text{mm}$

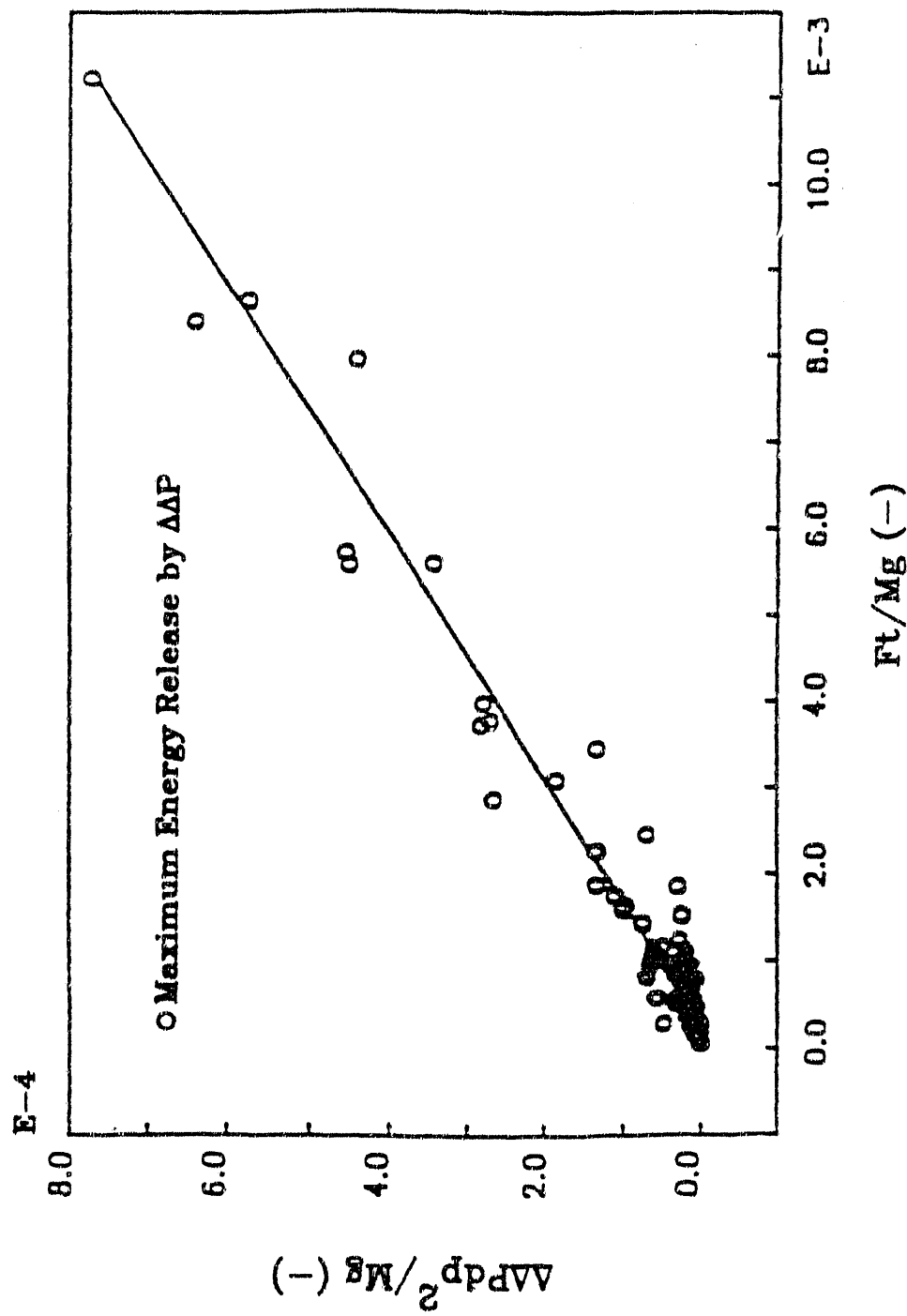


Figure 8. Dimensionless Numbers Correlation, F_t/Mg versus $\Delta\Delta P \cdot d_p^2 / Mg^2$

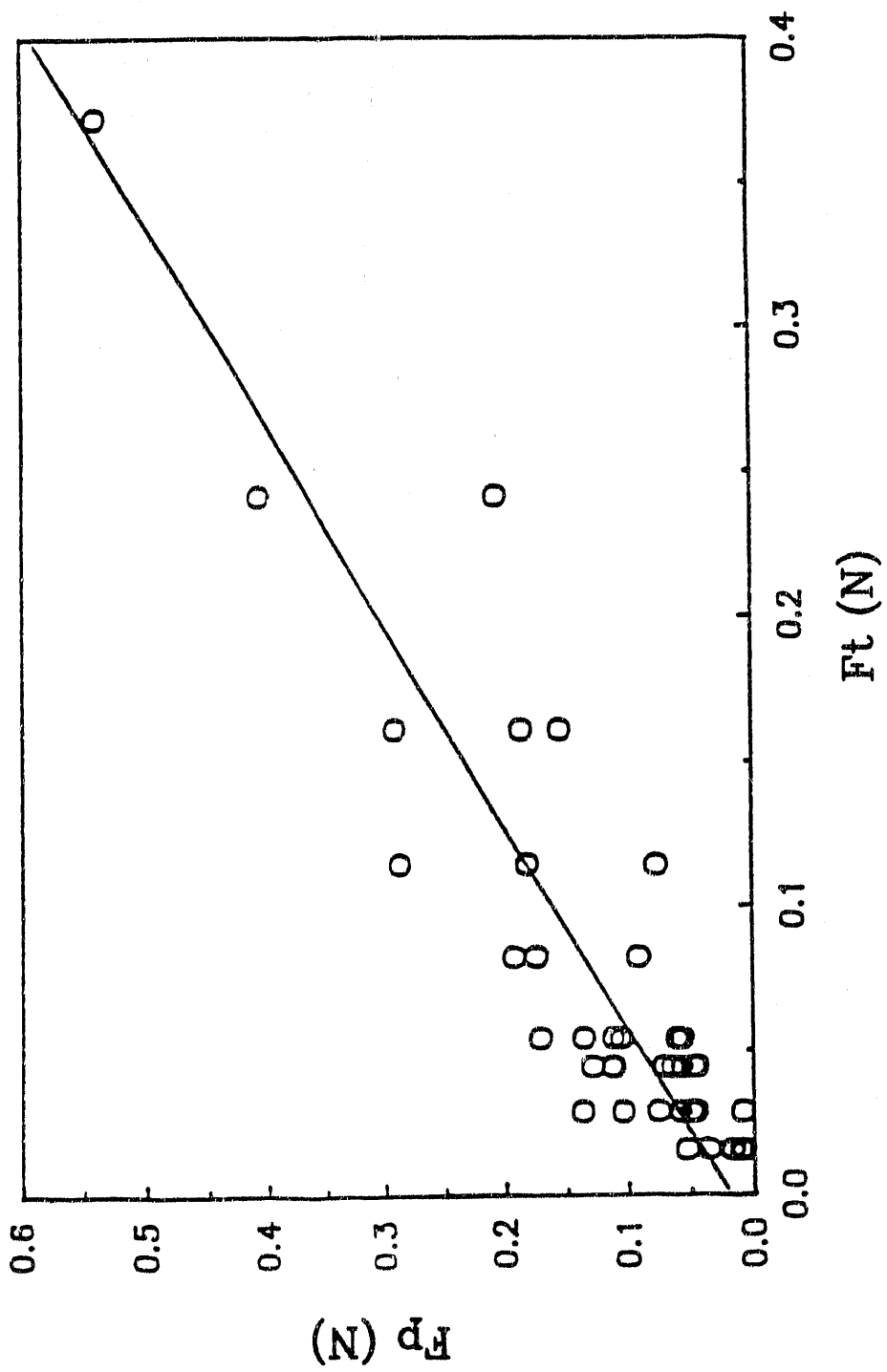


Figure 9 F_p versus F_t , Comparison of Force Measured by Piezo-electric and Fracture Sensitive Methods.

technically complicated, the gas phase pressure fluctuation method is relatively easy and convenient, particularly this method can directly be applied to high temperature and pressure. Consequently, the $\Delta\Delta P$ approach would be the best choice for our synchronized force-bubble behavior study.

4.3. Experimental Data of Transient Solid Particle Force Synchronized with METC's Image Analysis

Synchronized experiments were conducted in METC in order to study the relationship between transient solid particle force and transient bubble motion. The experimental data were recorded by the computer system to compare with METC's bubble image data. Four experiment runs were executed. For each experiment run, 5 seconds data were extracted and plotted. The starting point of the plots are the same as METC's bubble image data. Also, for the purpose of extensive study, 60 seconds data were maintained. Figure 10 through 13 show the transient force fluctuation as time elapses in four different experimental runs. These data are already provided to METC in disk format. For better representation, here we use pressure as Y axis in the unit of 1000 Pa. The operating conditions of four experiments are listed in table 2.

Comparing the Figure 10 with METC's bubble data figure indicates a reasonable match, although a detailed study and more experiments should be conducted to explore the relationship (See section 4.5 for correlation analysis). A series of experiments based on multiple measurement points were recommended in the next year proposal, as part of the fundamental study on transient bubble behavior by characterizing transient forces of solid particles in fluidized beds.

4.4. Consideration on the Data Processing Approach to Intensity Distribution of Gas Phase Pressure Fluctuation

In order to study the relationship between transient forces of solid particles and transient motion of bubble behavior, the gas phase pressure fluctuation method was used. This requires an appropriate approach on how to process the data of pressure fluctuation and bubble motion. Data from synchronized experiments were processed and analyzed. The distribution of pressure fluctuation were plotted, using 5 seconds data (synchronized operation) as well as 60 seconds data (extended operation). Figures 14 through 17 give the distribution of pressure fluctuation intensity for each experimental run using 5 seconds

PRESSURE FLUCTUATION

$U_0 = .259 \text{ m/s}$

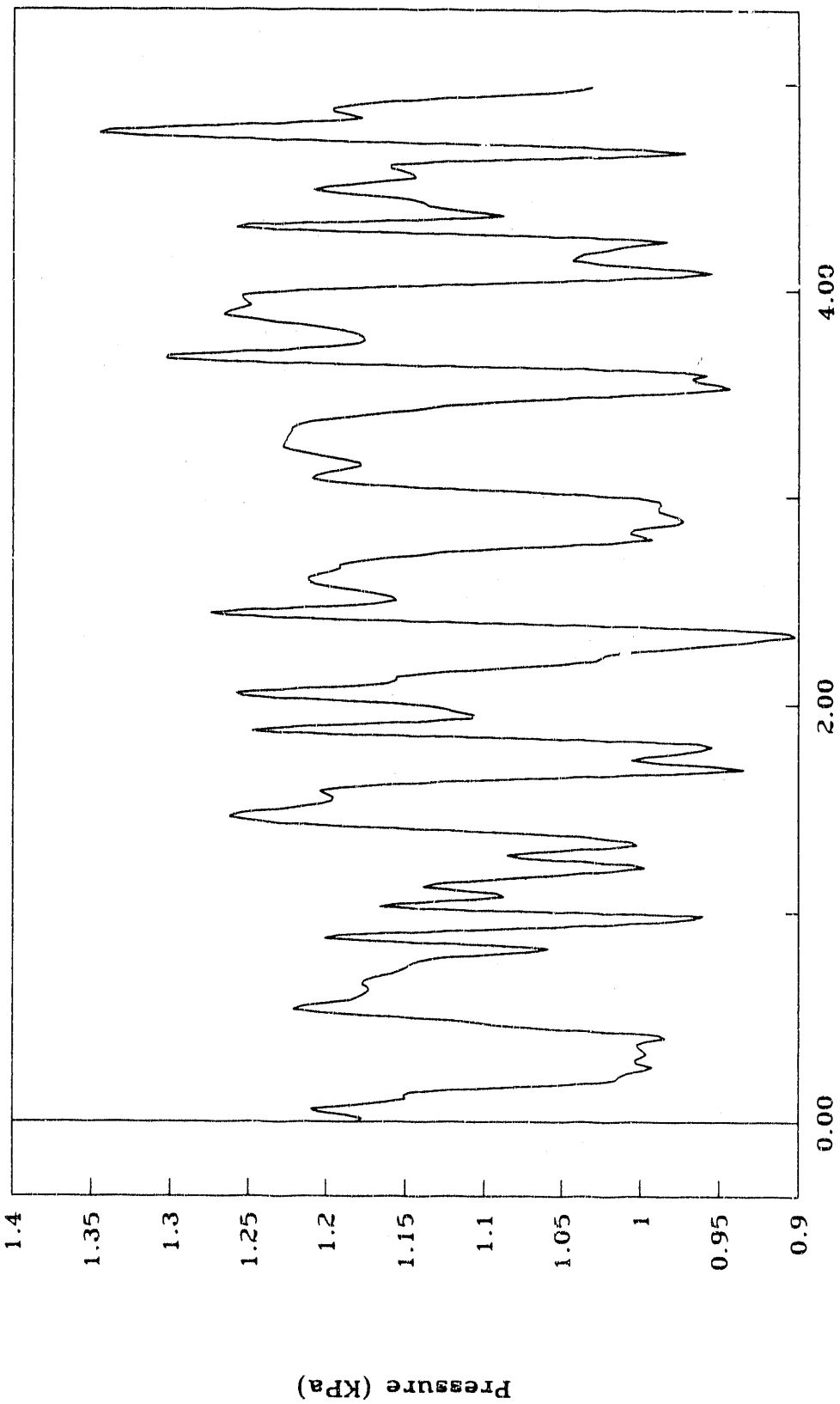


Figure 10. Pressure Fluctuation ($U_0 = 0.259 \text{ m/s}$)

PRESSURE FLUCTUATION

$U_0 = .316 \text{ m/s}$

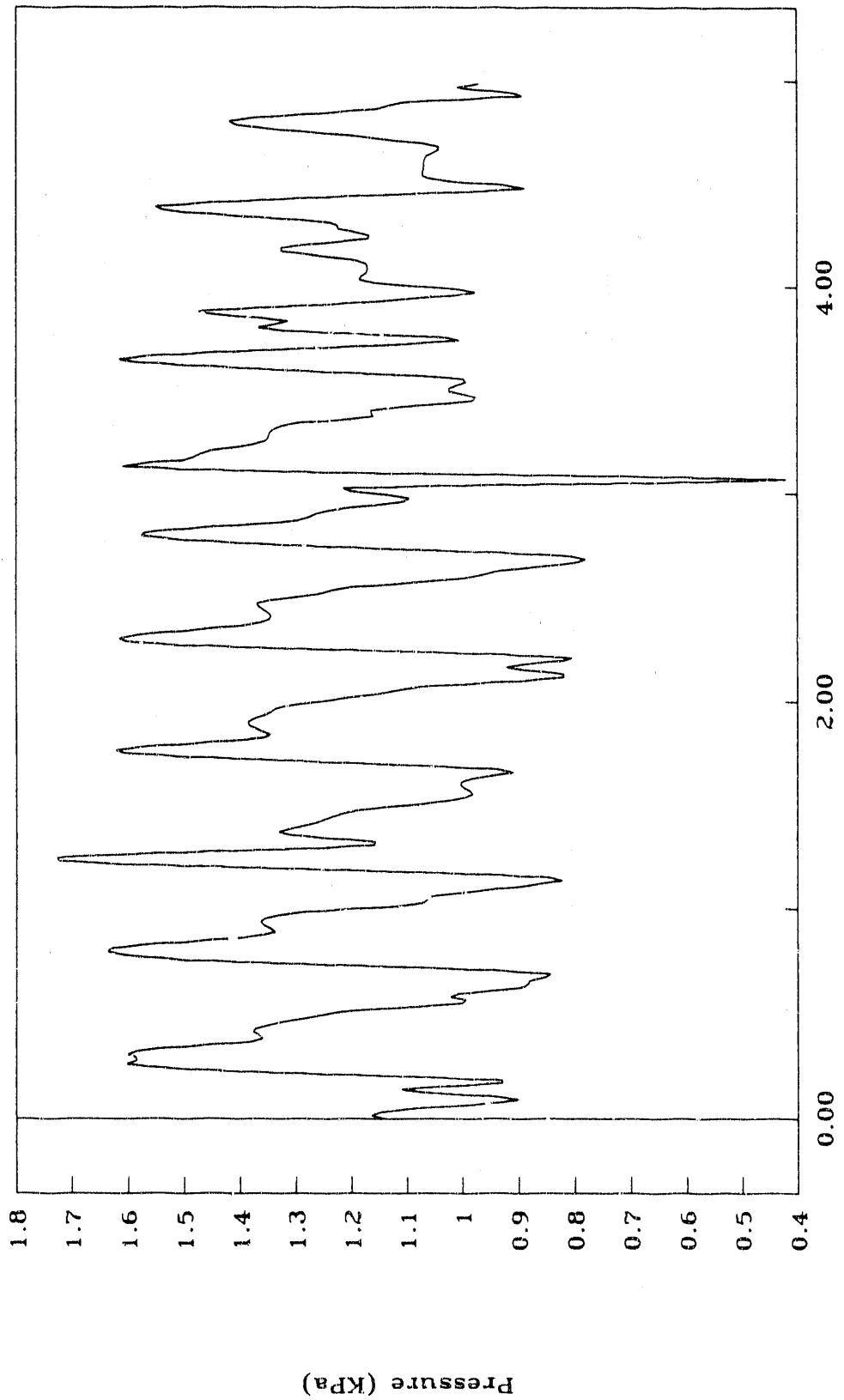


Figure 11. Pressure Fluctuation ($U_0 = 0.316 \text{ m/s}$)

PRESSURE FLUCTUATION

$U_0 = .361 \text{ m/s}$

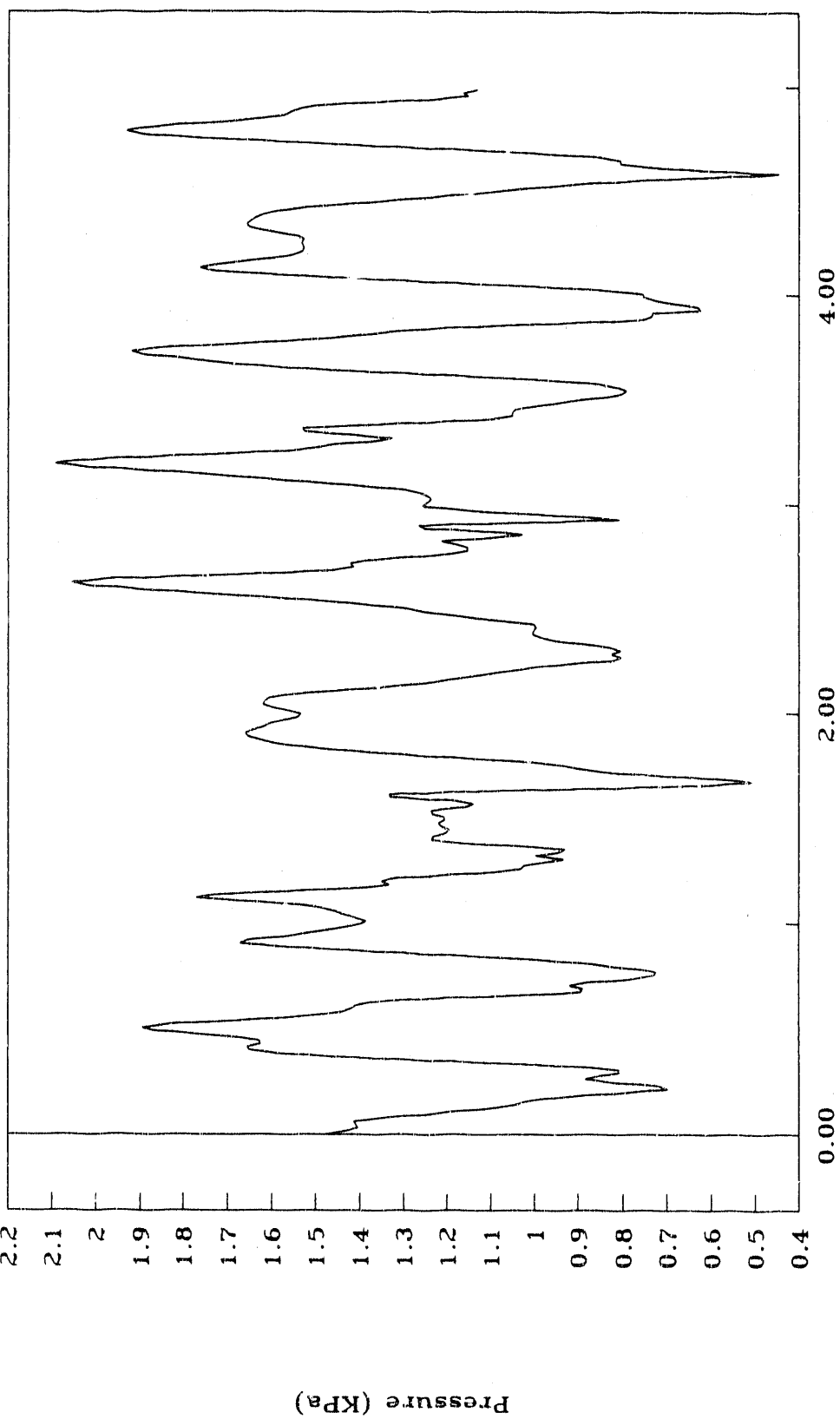


Figure 12. Pressure Fluctuation ($U_0 = 0.361 \text{ m/s}$)

PRESSURE FLUCTUATION

$U_0 = .220 \text{ m/s}$

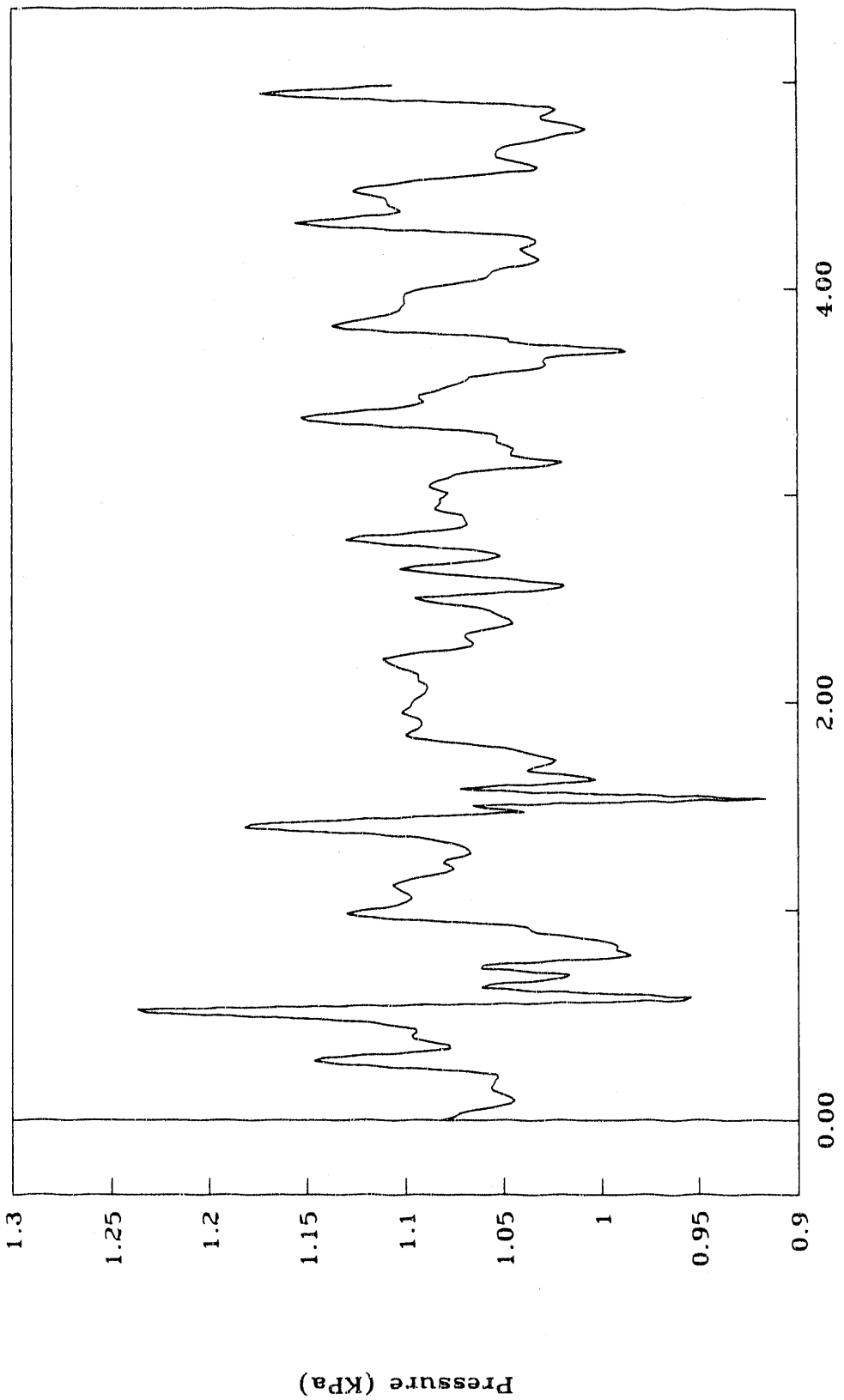


Figure 13. Pressure Fluctuation ($U_0 = 0.220 \text{ m/s}$)

TABLE 2 OPERATING CONDITIONS OF FOUR EXPERIMENTS
 (bed material is plastic particles)

RUN NUMBER	U_0 (m/sec)	D_t (inches)	H (inches)	d_p (μ)
1	.259	6	16	700
2	.316	6	16	700
3	.361	6	16	700
4	.220	6	16	700

DISTRIBUTION OF PRESSURE FLUCTUATION
(The First Run, 5 Seconds)

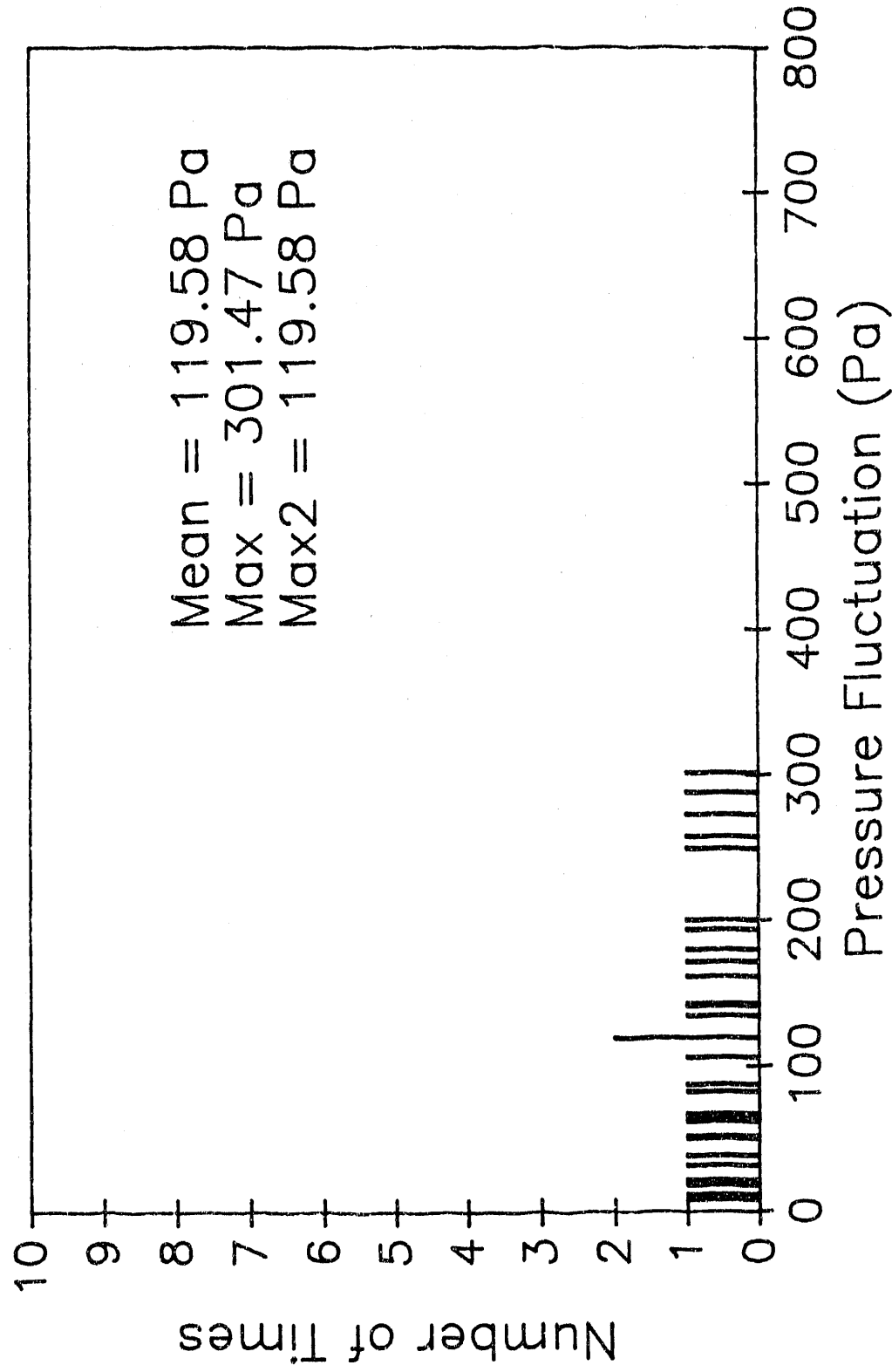


Figure 14. Intensity Distribution of Gas Phase Pressure Fluctuation
(Run 1, 5 seconds)

DISTRIBUTION OF PRESSURE FLUCTUATION
(The Second Run, 5 Seconds)

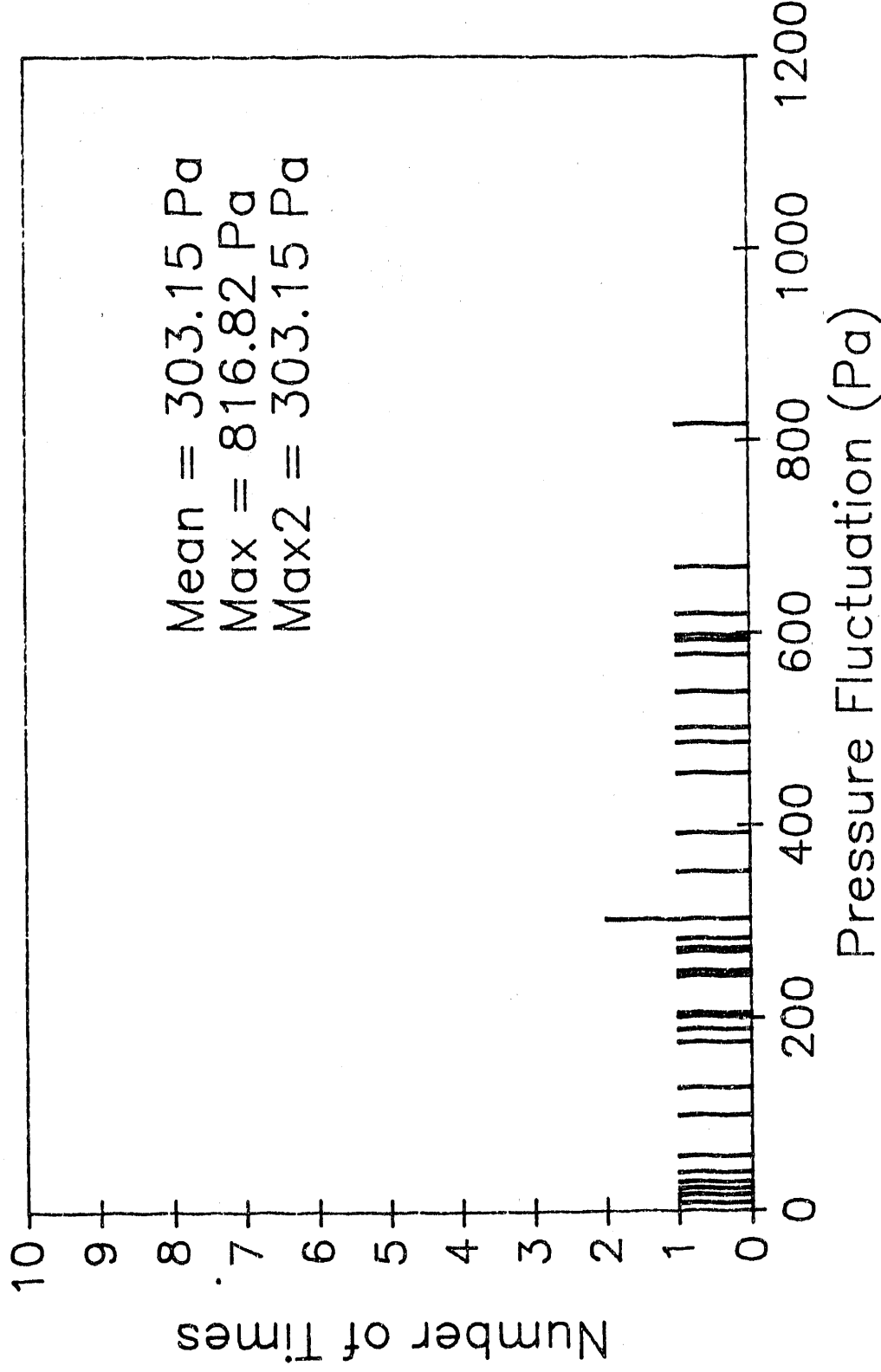


Figure 15. Intensity Distribution of Gas Phase Pressure Fluctuation
(Run 2, 5 seconds)

DISTRIBUTION OF PRESSURE FLUCTUATION
(The Third Run, 5 Seconds)

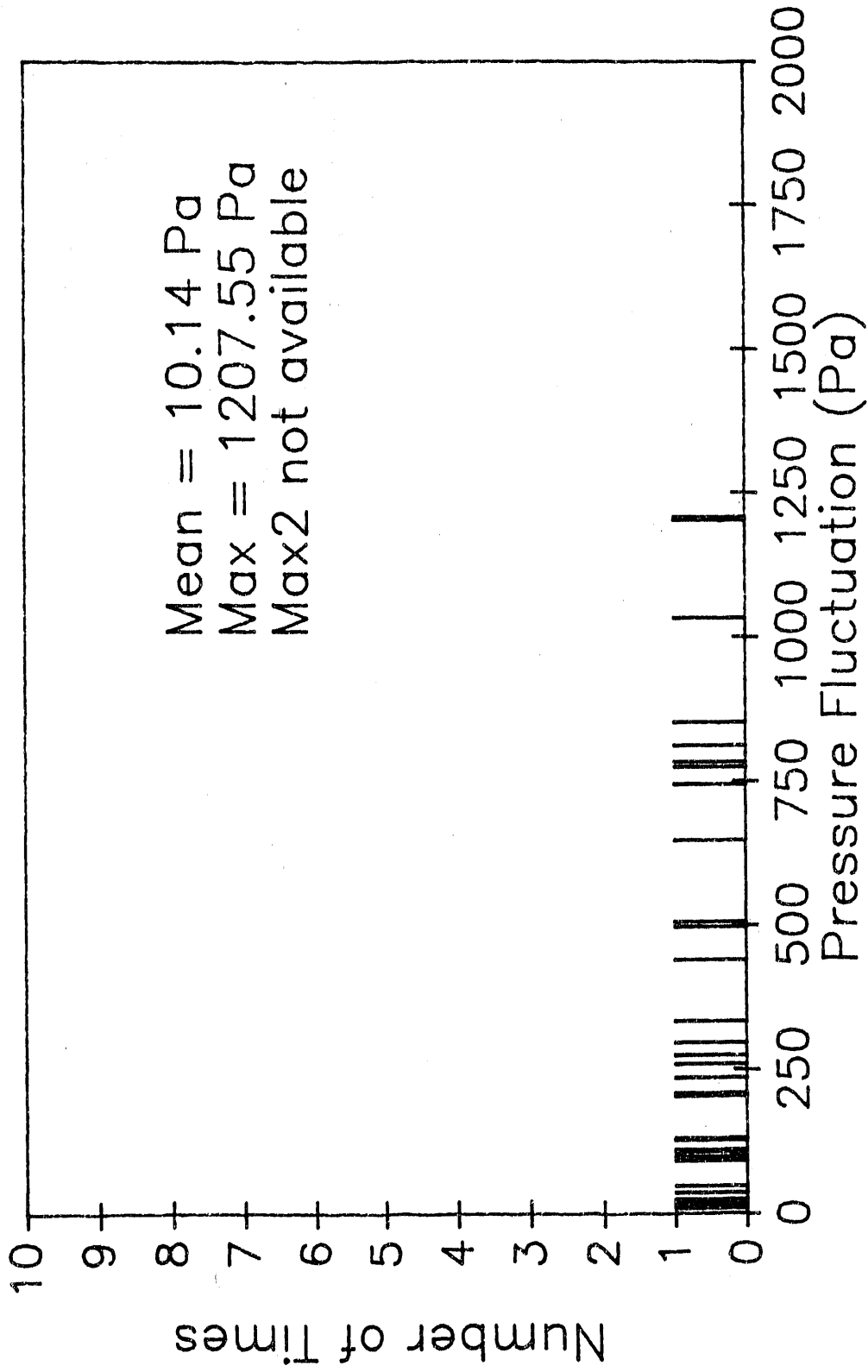


Figure 16. Intensity Distribution of Gas Phase Pressure Fluctuation
(Run 3, 5 seconds)

DISTRIBUTION OF PRESSURE FLUCTUATION
(The Fourth Run, 5 Seconds)

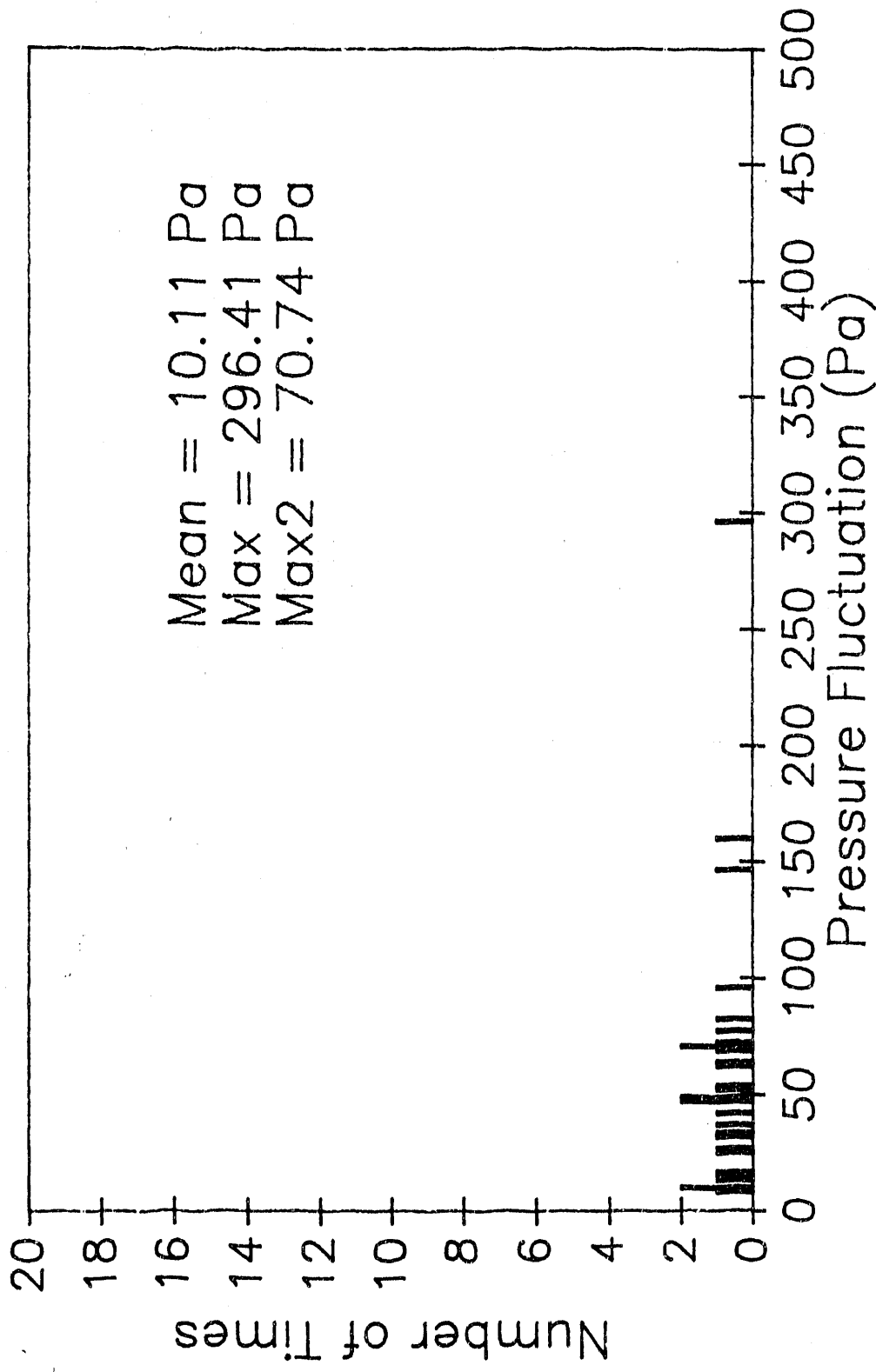


Figure 17. Intensity Distribution of Gas Phase Pressure Fluctuation
(Run 4, 5 seconds)

data. The distributions are flat in shape. The maximum frequency is 2, providing non-reliable information on prevailing force. When U_0/U_{mf} is high (the third run), the distribution becomes nearly uniform, and the second maximum is even not available. It is obvious that 5 second run time is too short to provide the satisfactory representative force information because of data shortage. Figures 18 through 21 show the distribution of pressure fluctuation using 60 second data (55 second for the first run). It is clear that 60 second data provide realistic representation of the pressure fluctuation intensity distribution. Further study of 15 second data and 30 second data will lead to the following conclusion: the higher the U_0/U_{mf} ratio, the longer the run time required to represent the transiently prevailing forces of solid particles in the system. For the synchronized experiment, when U_0 is low (run 4, 0.220m/sec), at least 15 second data may be collected, but when U_0 is high (run 3, 0.361m/sec) at least 60 second data should be obtained. The intensity distributions of pressure fluctuation for each run using 15 second and 30 second data are provided in Figures 22 through 29.

To more reasonably manage the data taking process, smaller sampling rate (per second) may be used to minimize the total number of samples. However further study on this subject is necessary to maintain the quality of sampling process.

Currently the sampling rate of METC's transient bubble image analysis is 60 samples per second, and that of our transient forces of solid particle is 100 samples per second. For the purpose of the correlation study, these sampling rate should be the same or in multiple. Therefore, an adjustment would be necessary for the future synchronized experiments.

By observing these experimental data processing, the data of the transient forces of solid particle can already help understanding the transient bubble signal, hinting that the transient bubble signals should be obtained more, or the sampling taking time should be at least 15 or 30 seconds.

4.5. Correlation Analysis on Synchronized Bubble Image and Pressure Fluctuation

Based on the data obtained from joint experiment in METC, we investigated to correlate the voidage signals (obtained by METC's capacitance method) with the transient force signals (obtained by our method) in fluidized beds.

There is obvious a clear correspondency between the above two

DISTRIBUTION OF PRESSURE FLUCTUATION (The First Run, 55 Seconds)

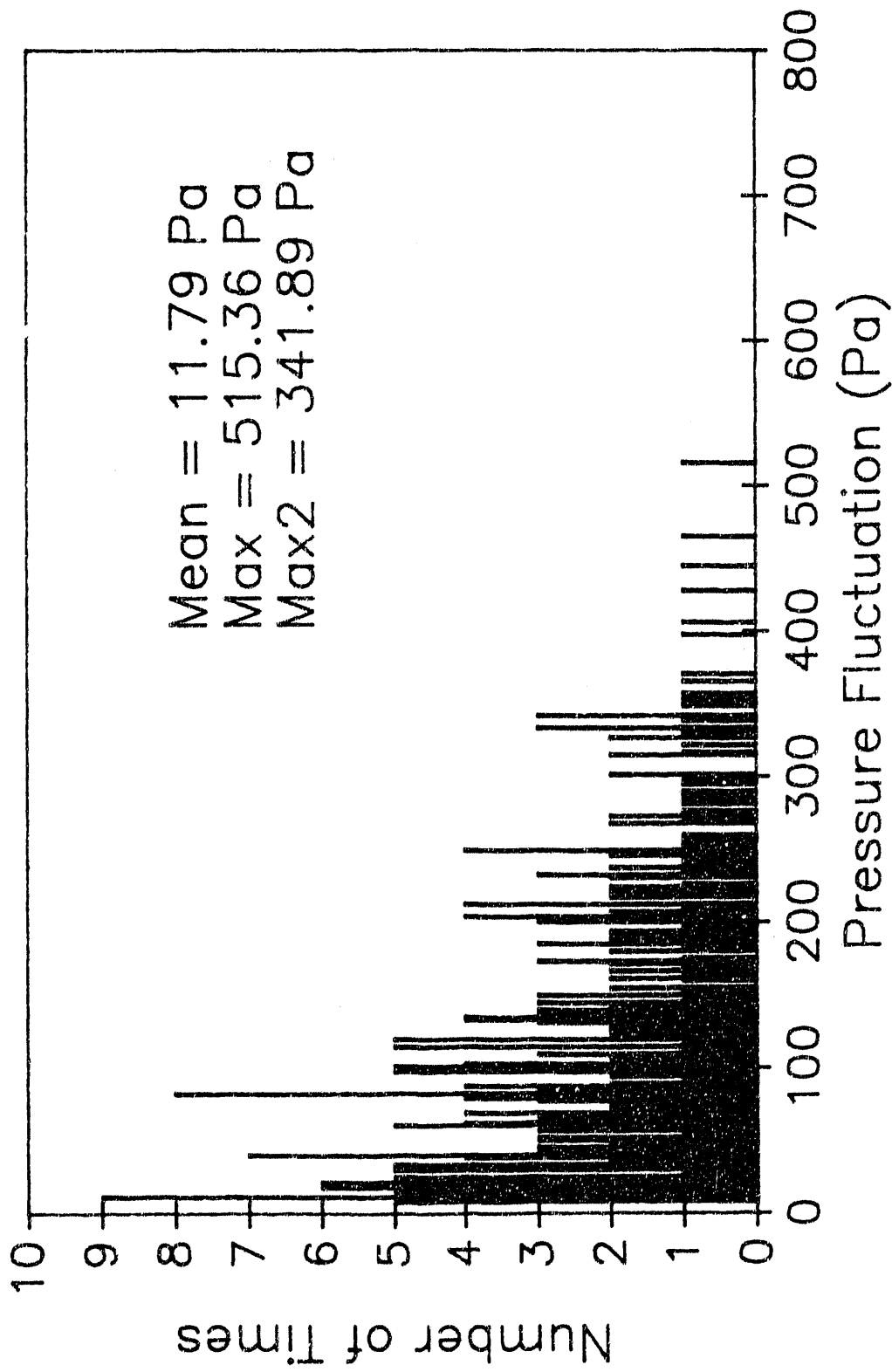


Figure 18. Intensity Distribution of Gas Phase Pressure Fluctuation
(Run 1, 55 seconds)

DISTRIBUTION OF PRESSURE FLUCTUATION
(The Second Run, 60 Seconds)

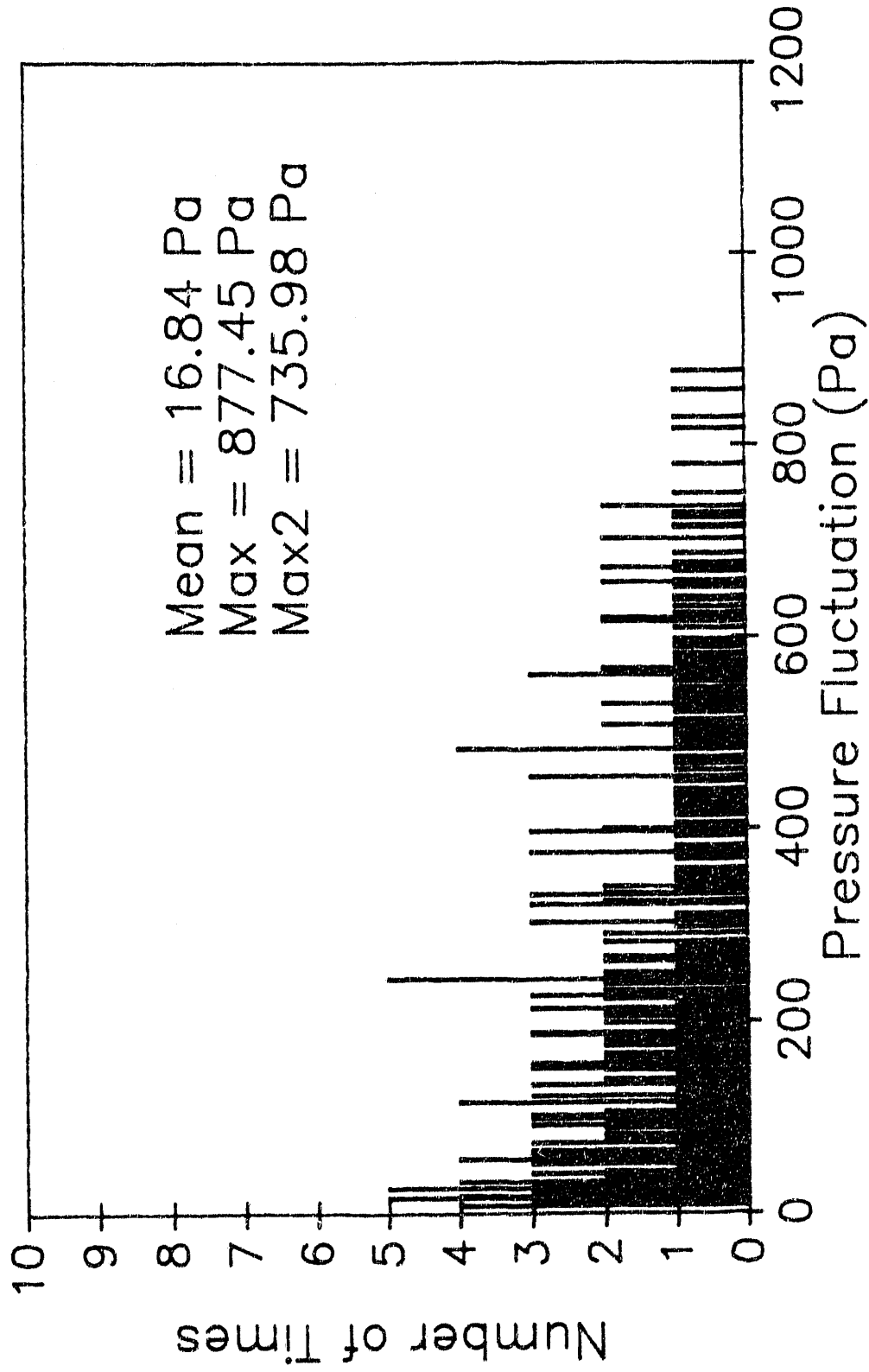


Figure 19. Intensity Distribution of Gas Phase Pressure Fluctuation
(Run 2, 60 seconds)

DISTRIBUTION OF PRESSURE FLUCTUATION
(The Third Run, 60 Seconds)

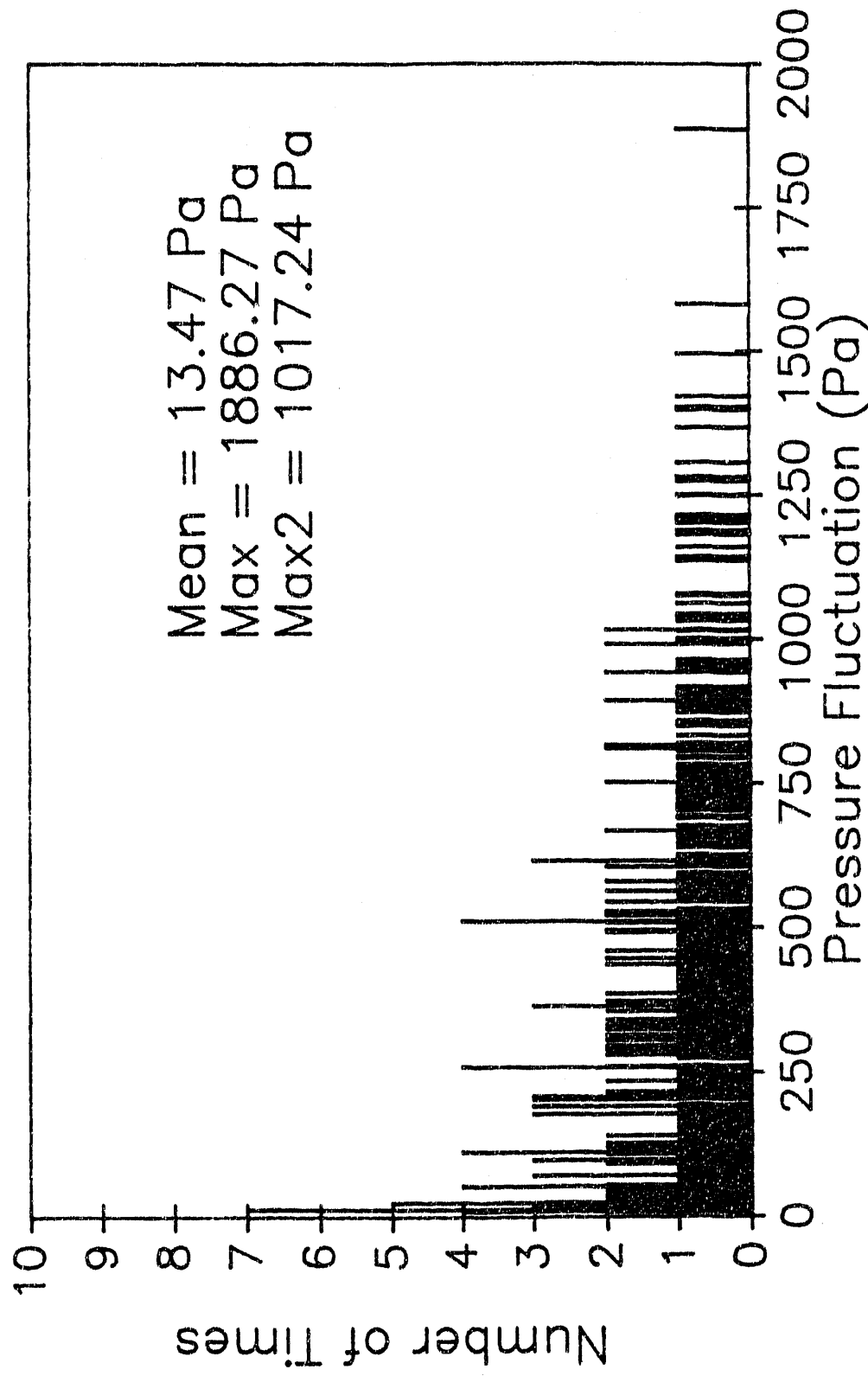


Figure 20. Intensity Distribution of Gas Phase Pressure Fluctuation
(Run 3, 60 seconds)

DISTRIBUTION OF PRESSURE FLUCTUATION
(The Fourth Run, 60 Seconds)

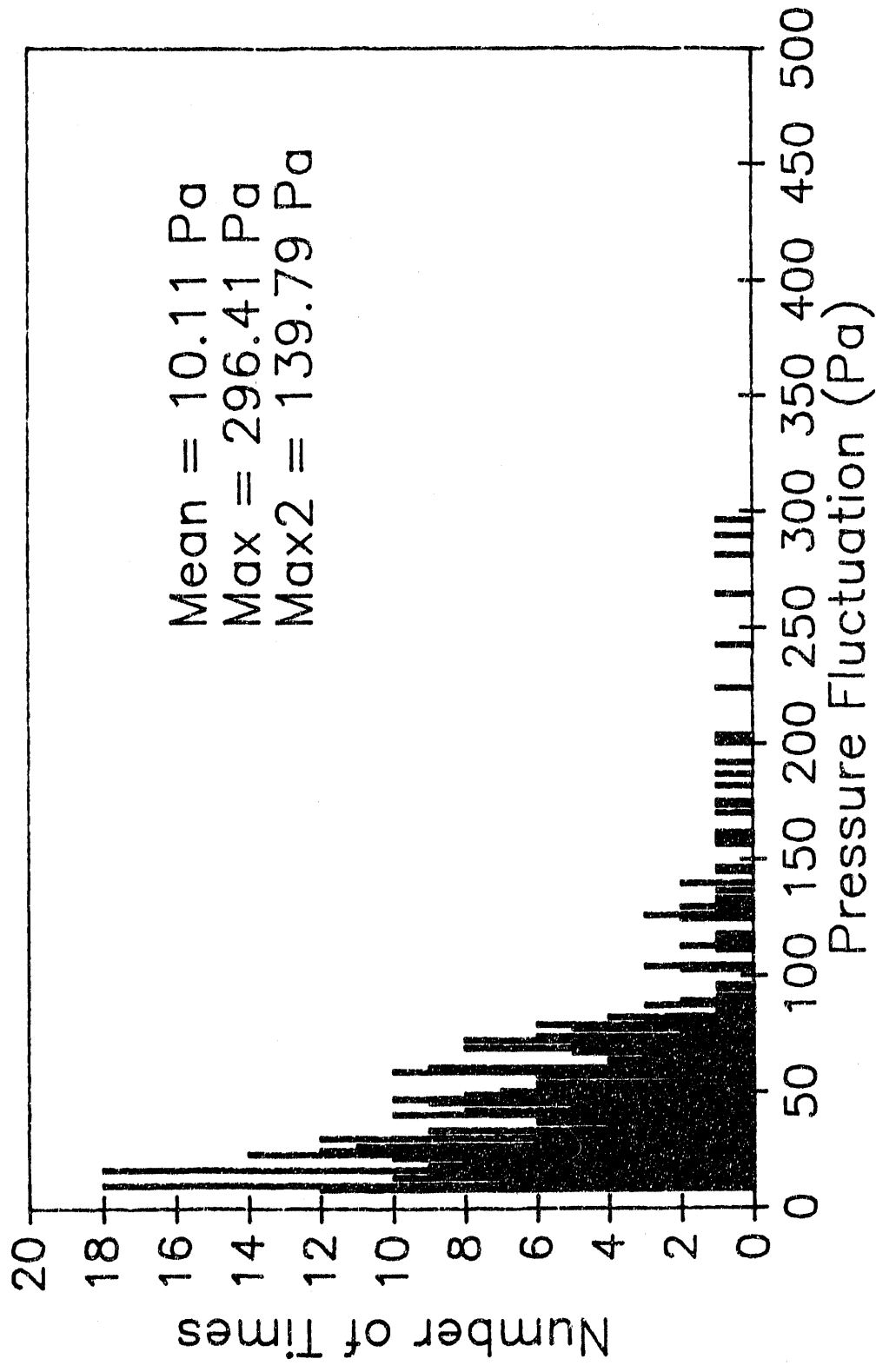


Figure 21. Intensity Distribution of Gas Phase Pressure Fluctuation
(Run 4, 60 seconds)

DISIBUTION OF PRESSURE FLUCTUATION
(The First Run, 15 SECONDS)

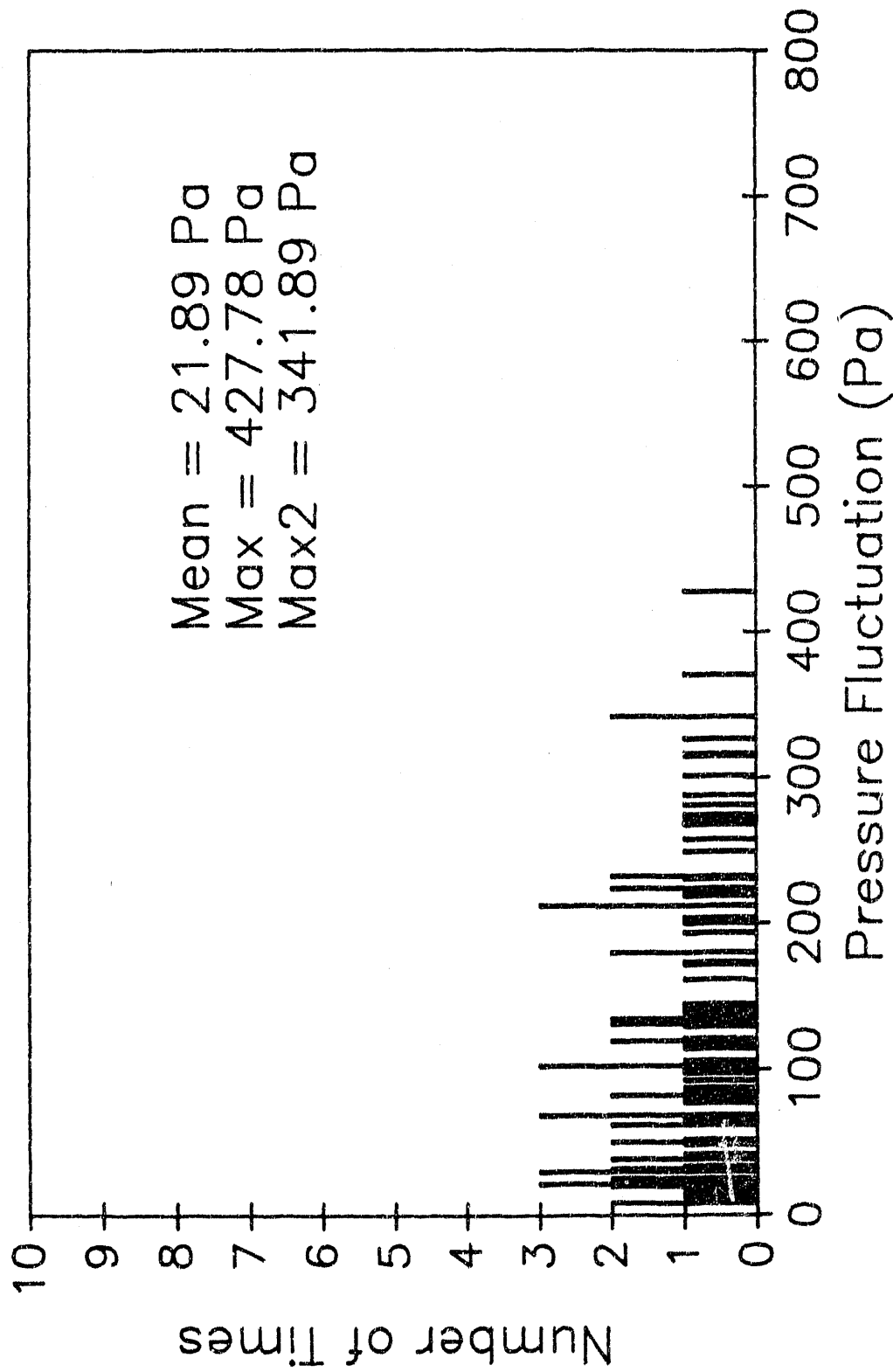


Figure 22. Intensity Distribution of Gas Phase Pressure Fluctuation
(Run 1, 15 seconds)

DISTRIBUTION OF PRESSURE FLUCTUATION
(The Second Run, 15 Seconds)

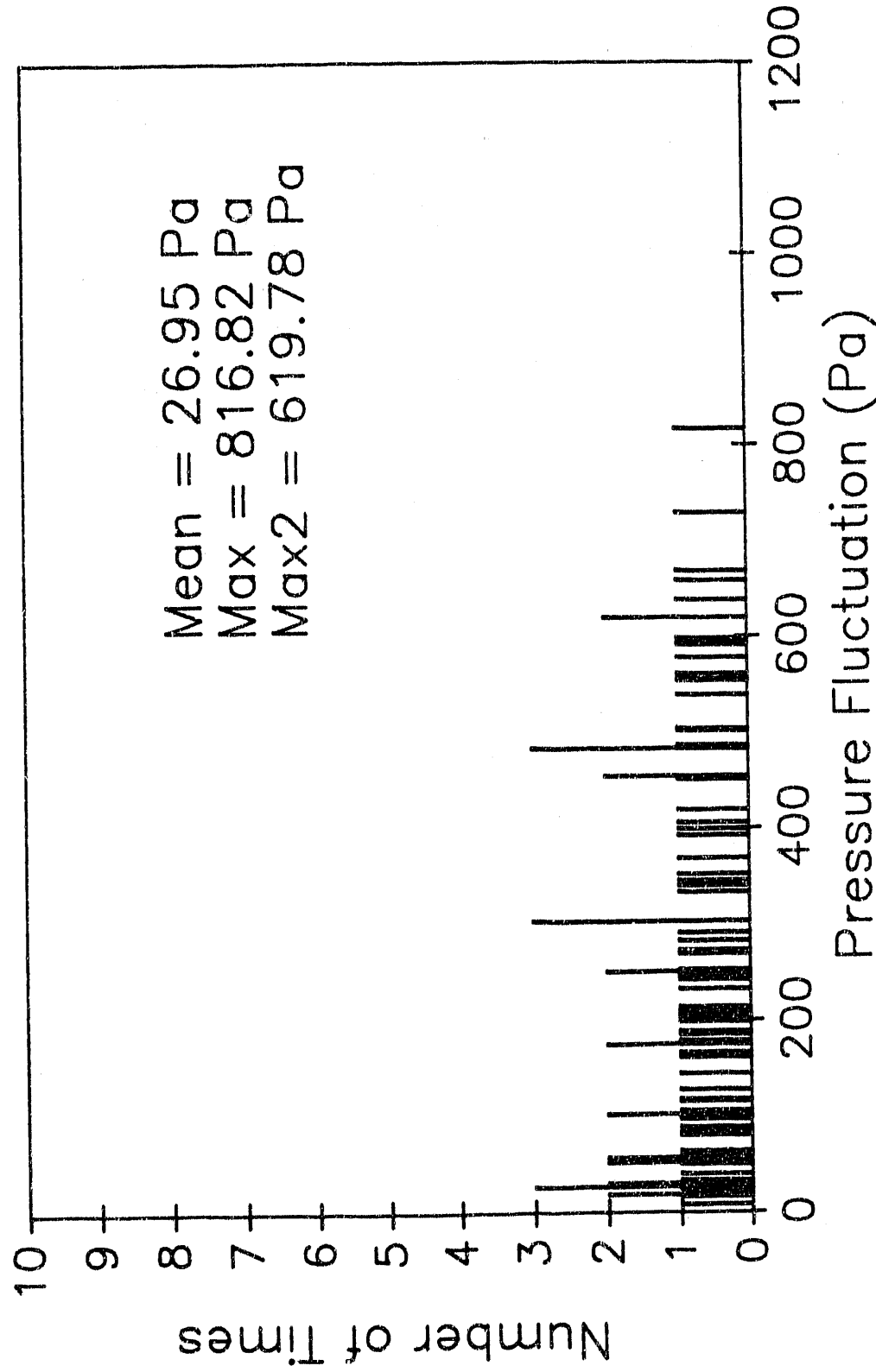


Figure 23. Intensity Distribution of Gas Phase Pressure Fluctuation
(Run 2, 15 seconds)

DISTRIBUTION OF PRESSURE FLUCTUATION
(The Third Run, 15 Second)

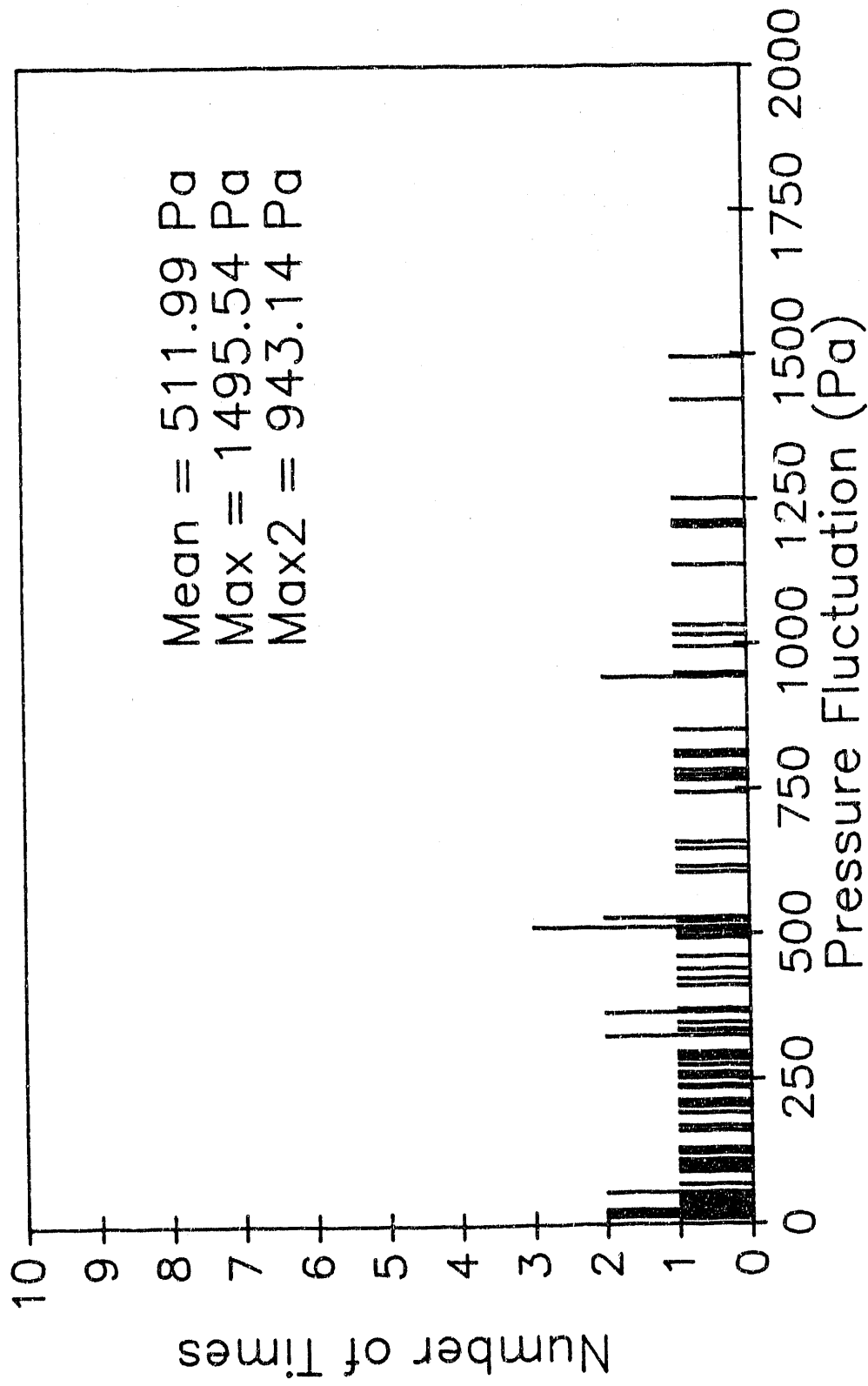


Figure 24. Intensity Distribution of Gas Phase Pressure Fluctuation
(Run 3, 15 seconds)

DISTRIBUTION OF PRESSURE FLUCTUATION
(The Fourth Run, 15 Seconds)

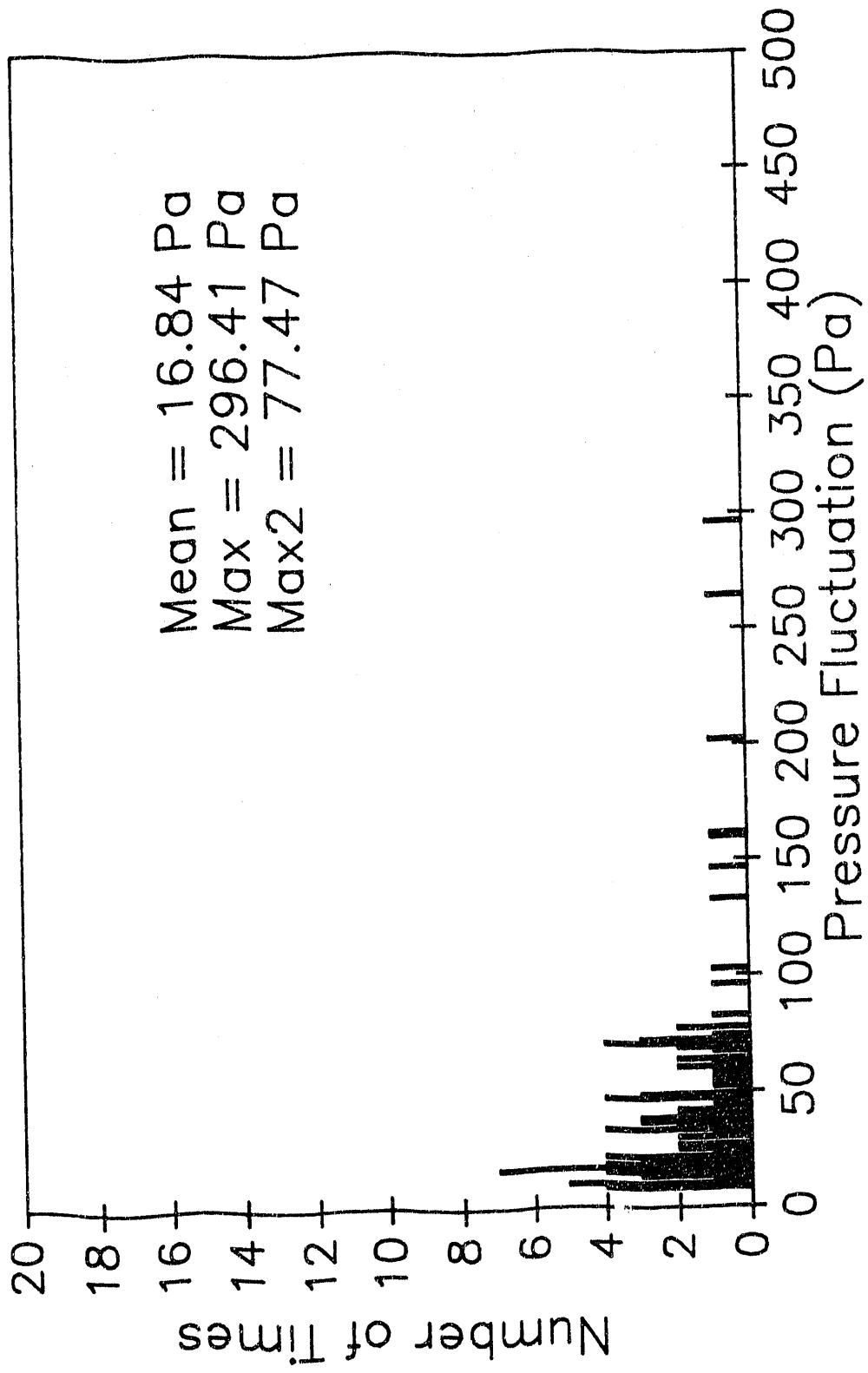


Figure 25. Intensity Distribution of Gas Phase Pressure Fluctuation
(Run 4, 15 seconds)

DISTRIBUTION OF PRESSURE FLUCTUATION
(The First Run, 30 Seconds)

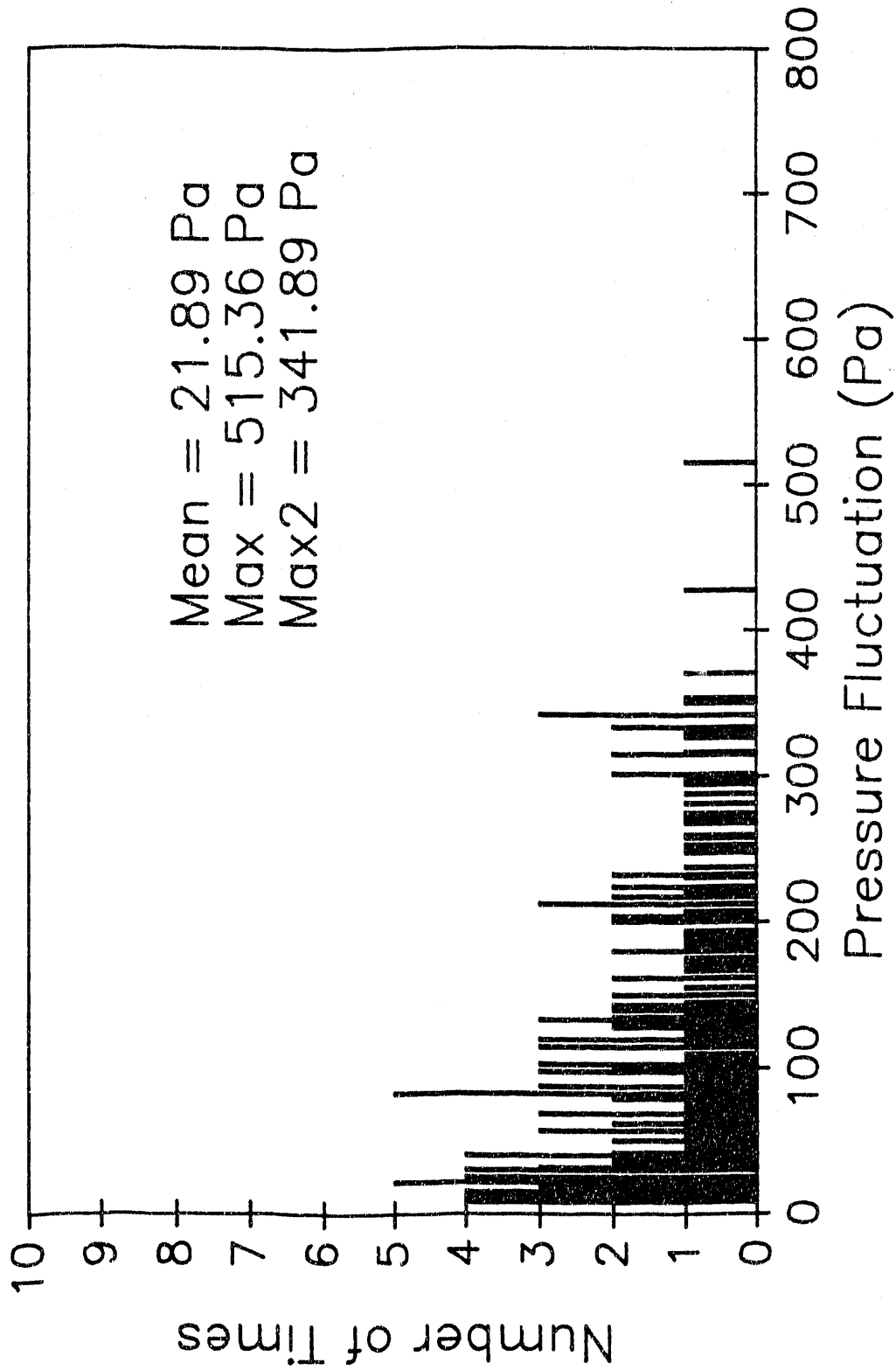


Figure 26. Intensity Distribution of Gas Phase Pressure Fluctuation
(Run 1, 30 seconds)

DISTRIBUTION OF PRESSURE FLUCTUATION
(The Second Run, 30 Seconds)

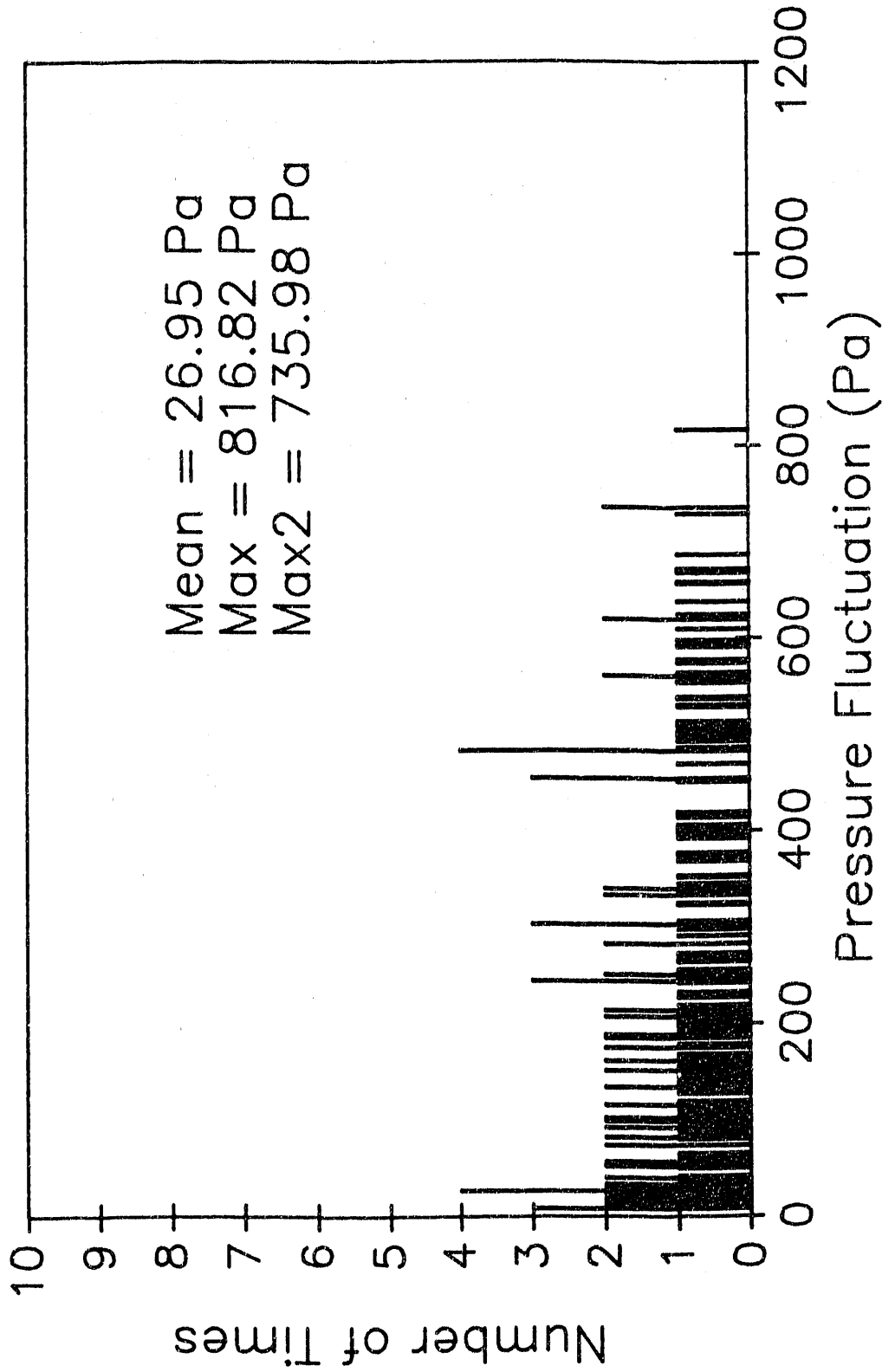


Figure 27. Intensity Distribution of Gas Phase Pressure Fluctuation
(Run 2, 30 seconds)

DISTRIBUTION OF PRESSURE FLUCTUATION
(The Third Run, 30 Seconds)

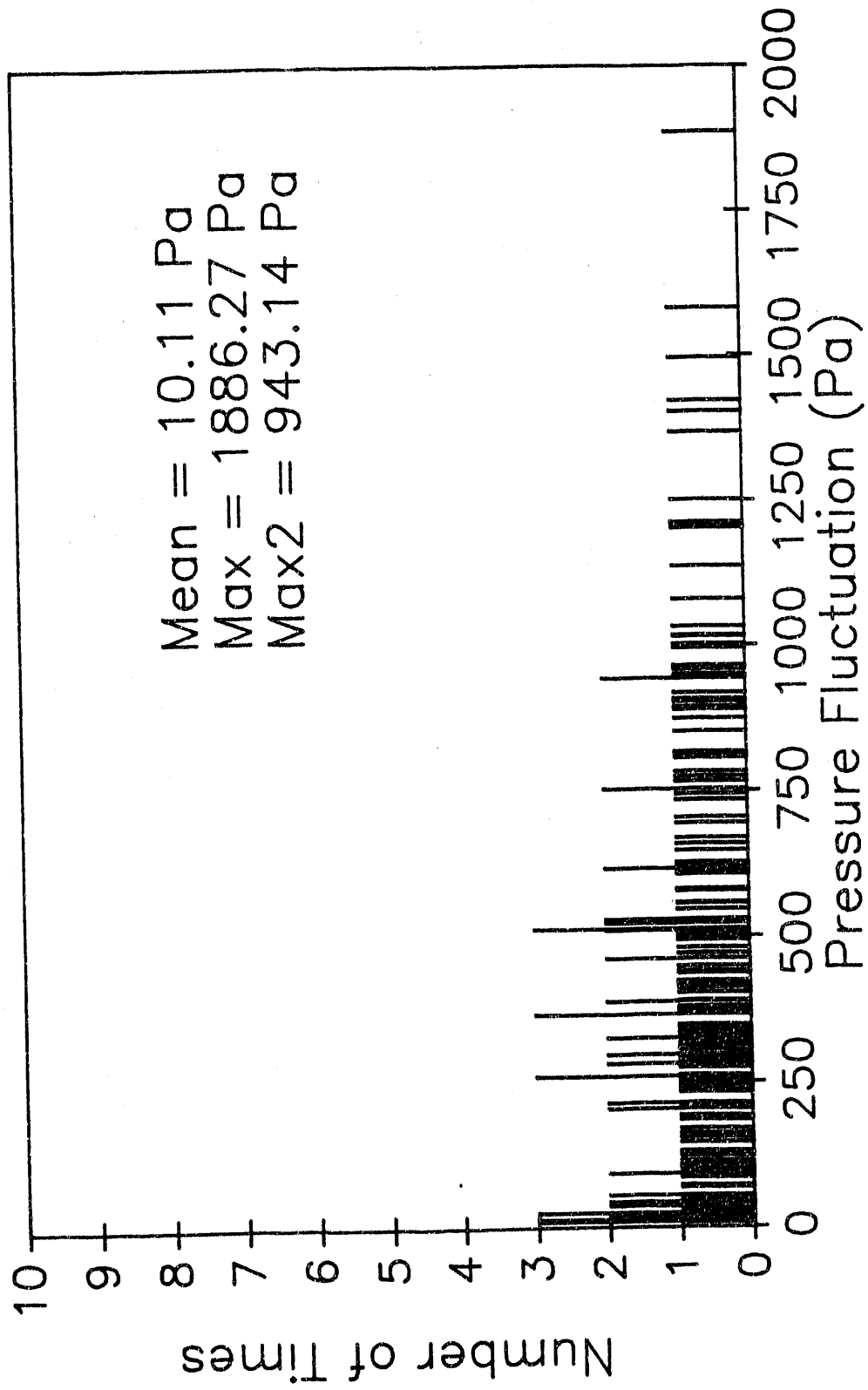


Figure 28. Intensity Distribution of Gas Phase Pressure Fluctuation
(Run 3, 30 seconds)

DISTRIBUTION OF PRESSURE FLUCTUATION
(The Fourth Run, 30 Seconds)

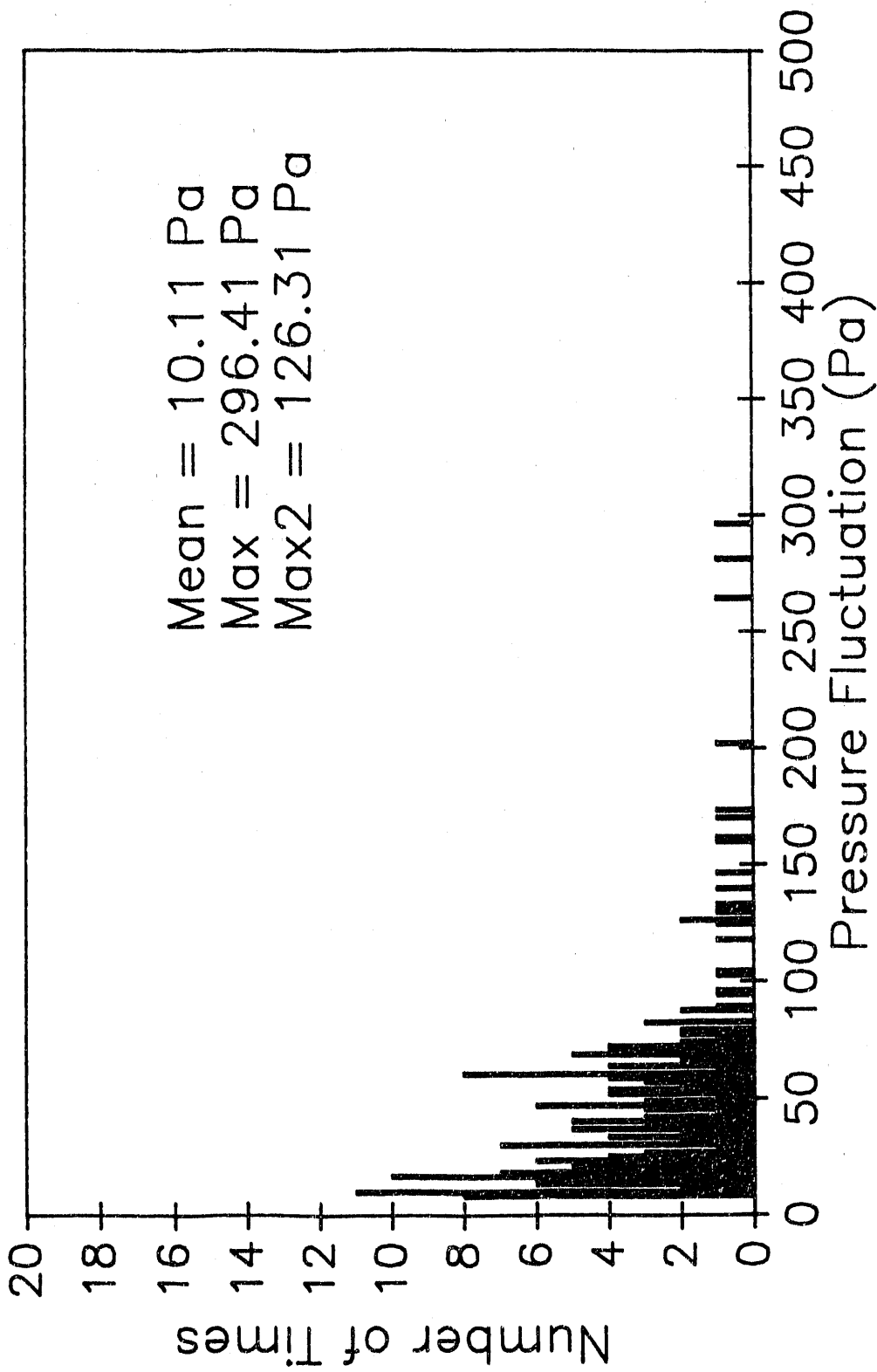


Figure 29. Intensity Distribution of Gas Phase Pressure Fluctuation
(Run 4, 30 seconds)

signals by observing and comparing the figures. However, several early attempts failed. The reason for this is that only average voidage data were considered. In latter trials we used local voidage signals, and attempted to develop a most appropriate numerical characterization approach to quantitatively express the correspondency. Results show that bubble image can well be correlated to the transient force signal of solid particles.

Local data obtained from METC's capacitance method are expressed by levels and cells. At each level, the horizontal section of the bed is divided into 193 cells. Figure 30 shows the pixel definitions. The transient force signals in terms of pressure fluctuation were measured at the center and near level 3. Therefore, the local voidage of cell 1 (cell A in Figure 30) and of cell 1 through 33 (cell A, and 1 through 32 in Figure 30) are better candidates than the averaged voidage for correlation analysis. Figure 31 through 46 show the averaged voidage in level 1, 2, 3 and 4 for four experiments. Figure 47 through 62 show the local voidage of cell 1 (cell A in Figure 30) at four levels for four experiments. Figure 63 through 78 show the local voidage of cell 1 through 33 (cell A, and 1 through 32 in Figure 30) at four levels for four experiments. Analysis shows that averaged voidage of cell 1 through 33 (cell A, and 1 through 32 in Figure 30) has close correlation with the gas phase pressure fluctuation.

The correlation study was based on the second experiment, when $U_0 = 0.259$. Local voidage data were processed to obtain the averaged voidage of cell 1 through 33. Pressure data were also processed to match time interval with METC's voidage data. From the synchronized data table, the voidage peaks were identified and corresponding pressure fluctuations were also recorded. Figure 79 shows that there is a reasonable match between voidage and pressure fluctuation.

Let V represents the voidage when it reaches the peak point, and $\Delta\Delta P$ represents the corresponding pressure fluctuation, the correlation can be expressed as:

$$\Delta\Delta P = e^{6.4366 V - 5.8490}$$

where e is the base of the natural logarithm function. The correlation coefficient is 0.79.

It is observed that at lower superficial gas velocity (U_0) the local voidage peak and pressure fluctuation are not well matched. The reason for this is that when U_0 is low, small bubbles are generated and the number of bubbles increases, one-point pressure

Pixel Definitions

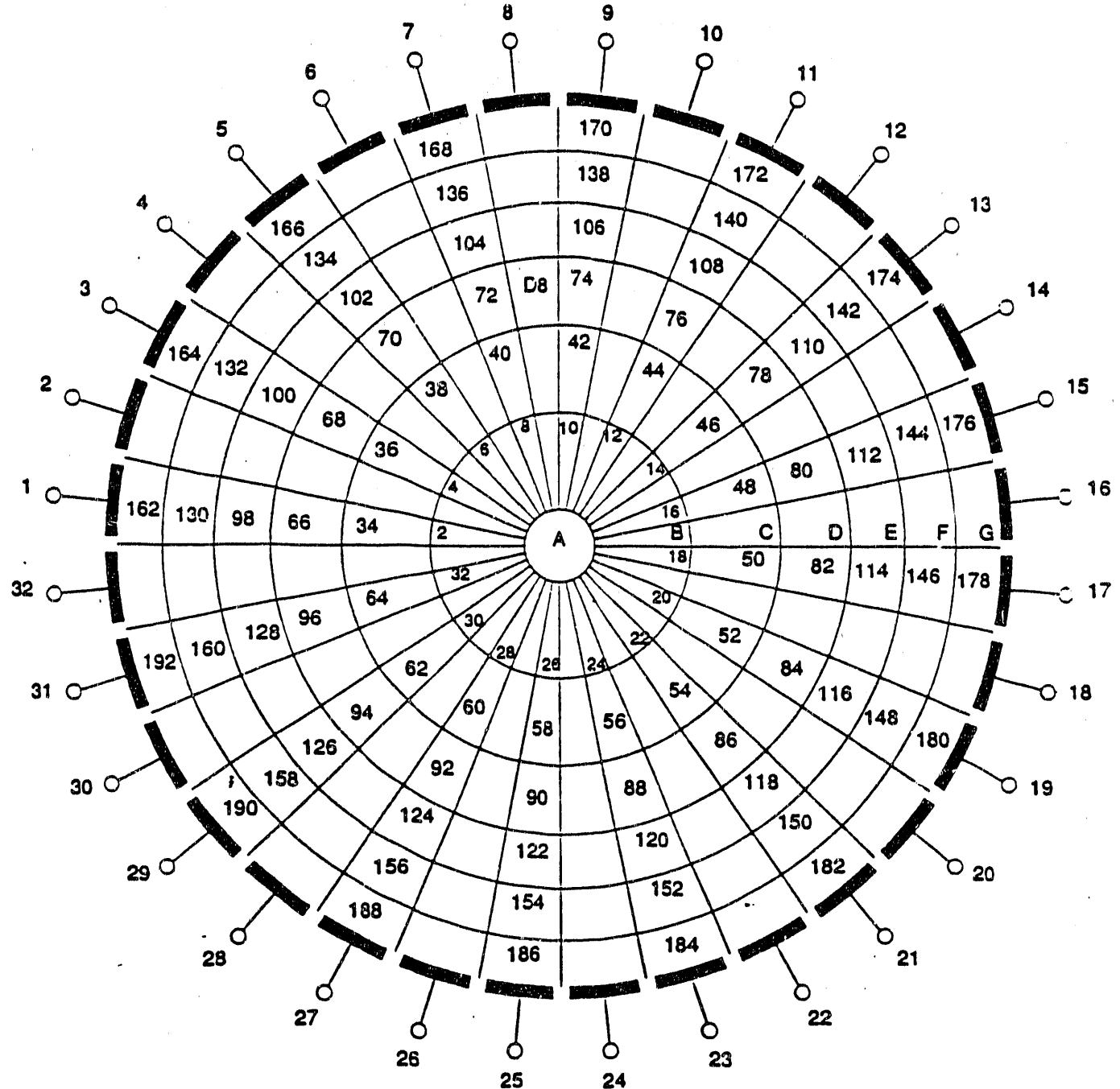


Figure 30. Pixel Definitions

VOIDAGE VERSUS TIME

$U_0 = .259 \text{ m/s}$

LEVEL 1

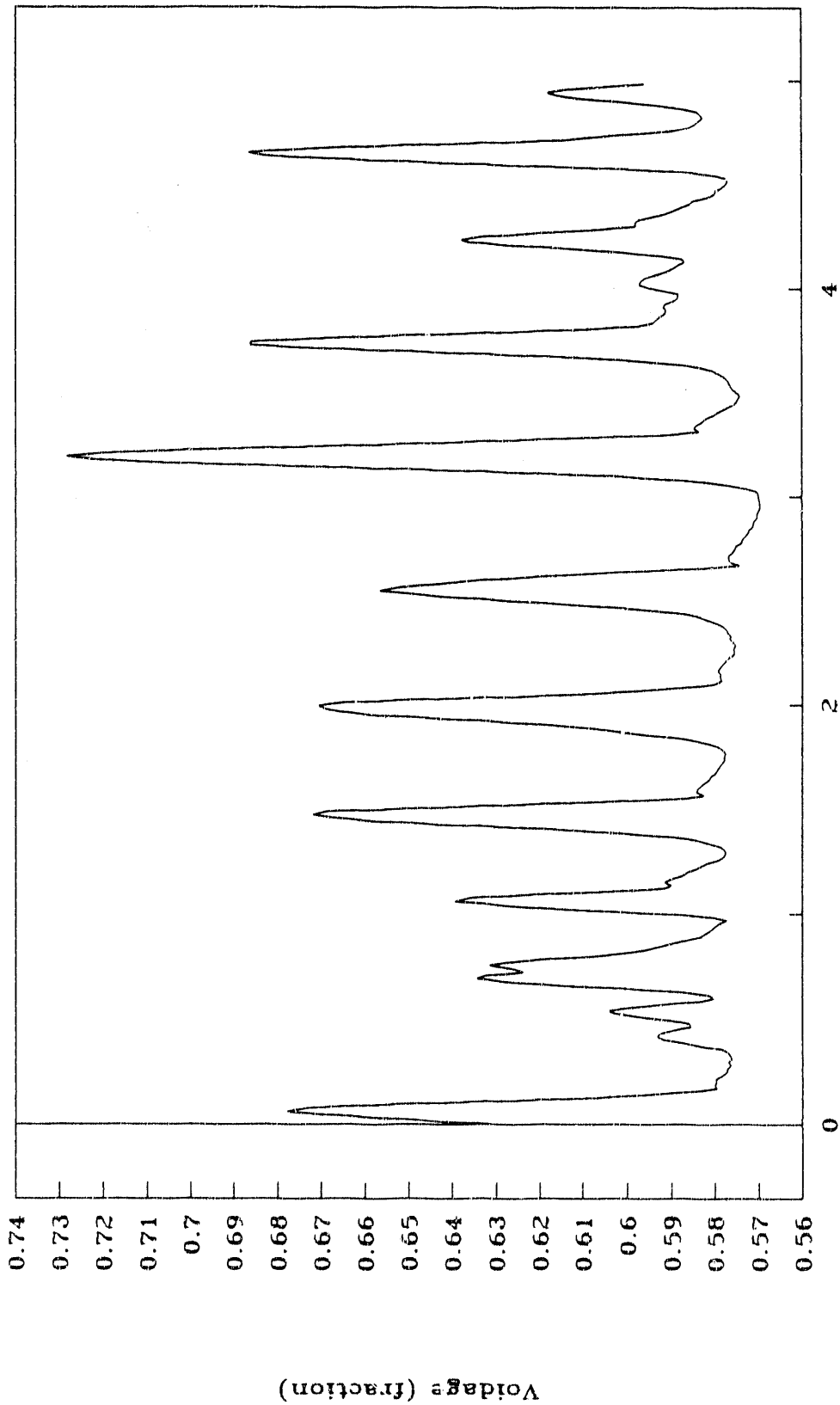


Figure 31. Average Voidage versus Time ($U_0=.259$, level 1)
Time (second)

VOIDAGE VERSUS TIME

$U_0 = .259 \text{ m/s}$ LEVEL 2

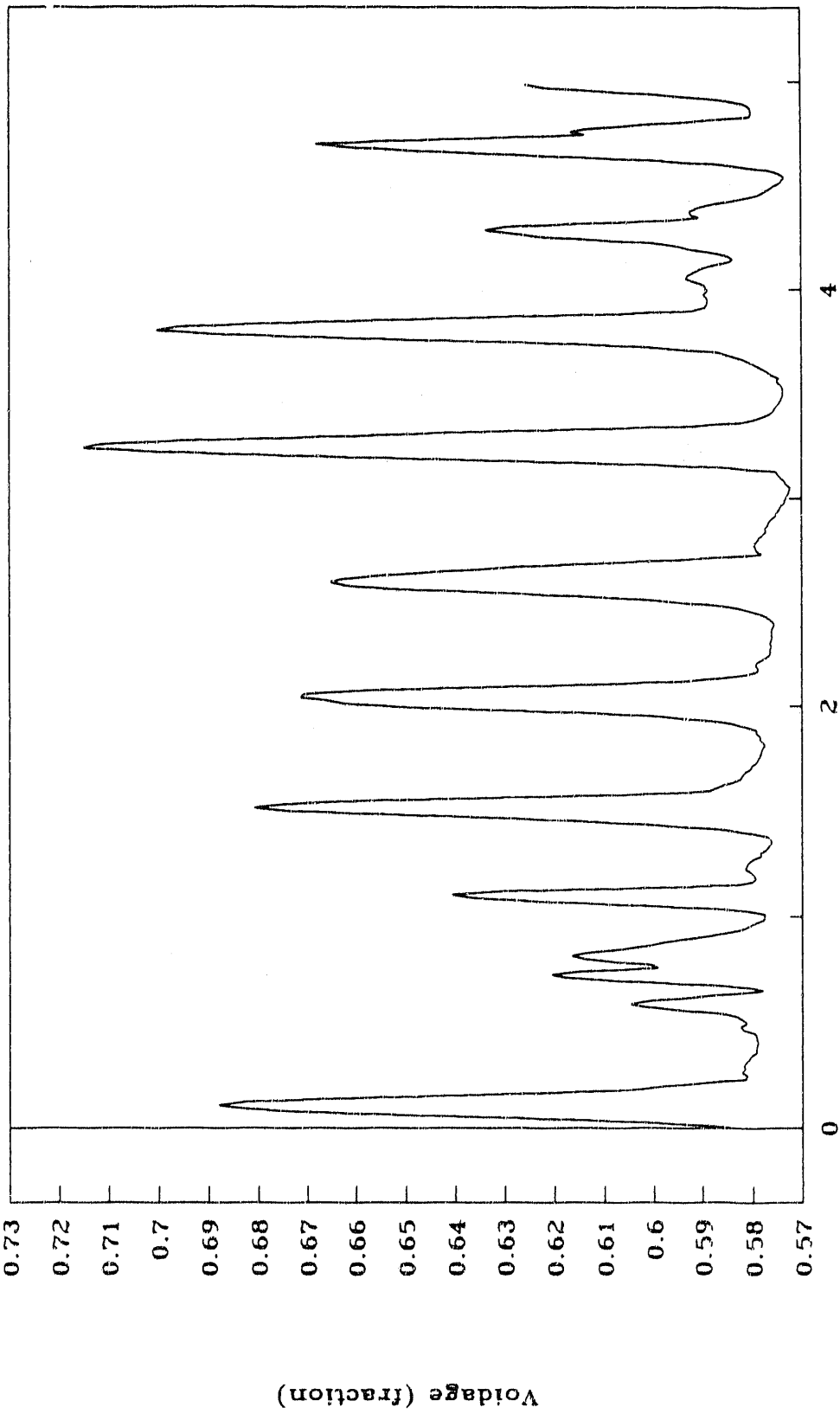


Figure 32. Average voidage versus Time ($U_0 = .259$, level 2)

VOIDAGE VERSUS TIME

$U_0 = .259 \text{ m/s}$ LEVEL 3

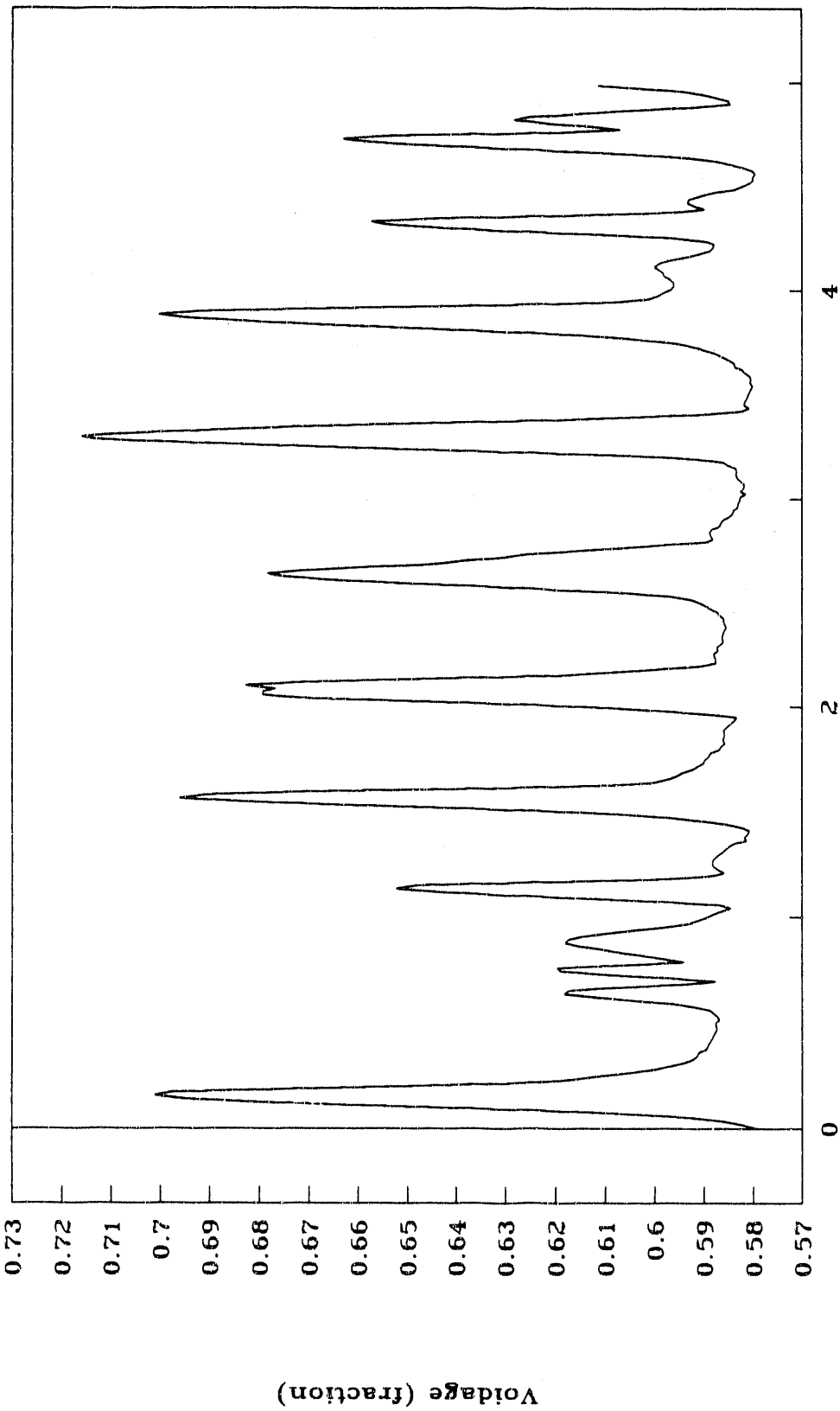


Figure 33. Average voidage versus Time ($U_0 = .259$, level 3)

VOIDAGE VERSUS TIME

$U_0 = .259 \text{ m/s}$ LEVEL 4

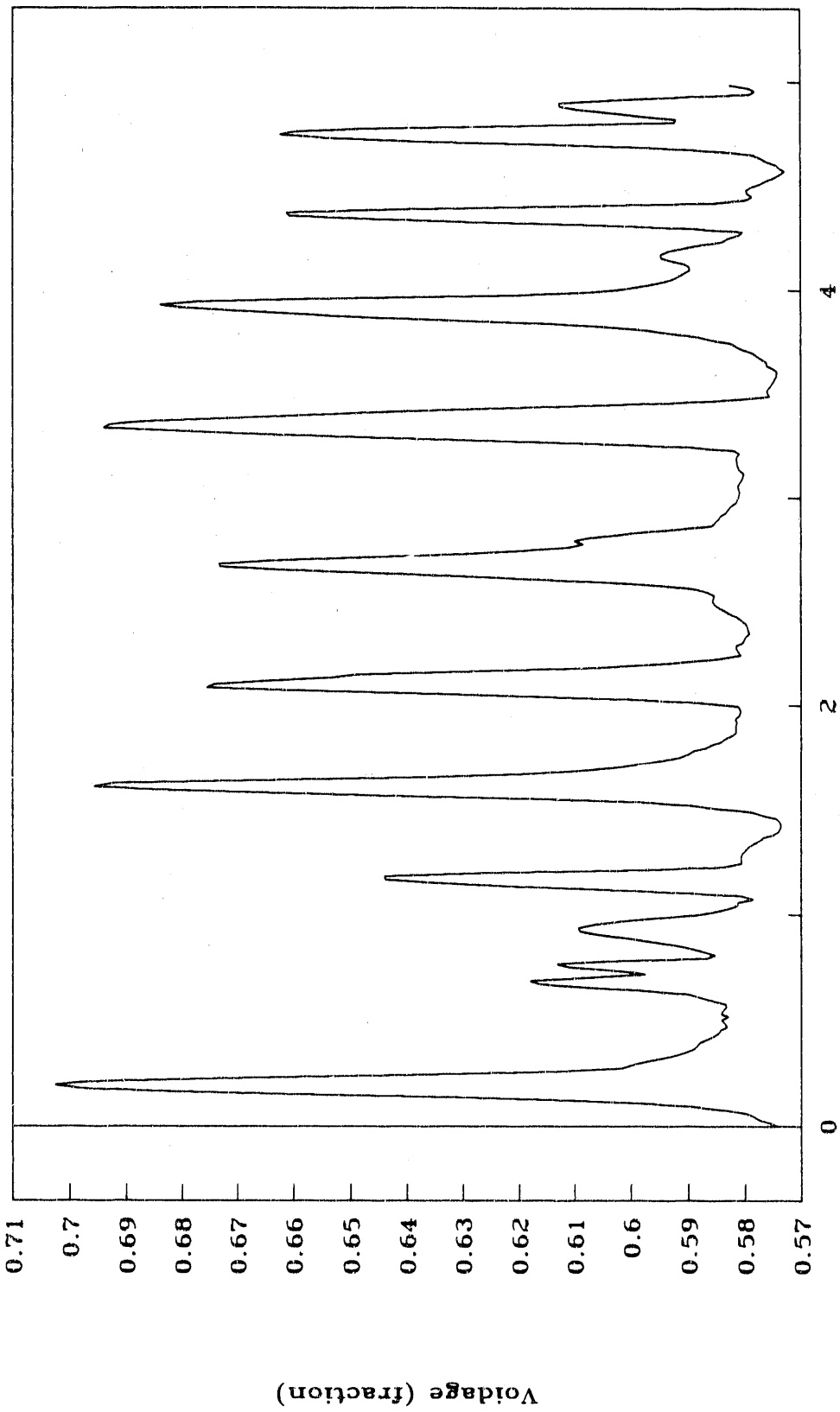


Figure 34. Average Voidage versus Time ($U_0 = .259$, level 4)

VOIDAGE VERSUS TIME

$U_0 = .316 \text{ m/s}$ LEVEL 1

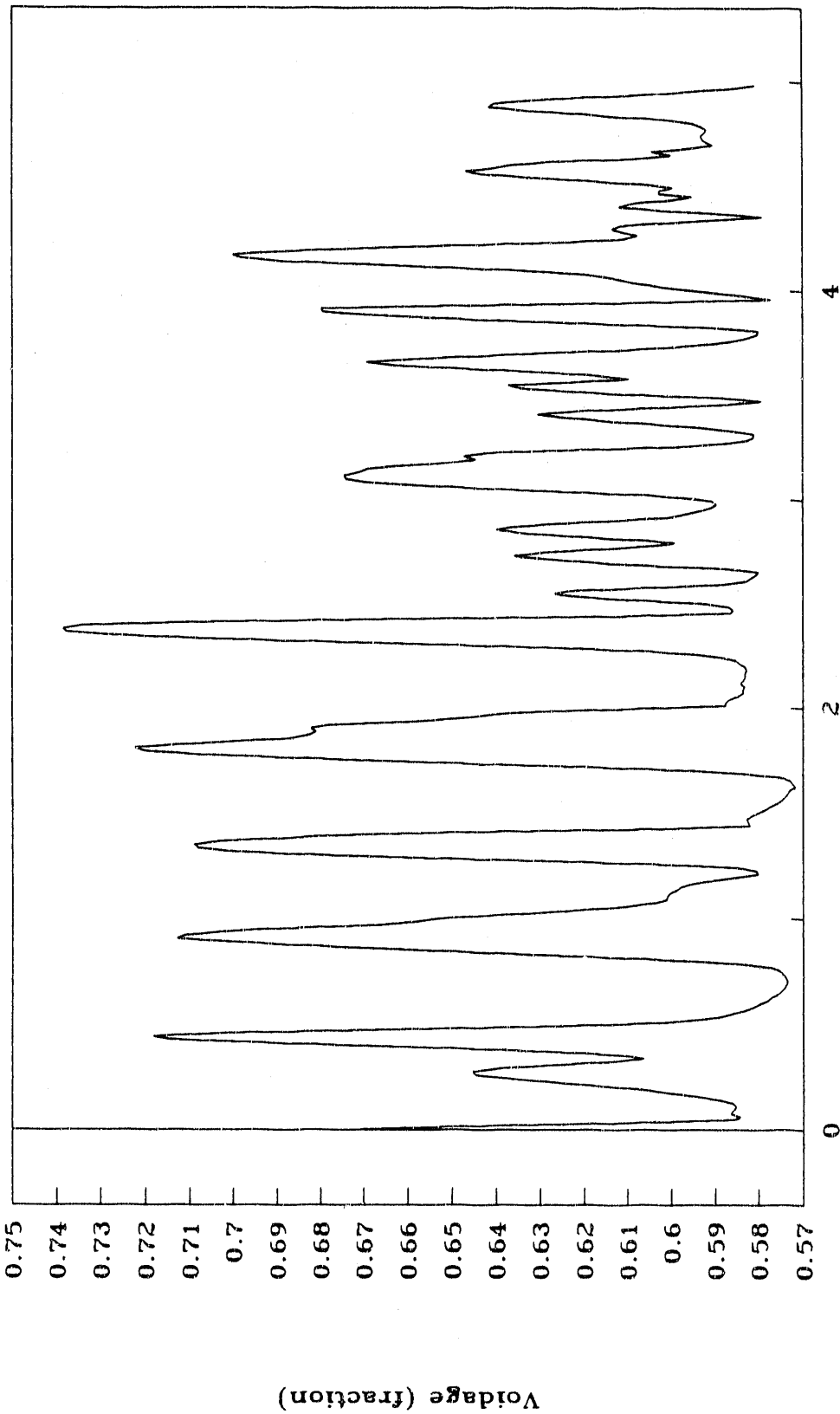


Figure 35. Average Voidage versus Time ($U_0 = .316$, level 1)

VOIDAGE VERSUS TIME

$U_0 = .316 \text{ m/s}$ LEVEL 2

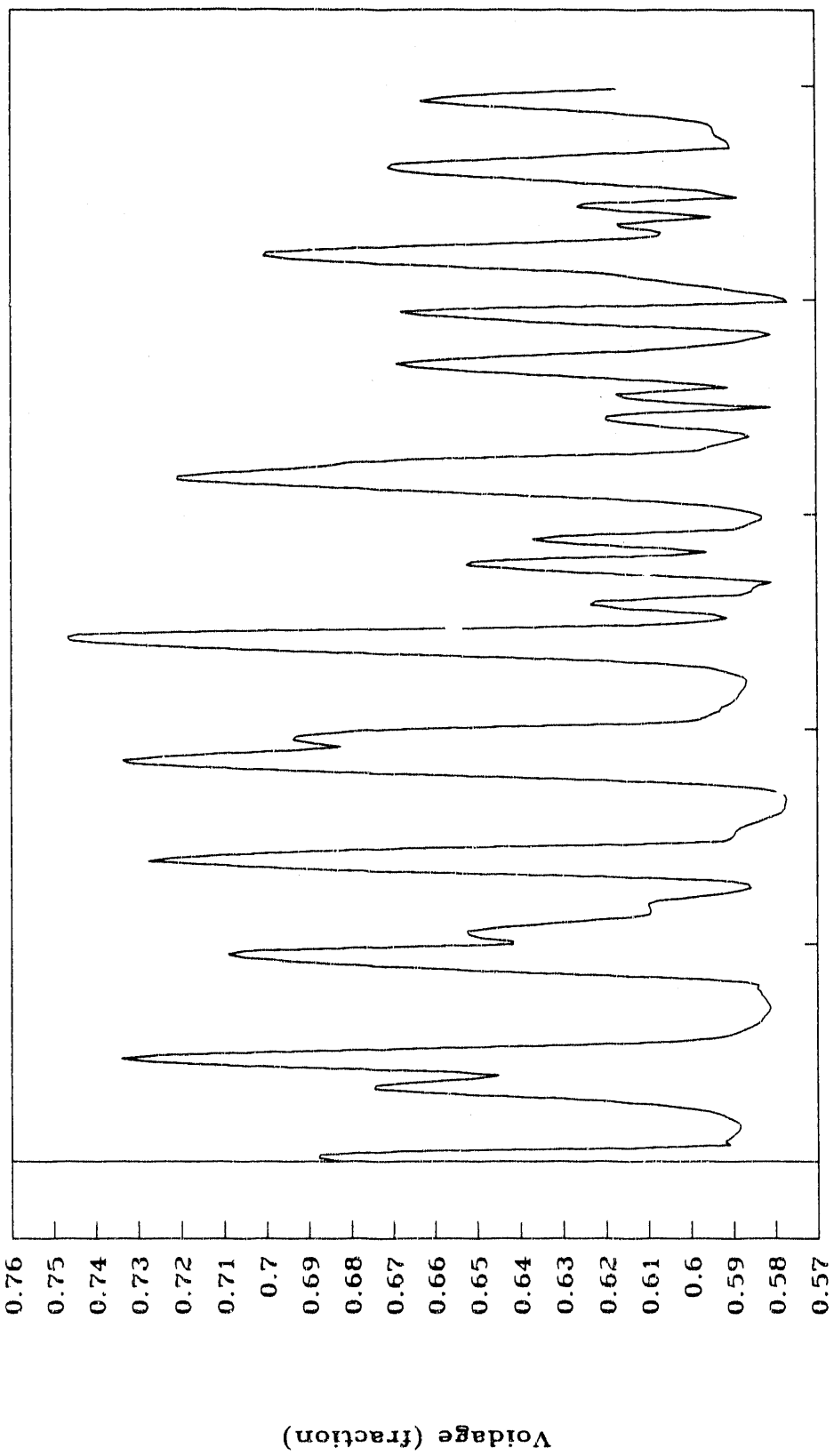


Figure 36. Average voidage versus Time ($U_0=.316$, level 2)

VOIDAGE VERSUS TIME

$U_0 = .316 \text{ m/s}$ LEVEL 3

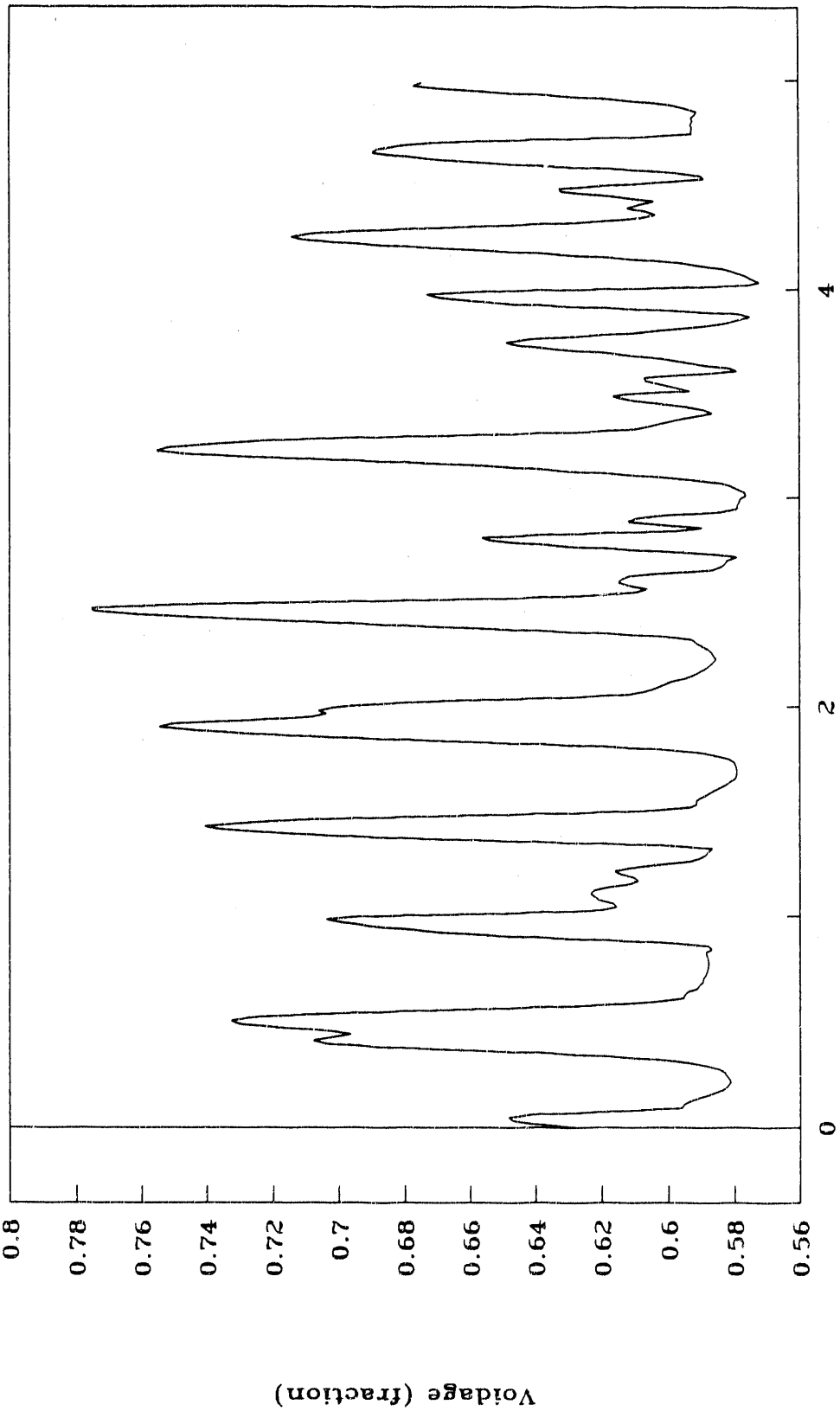


Figure 37. Average Voidage versus Time ($U_0 = .316$, level 3)

VOIDAGE VERSUS TIME

$U_0 = .3116 \text{ m/s}$

LEVEL 4

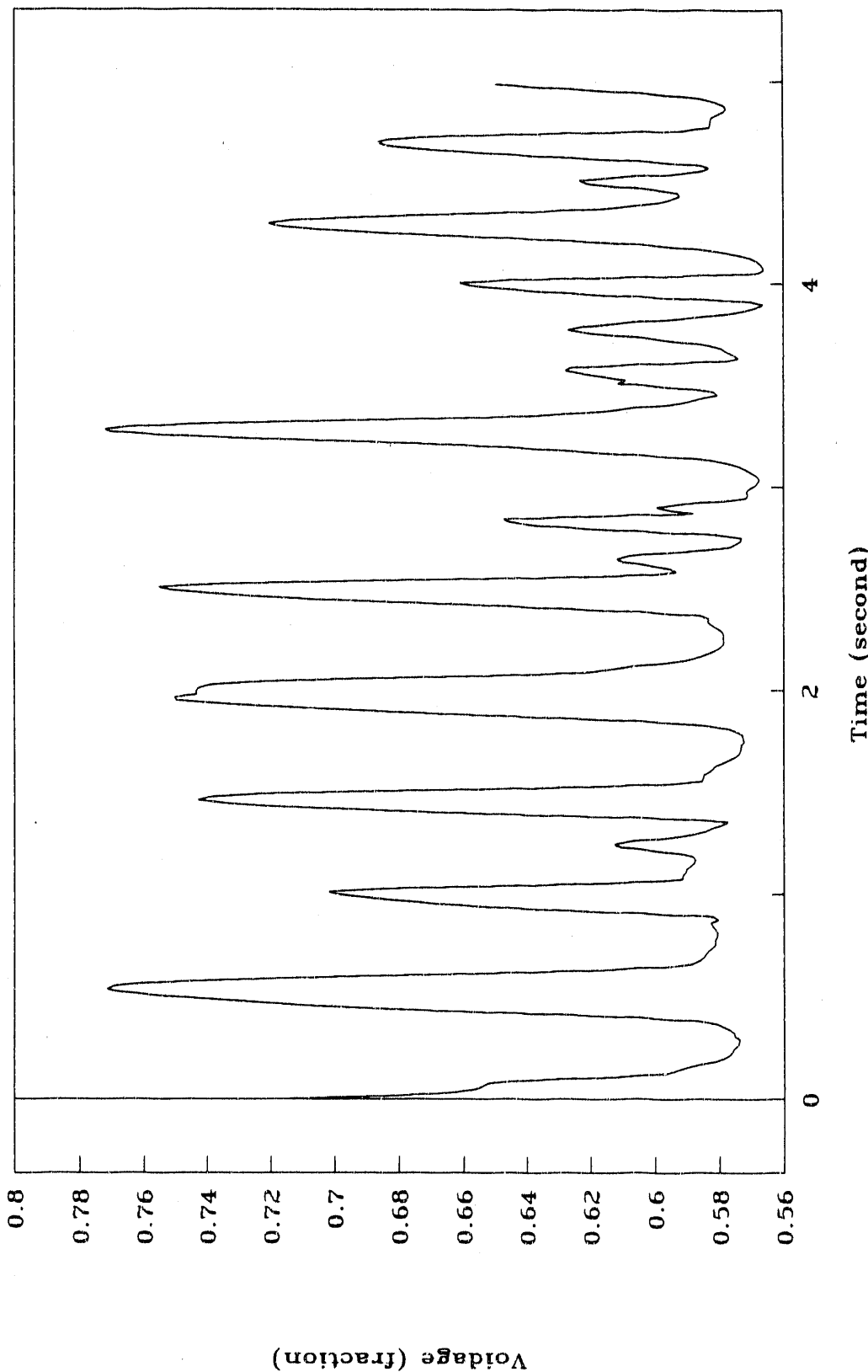


Figure 38. Average Voidage versus Time ($U_0 = .3116$, level 4)

VOIDAGE VERSUS TIME

$U_0 = .361 \text{ m/s}$

LEVEL 1

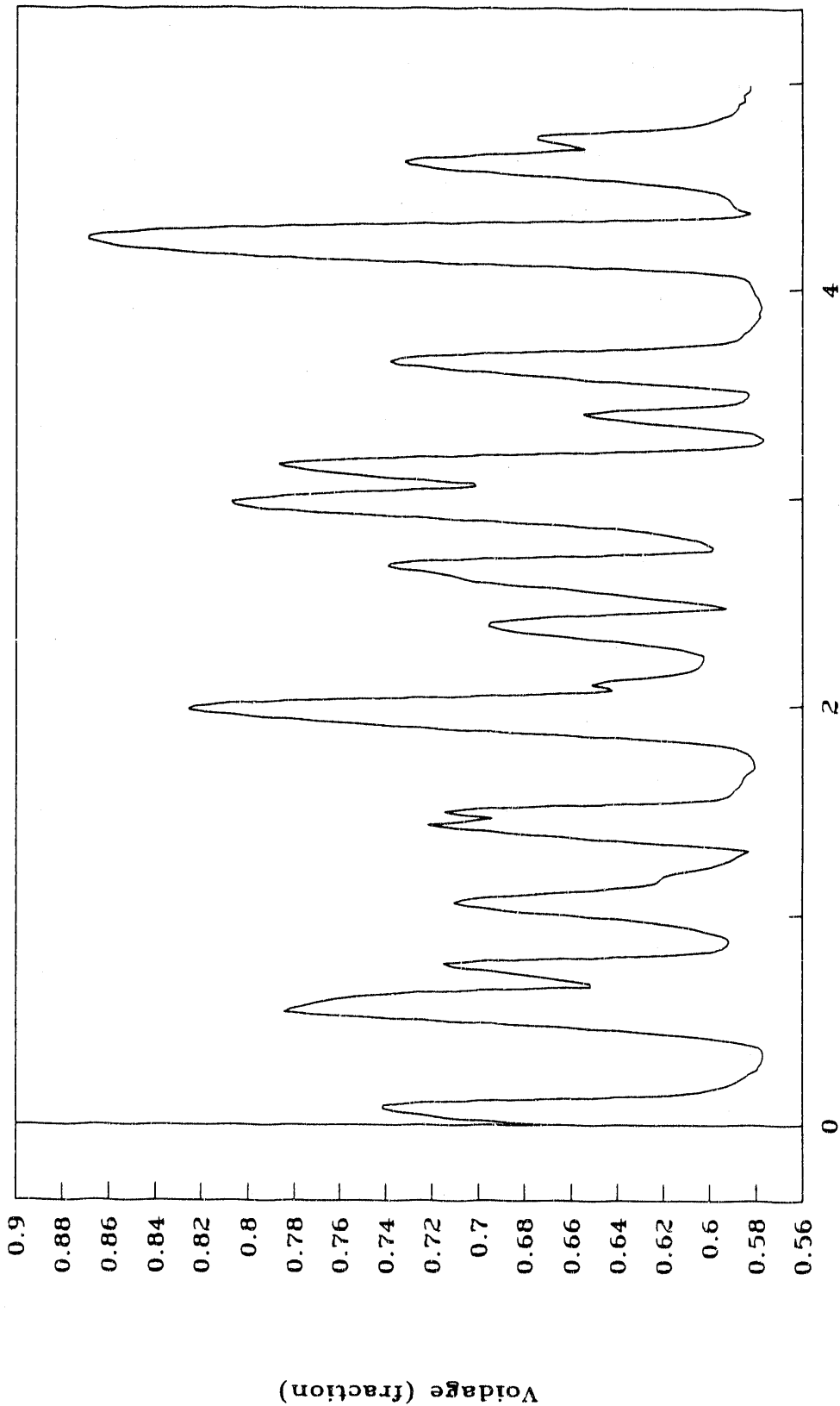


Figure 39. Average Voidage versus Time ($U_0 = .361$, level 1)

VOIDAGE VERSUS TIME

$U_0 = .361 \text{ m/s}$

LEVEL 2

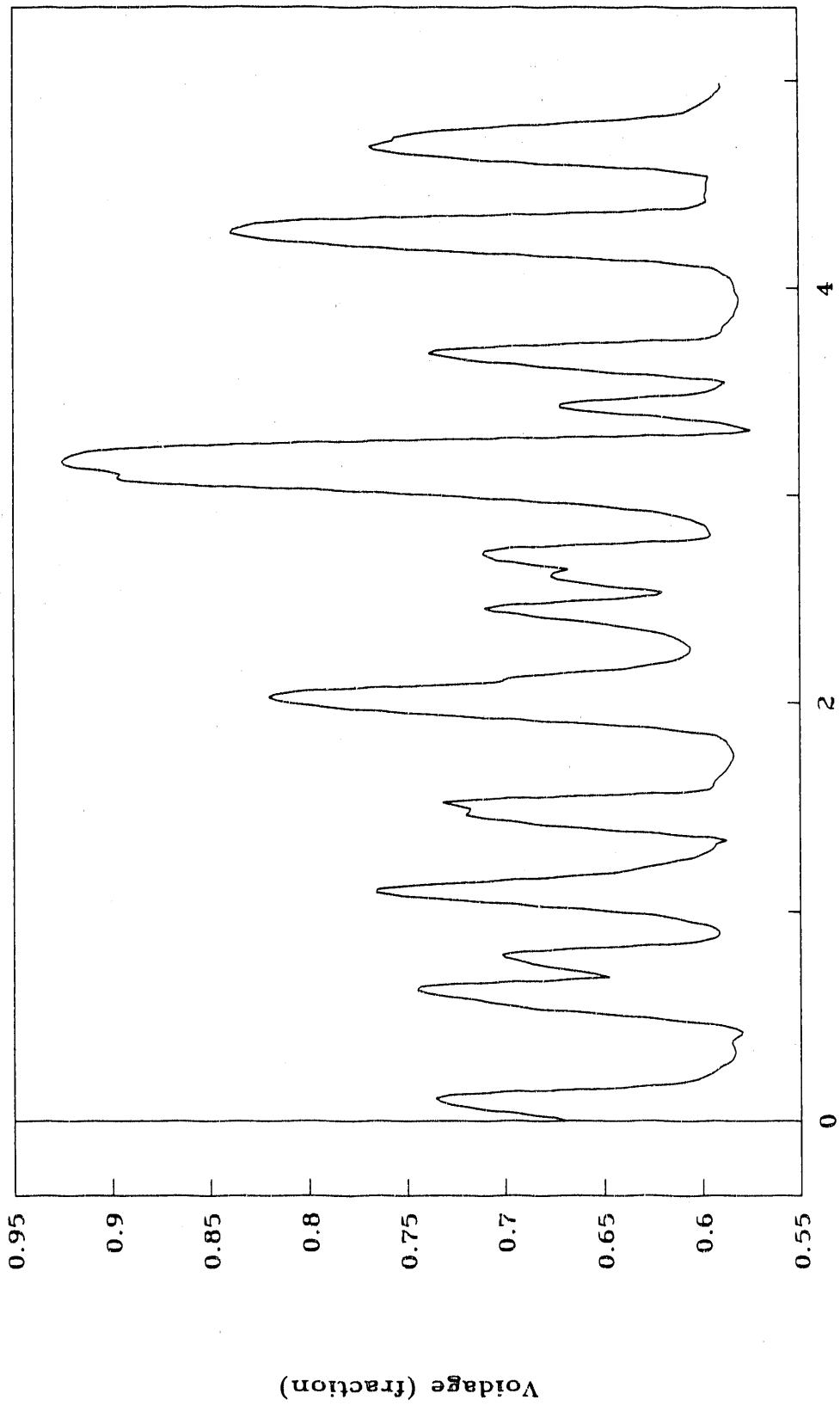


Figure 40. Average Voidage versus Time ($U_0 = .361$, level 2)

VOIDAGE VERSUS TIME

$U_0 = .361 \text{ m/s}$

LEVEL 3

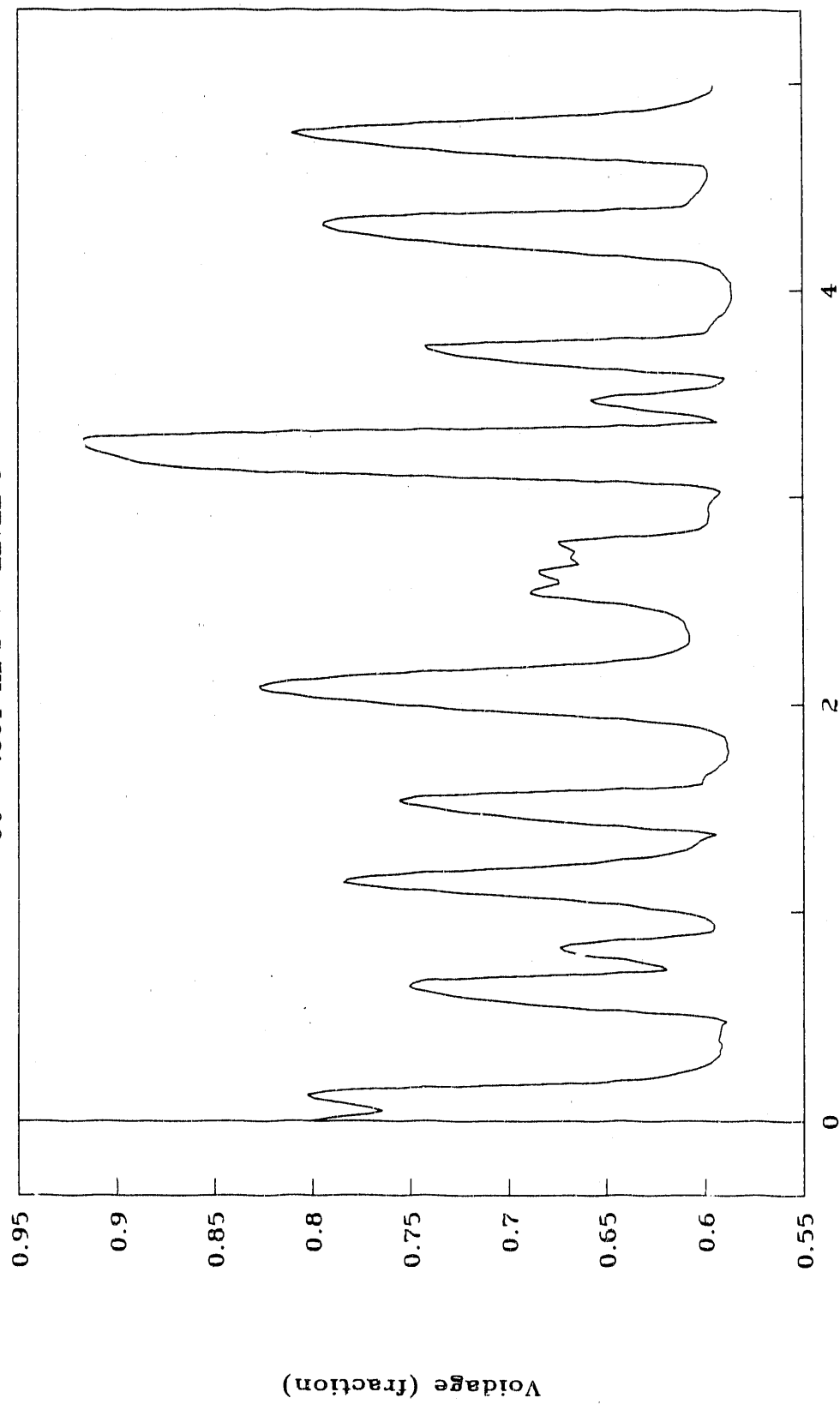


Figure 41. Average Voidage versus Time ($U_0 = .361$, level 3)

VOIDAGE VERSUS TIME

$U_0 = .361 \text{ m/s}$

LEVEL 4

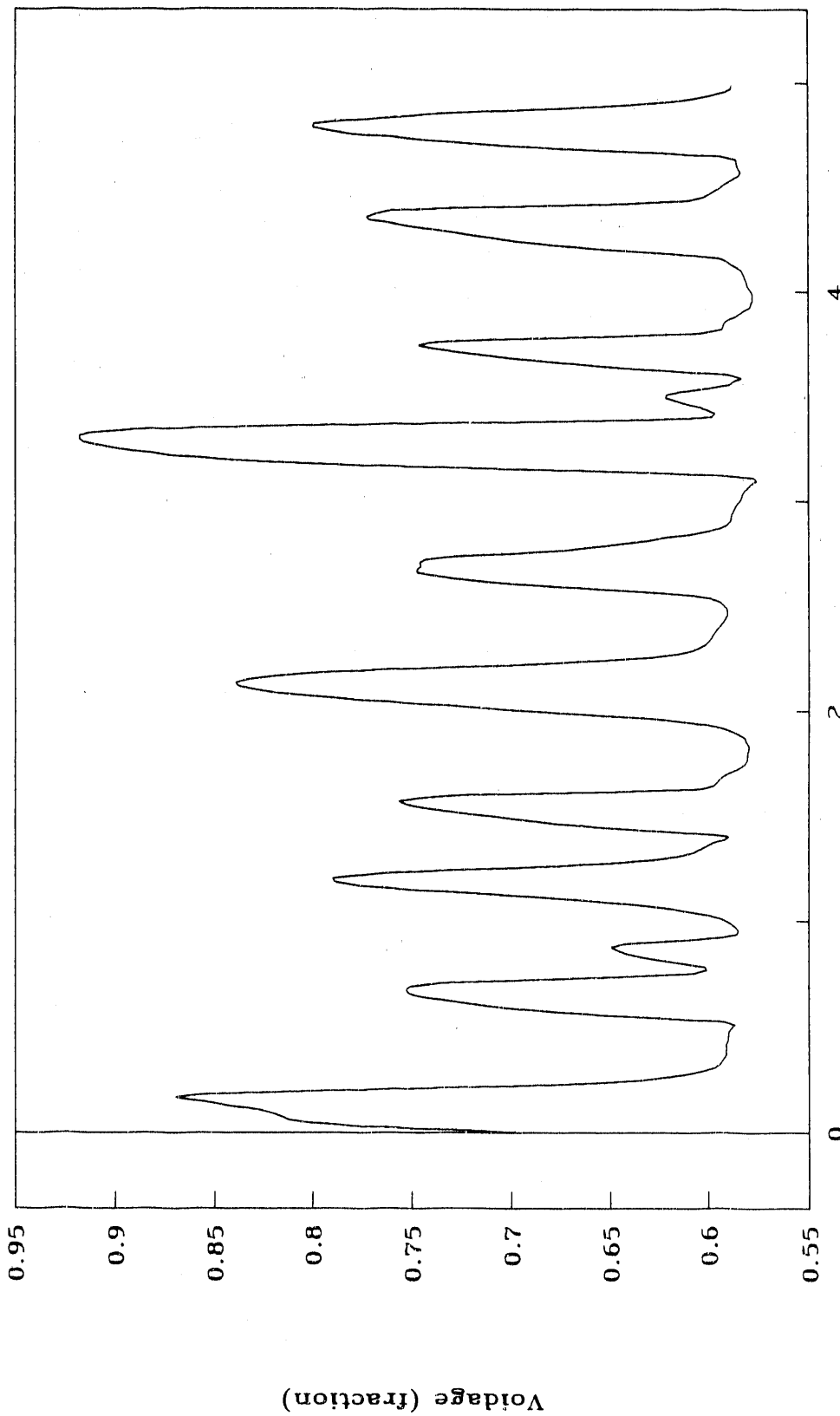


Figure 42. Average Voidage versus Time ($U_0=.361$, level 4)

VOIDAGE VERSUS TIME

$U_0 = .220 \text{ m/s}$ LEVEL 1

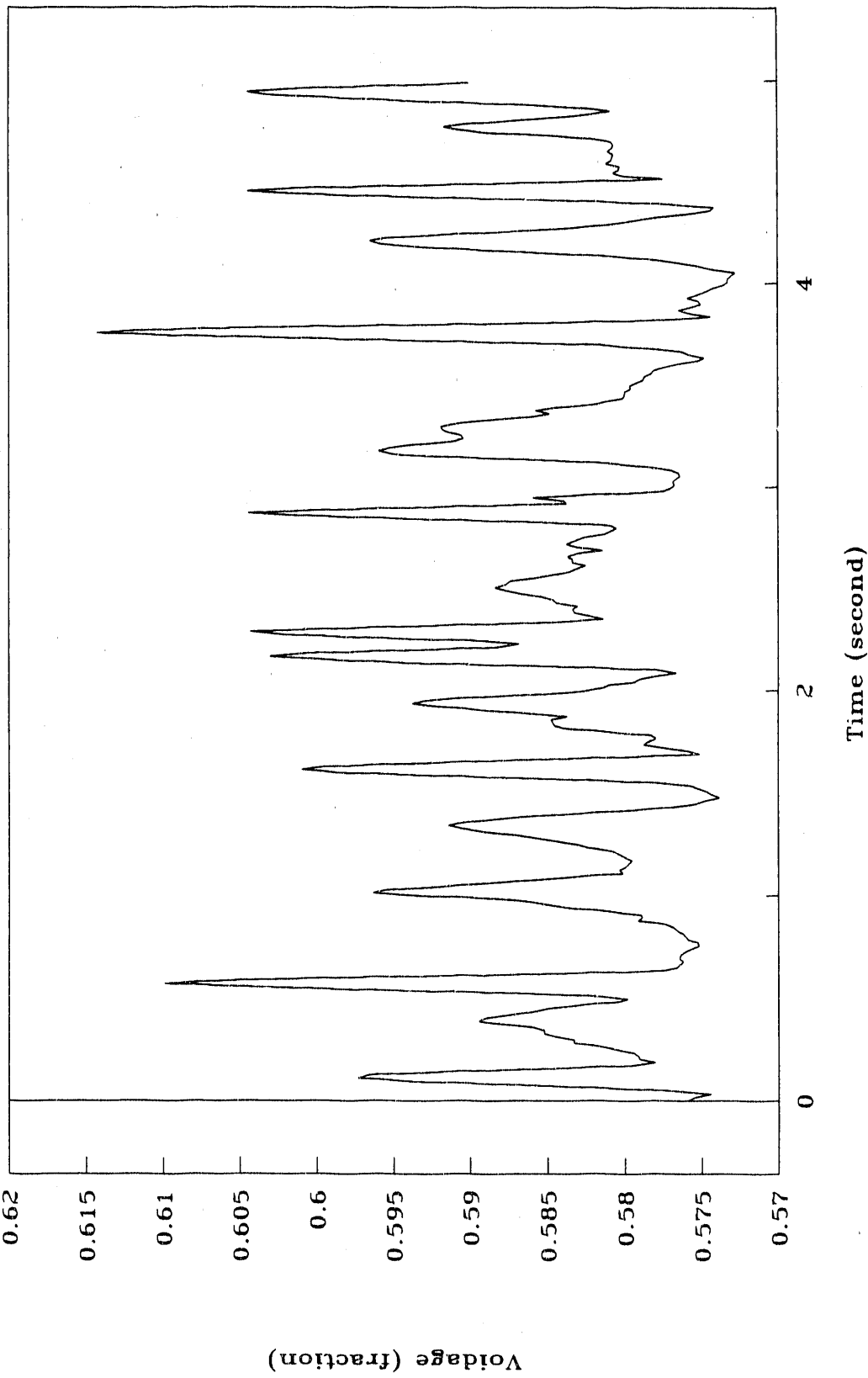


Figure 43. Average voidage versus Time ($U_0 = .220$, level 1)

VOIDAGE VERSUS TIME

$U_{i0} = .220 \text{ m/s}$ LEVEL 2

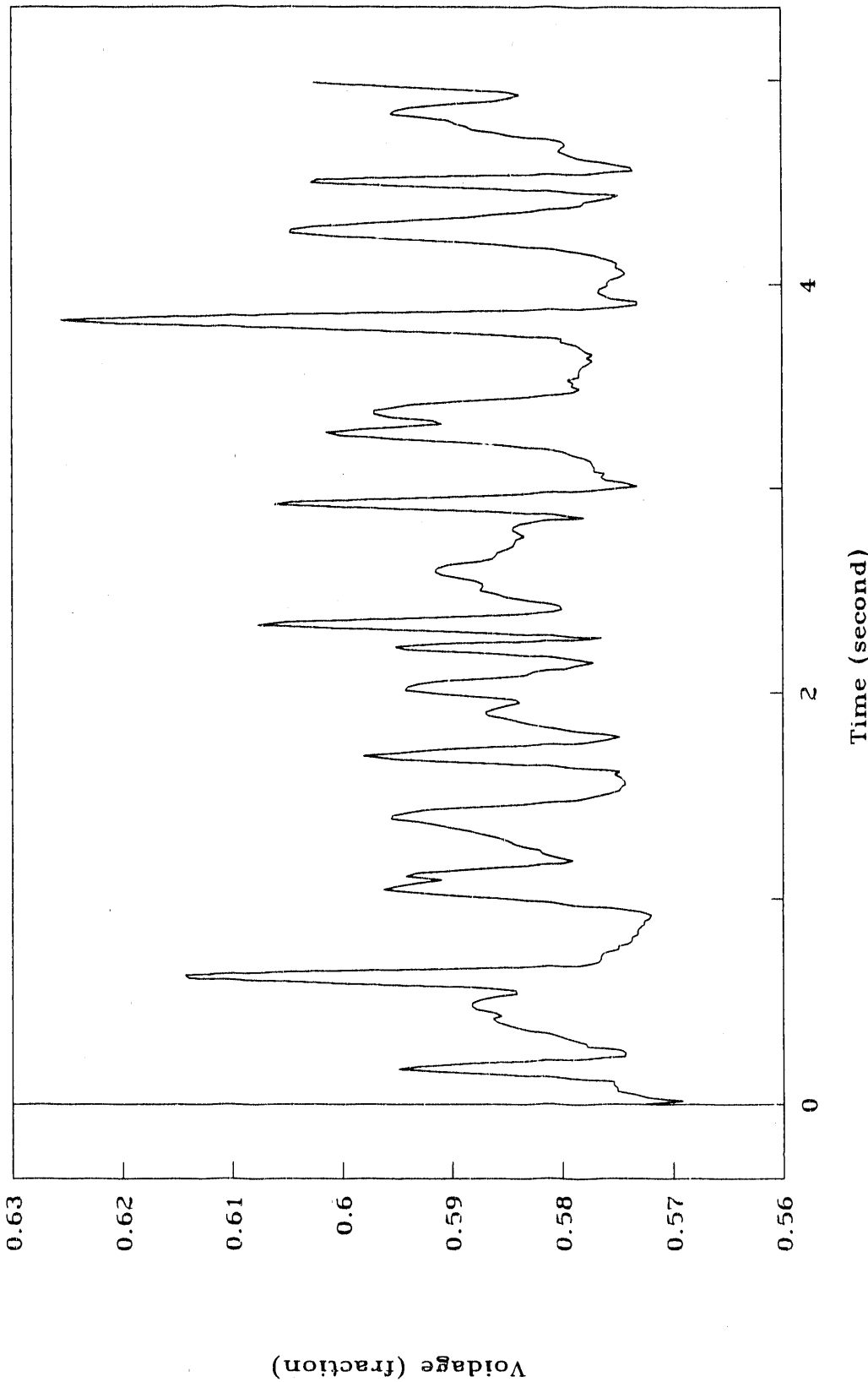


Figure 44. Average Voidage versus Time ($U_0 = .220$, level 2)

VOIDAGE VERSUS TIME

$U_0 = .220 \text{ m/s}$ LEVEL 3

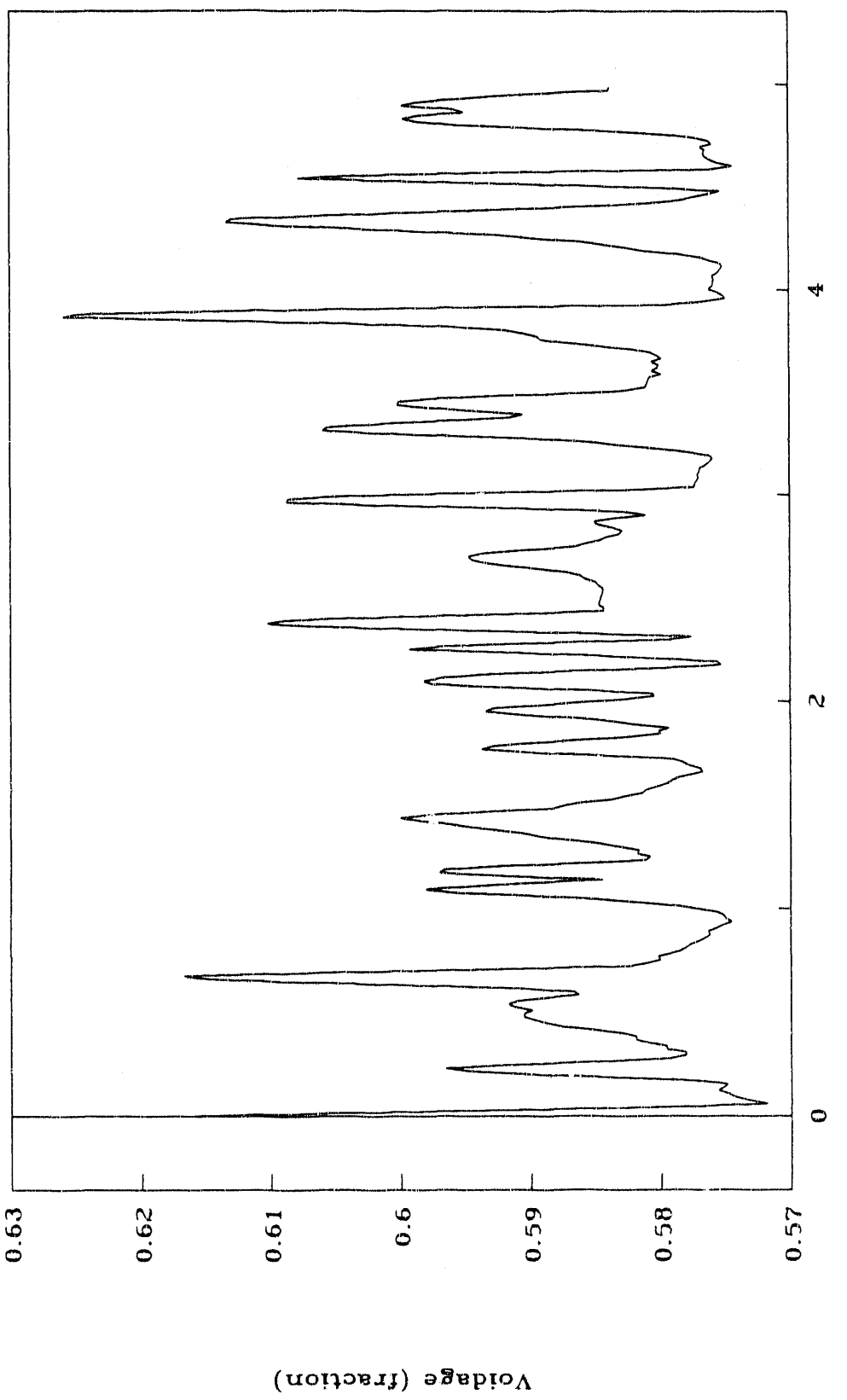


Figure 45. Average voidage versus Time ($U_0 = .220$, level 3)

VOIDAGE VERSUS TIME

$U_0 = .220 \text{ m/s}$

LEVEL 4

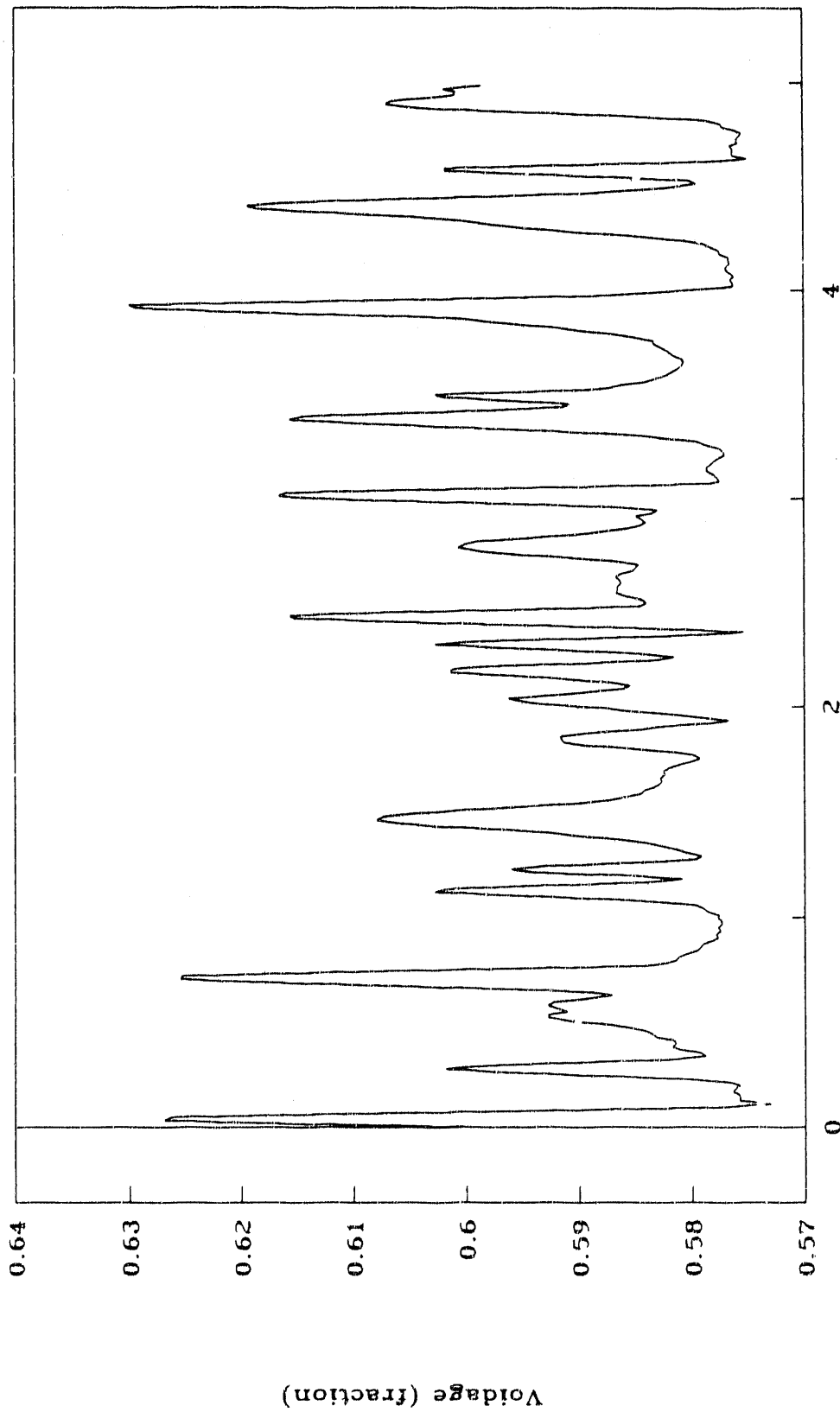


Figure 46. Average Voidage versus Time ($U_0 = .220$, level 4)

LOCAL VOIDAGE VERSUS TIME

$U_0 = .259 \text{ m/s}$ CELL 1 LEVEL 1

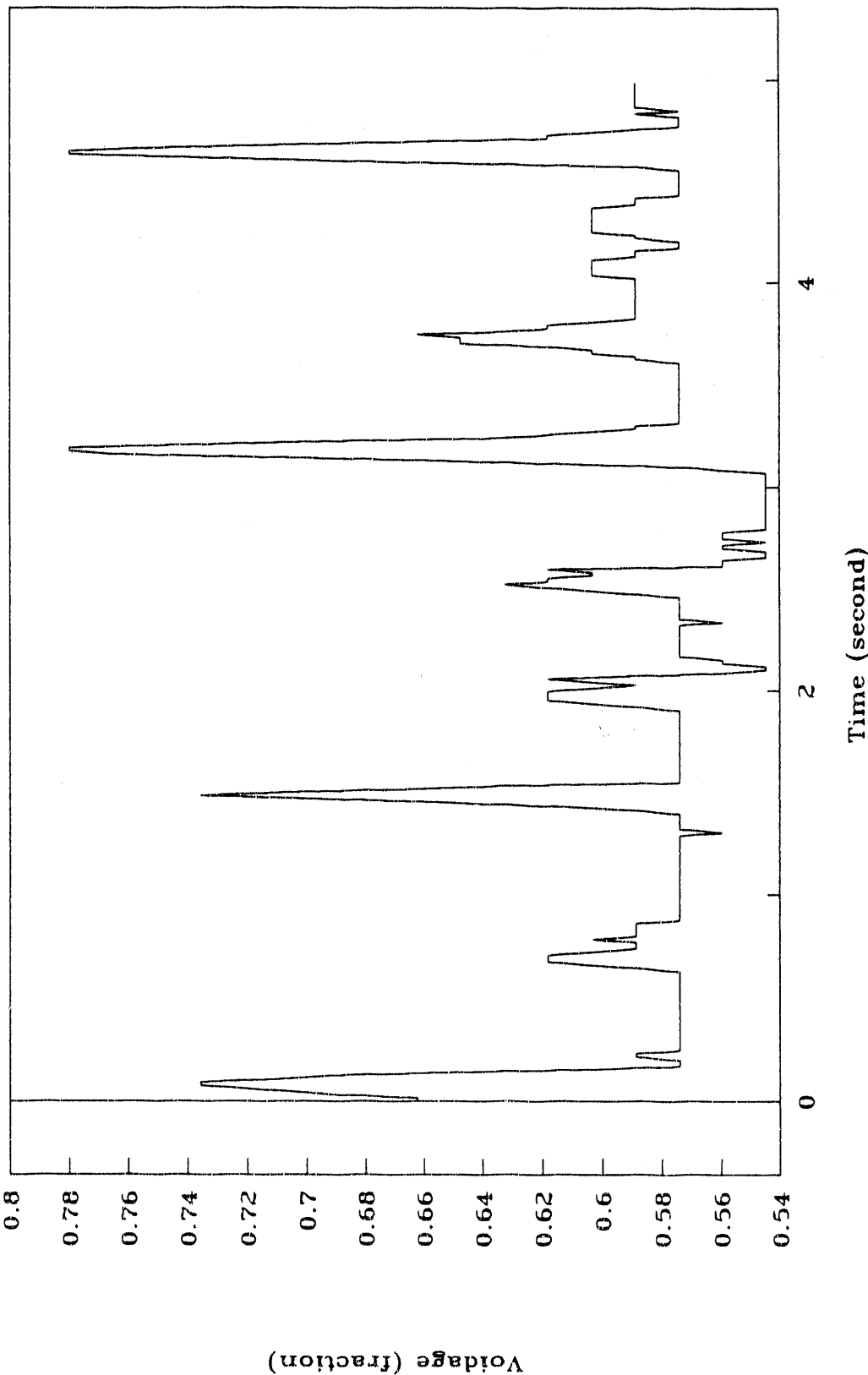


Figure 47. Local voidage versus time ($U_0 = .259$, cell 1, level 1)

LOCAL VOIDAGE VERSUS TIME

$U_0 = .259 \text{ m/s}$ CELL 1 LEVEL 2

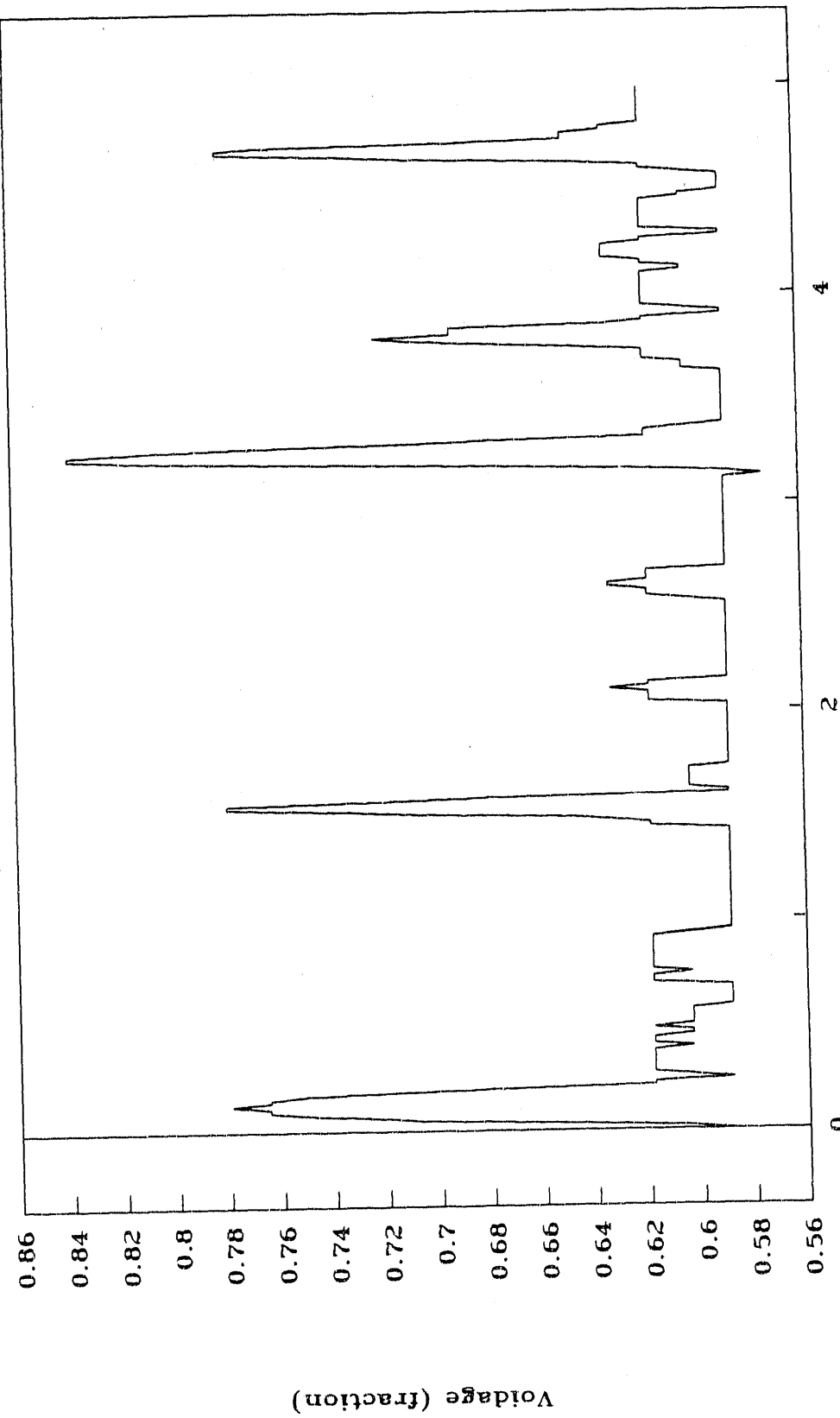


Figure 48. Local voidage versus Time ($U_0 = .259$, cell 1, level 2)

LOCAL VOIDAGE VERSUS TIME

$U_0 = .259 \text{ m/s}$ CELL 1 LEVEL 3

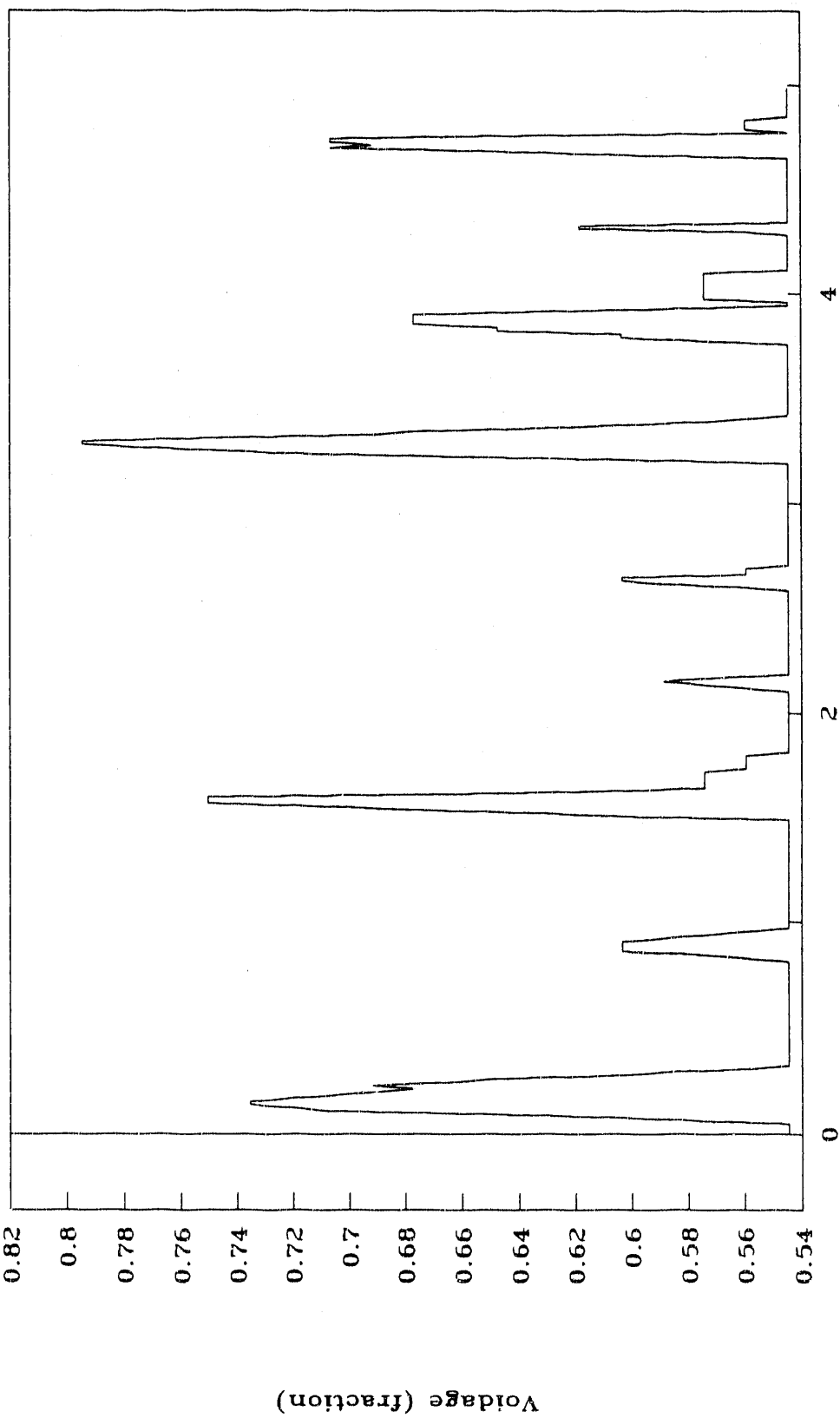


Figure 49. Local voidage versus Time ($U_0 = .259$, cell 1, level 3)

LOCAL VOIDAGE VERSUS TIME

$U_0 = .259 \text{ m/s}$ CELL 1 LEVEL 4

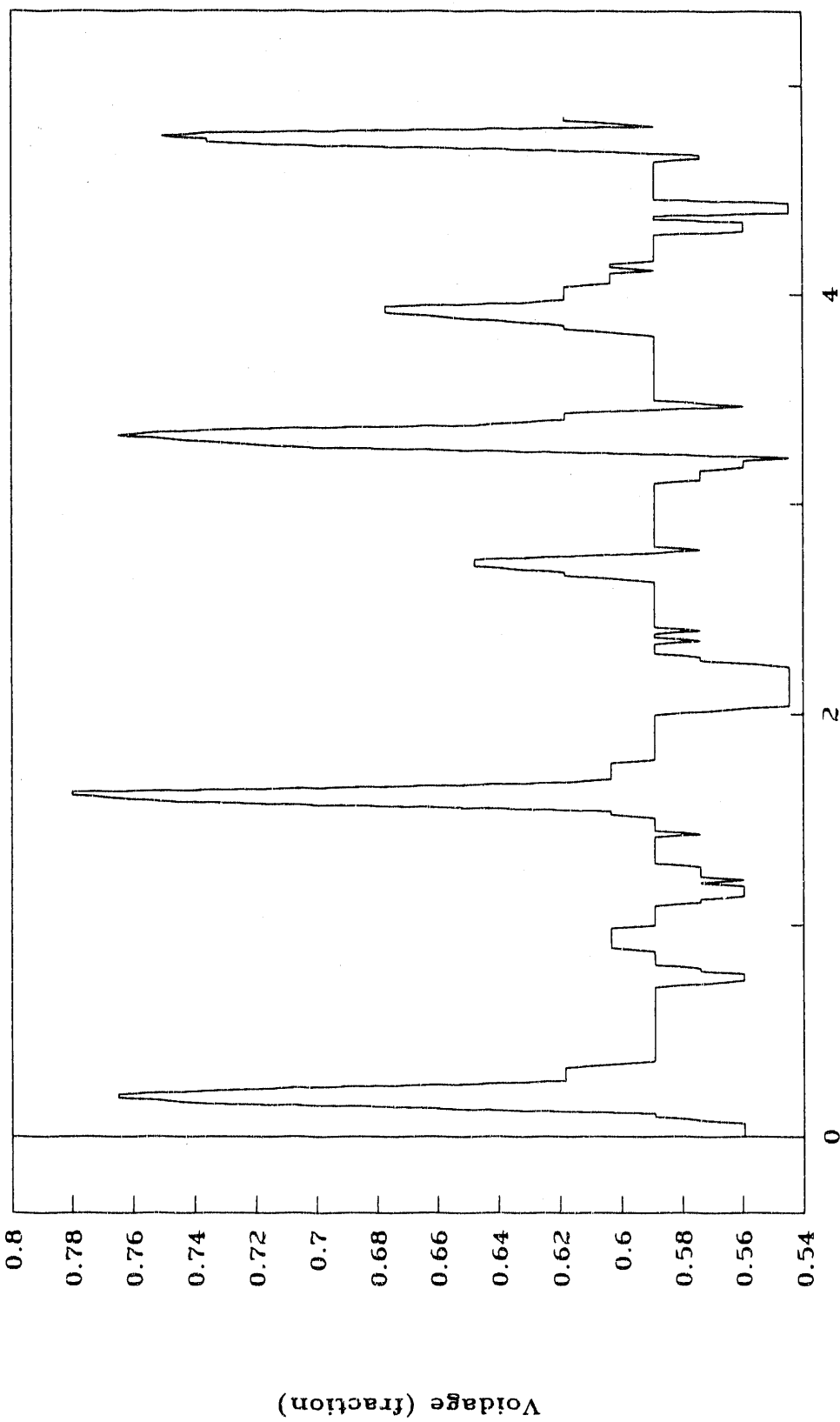


Figure 50. Local voidage versus time ($U_0 = .259$, cell 1, level 4)

LOCAL VOIDAGE VERSUS TIME

$U_0 = .316 \text{ m/s}$ CELL 1 LEVEL 1

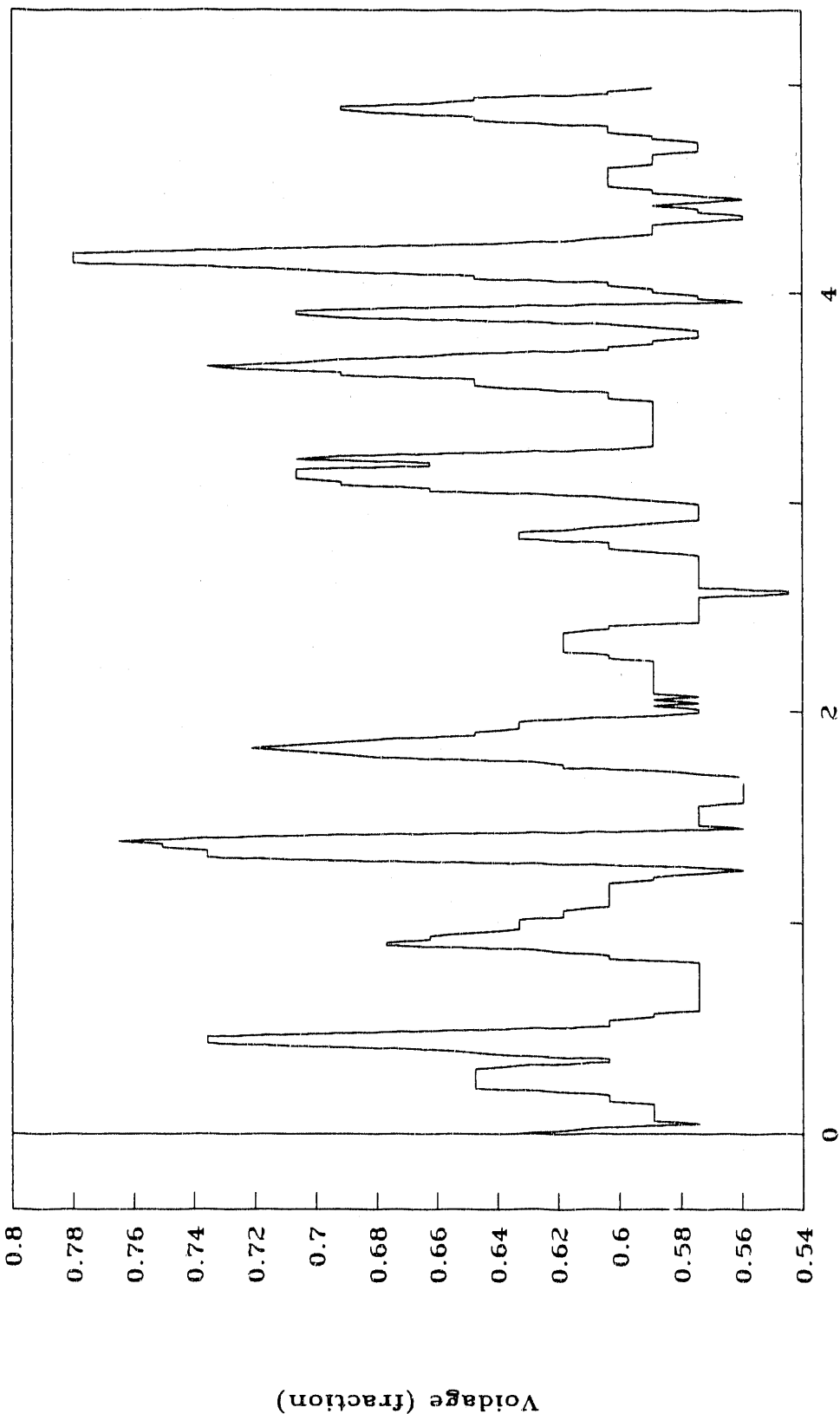


Figure 51. Local voidage versus Time ($U_0 = .316$, cell 1, level 1)

LOCAL VOIDAGE VERSUS TIME

$U_0 = .316 \text{ m/s}$ CELL 1 LEVEL 2

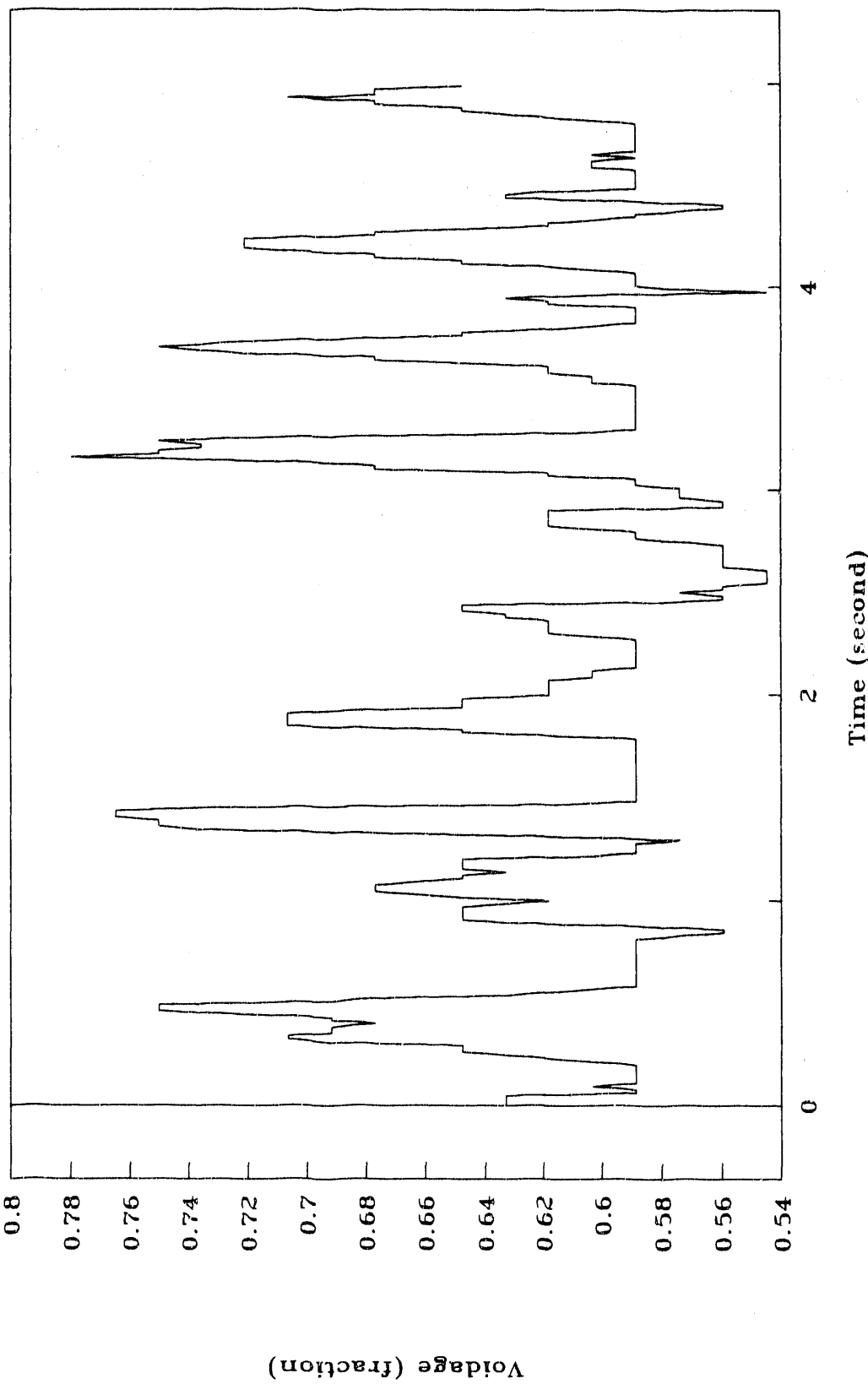


Figure 52. Local Voidage versus Time ($U_0 = .316$, cell 1, level 2)

LOCAL VOIDAGE VERSUS TIME

$U_0 = .316 \text{ m/s}$ CELL 1 LEVEL 3

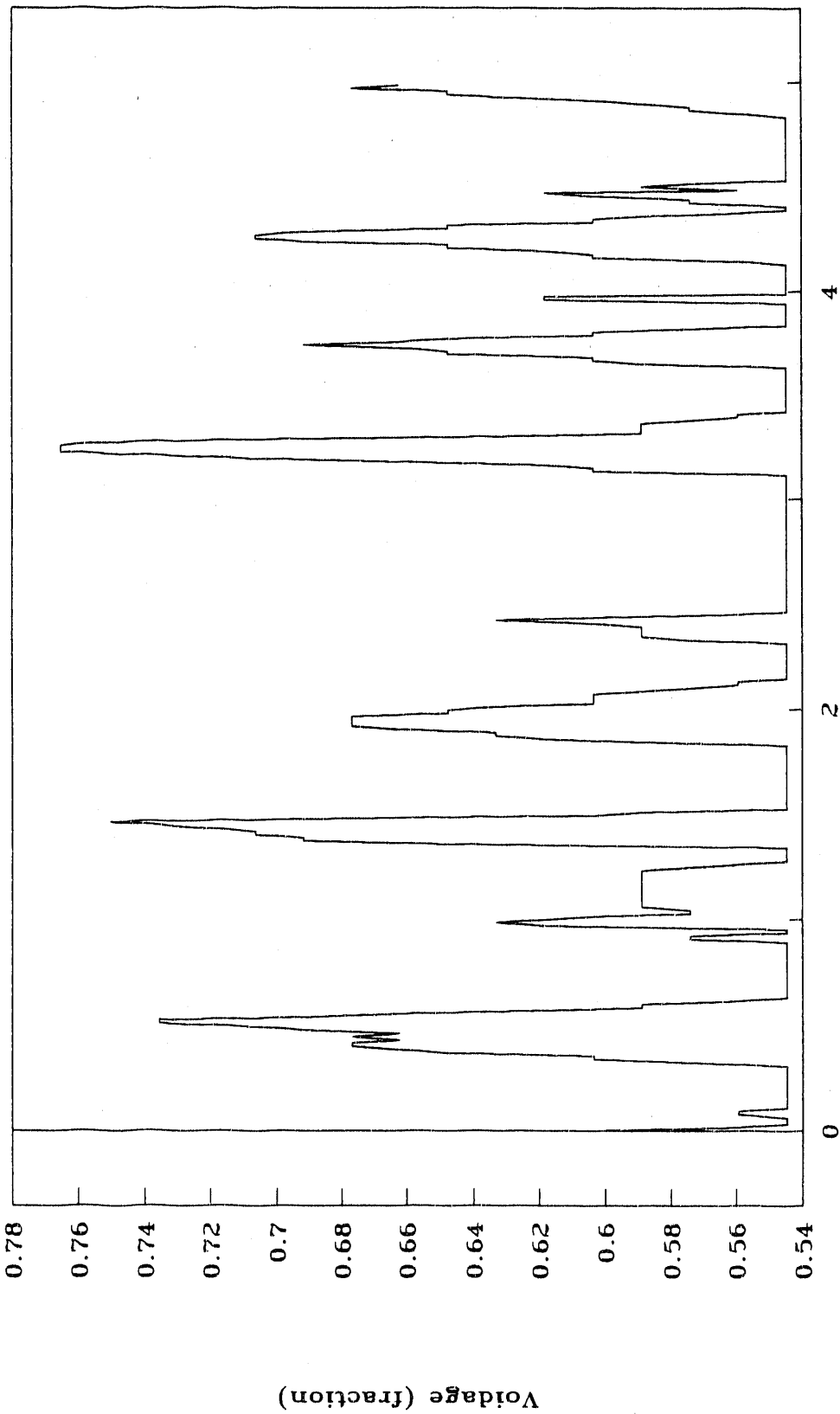


Figure 53. Local voidage versus Time ($U_0 = .316$, cell 1, level 3)

LOCAL VOIDAGE VERSUS TIME

$U_0 = .316 \text{ m/s}$ CELL 1 LEVEL 4

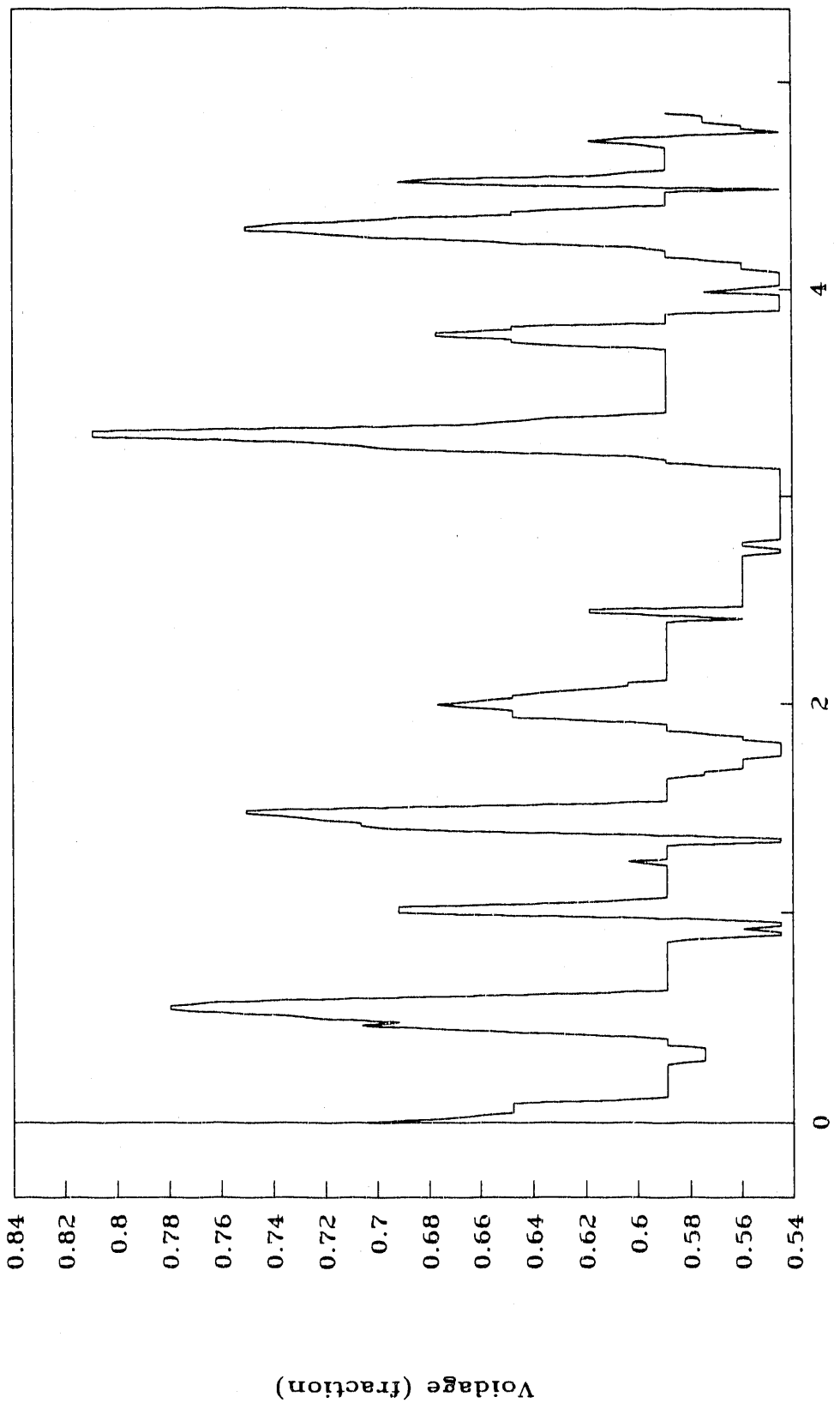


Figure 54. Local Voidage versus Time ($U_0 = .316$, cell 1, level 4)

LOCAL VOIDAGE VERSUS TIME

$U_0 = .361 \text{ m/s}$ CELL 1 LEVEL 1

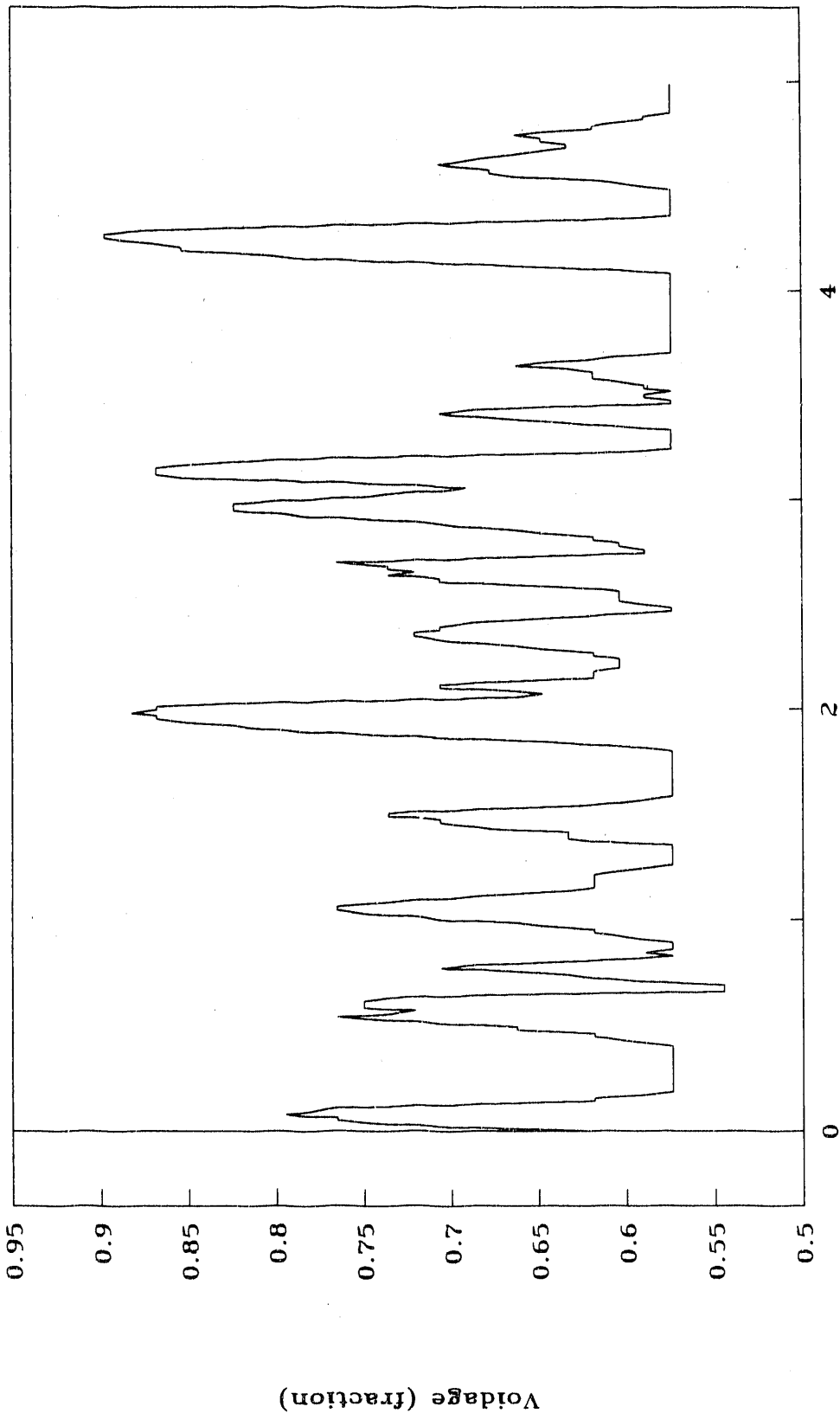


Figure 55. Local Voidage versus Time ($U_0 = .361$, cell 1, level 1)

LOCAL VOIDAGE VERSUS TIME

$U_0 = .361 \text{ m/s}$ CELL 1 LEVEL 2

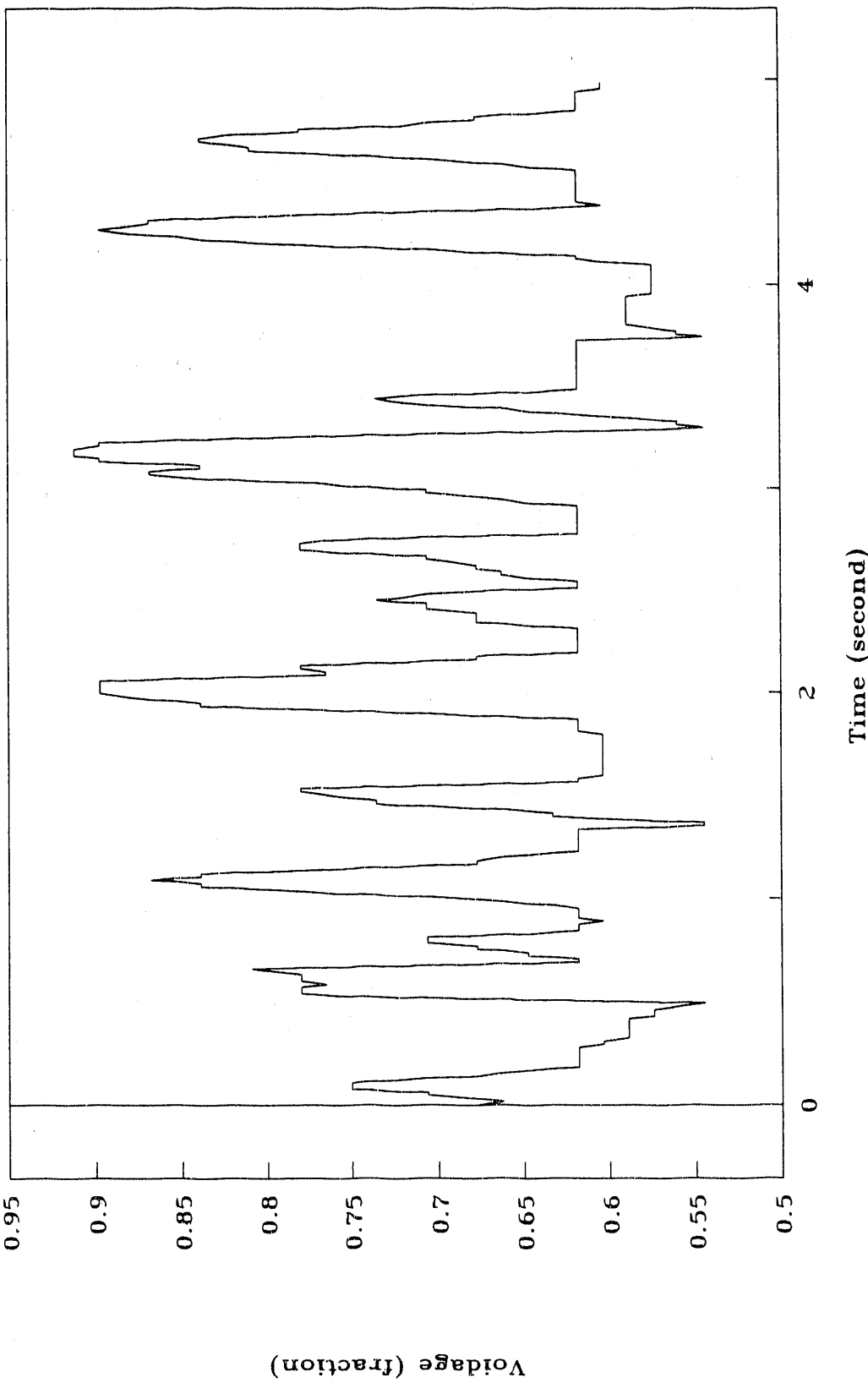


Figure 56. Local voidage versus time ($U_0 = .361$, cell 1, level 2)

LOCAL VOIDAGE VERSUS TIME

$U_0 = .361 \text{ m/s}$ CELL 1 LEVEL 3

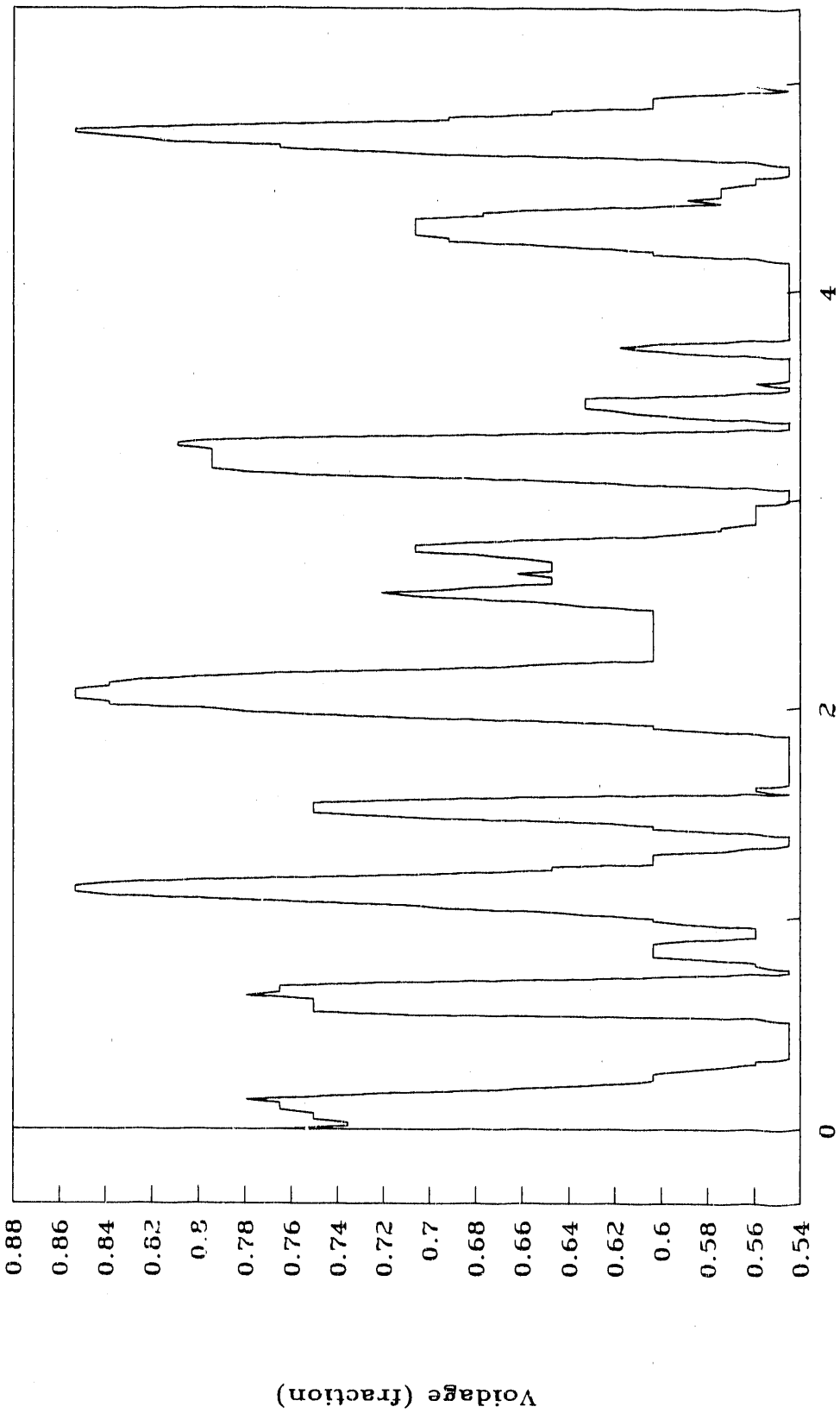


Figure 57. Local voidage versus Time ($U_0 = .361$, cell 1, level 3)

LOCAL VOIDAGE VERSUS TIME

$U_0 = .361 \text{ m/s}$ CELL 1 LEVEL 4

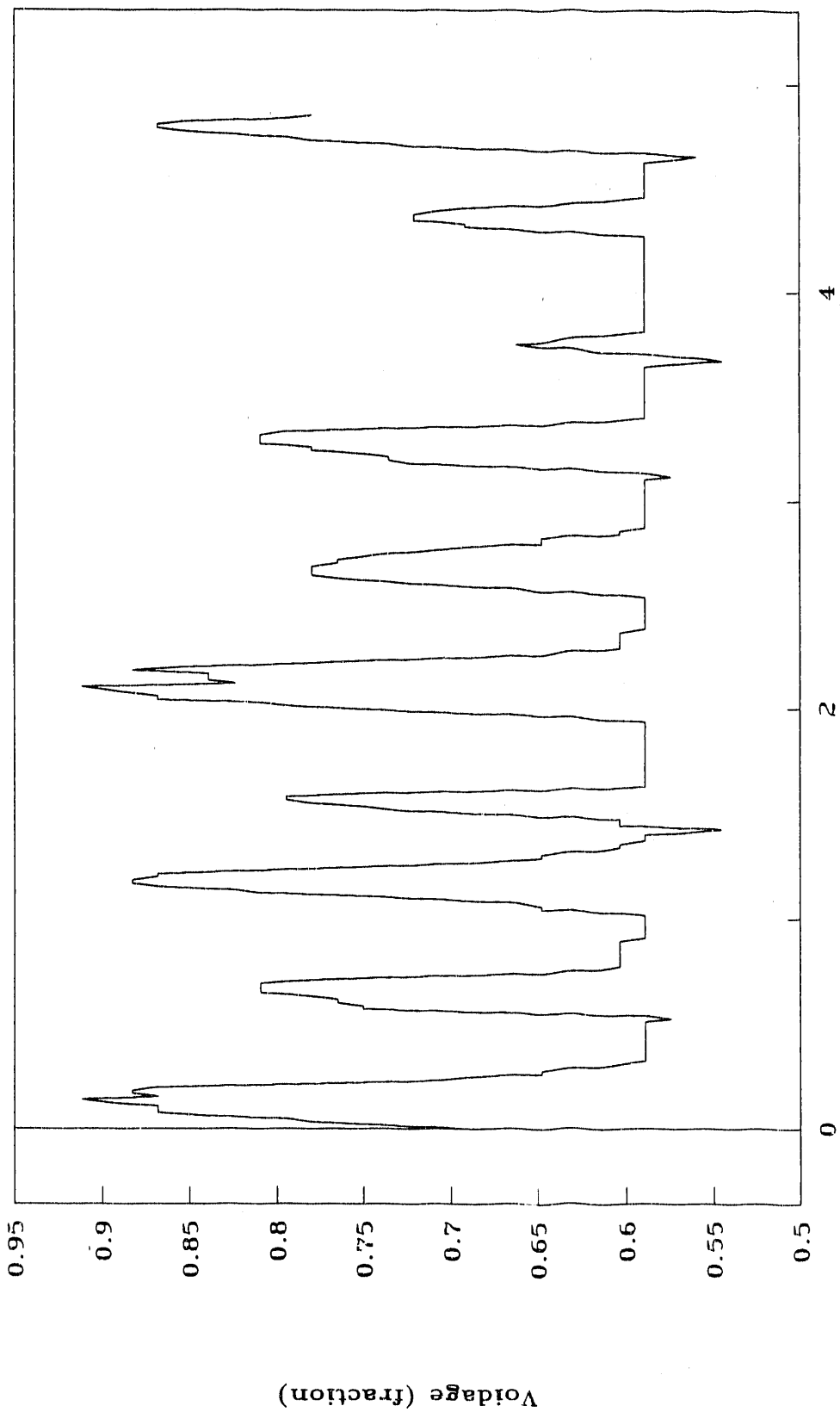


Figure 58. Local Voidage versus Time ($U_0 = .361$, cell 1, level 4)

LOCAL VOIDAGE VERSUS TIME

$U_0 = .220 \text{ m/s}$ CELL 1 LEVEL 1

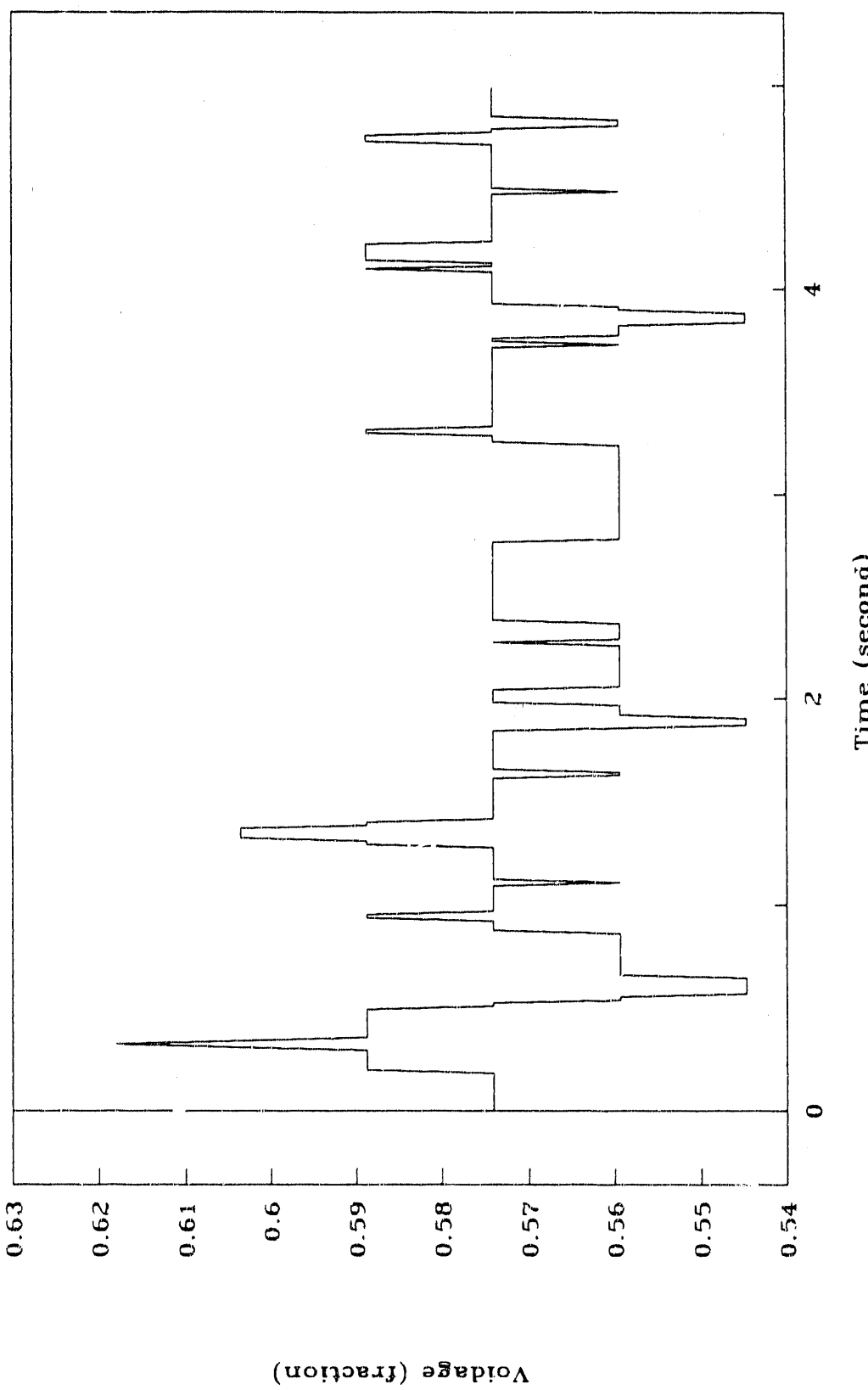


Figure 59. Local voidage versus Time ($U_0 = .220$, cell 1, level 1)

LOCAL VOIDAGE VERSUS TIME

$U_0 = .220 \text{ m/s}$ CELL 1 LEVEL 2

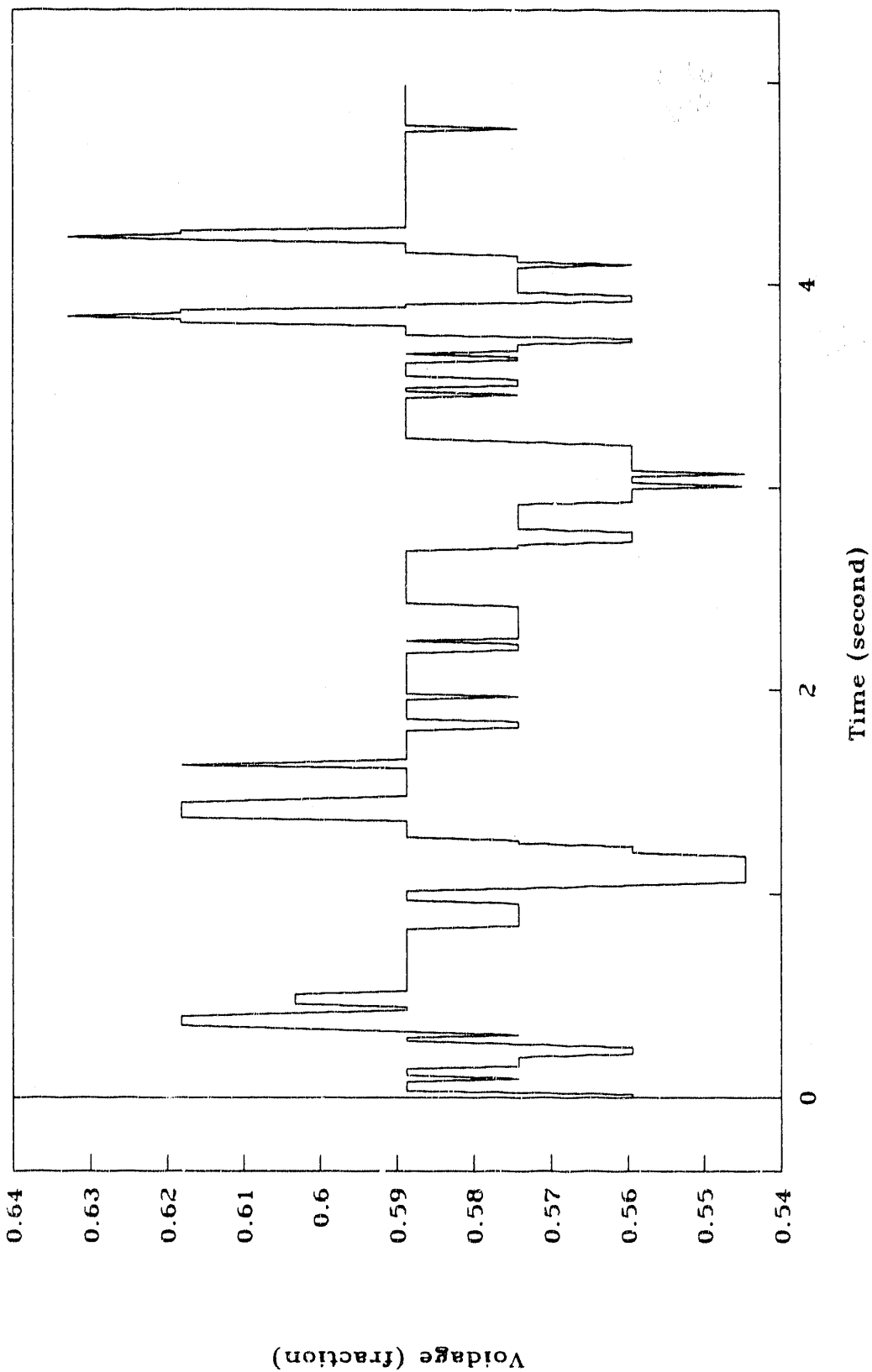


Figure 60. Local voidage versus time ($U_0 = .220$, cell 1, level 2)

LOCAL VOIDAGE VERSUS TIME

$U_0 = .220 \text{ m/s}$ CELL 1 LEVEL 3

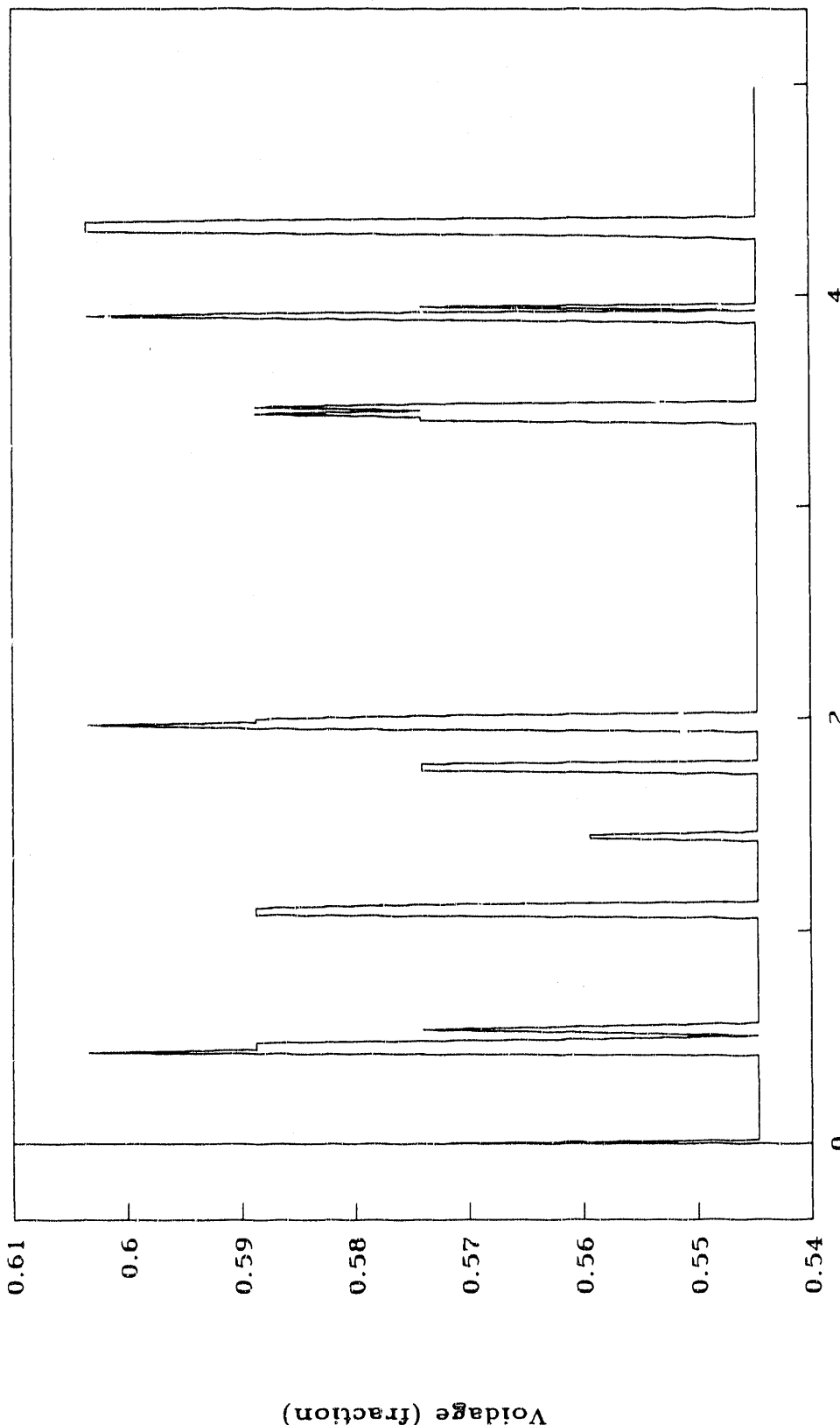


Figure 61. Local voidage versus Time ($U_0 = .220$, cell 1, level 3)

LOCAL VOIDAGE VERSUS TIME

$U_0 = .220 \text{ m/s}$ CELL 1 LEVEL 4

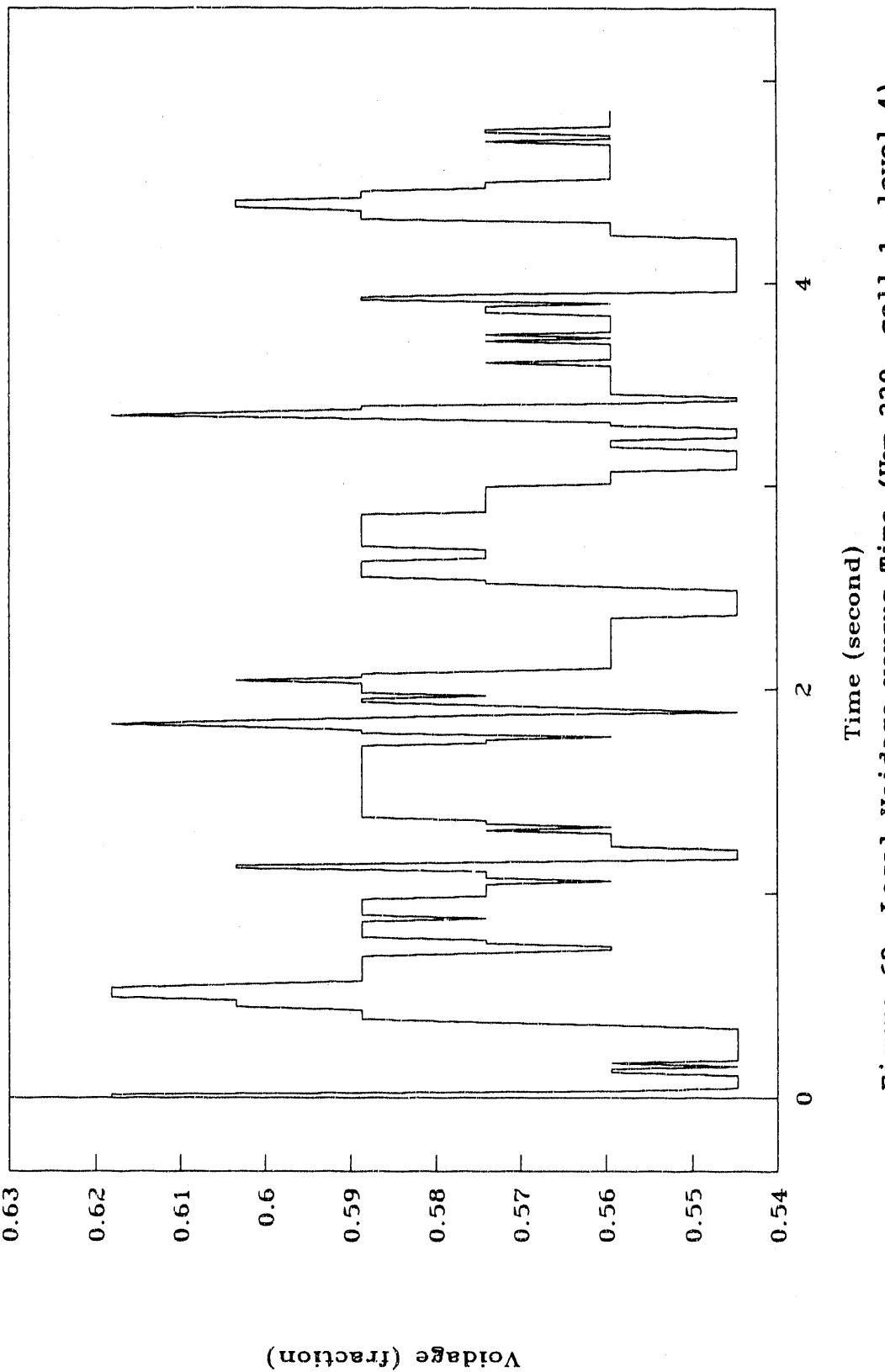


Figure 62. Local Voidage versus Time ($U_0 = .220$, cell 1, level 4)

LOCAL VOIDAGE VERSUS TIME

$U_0 = .259 \text{ m/s}$ CELL 1-33 LEVEL 1

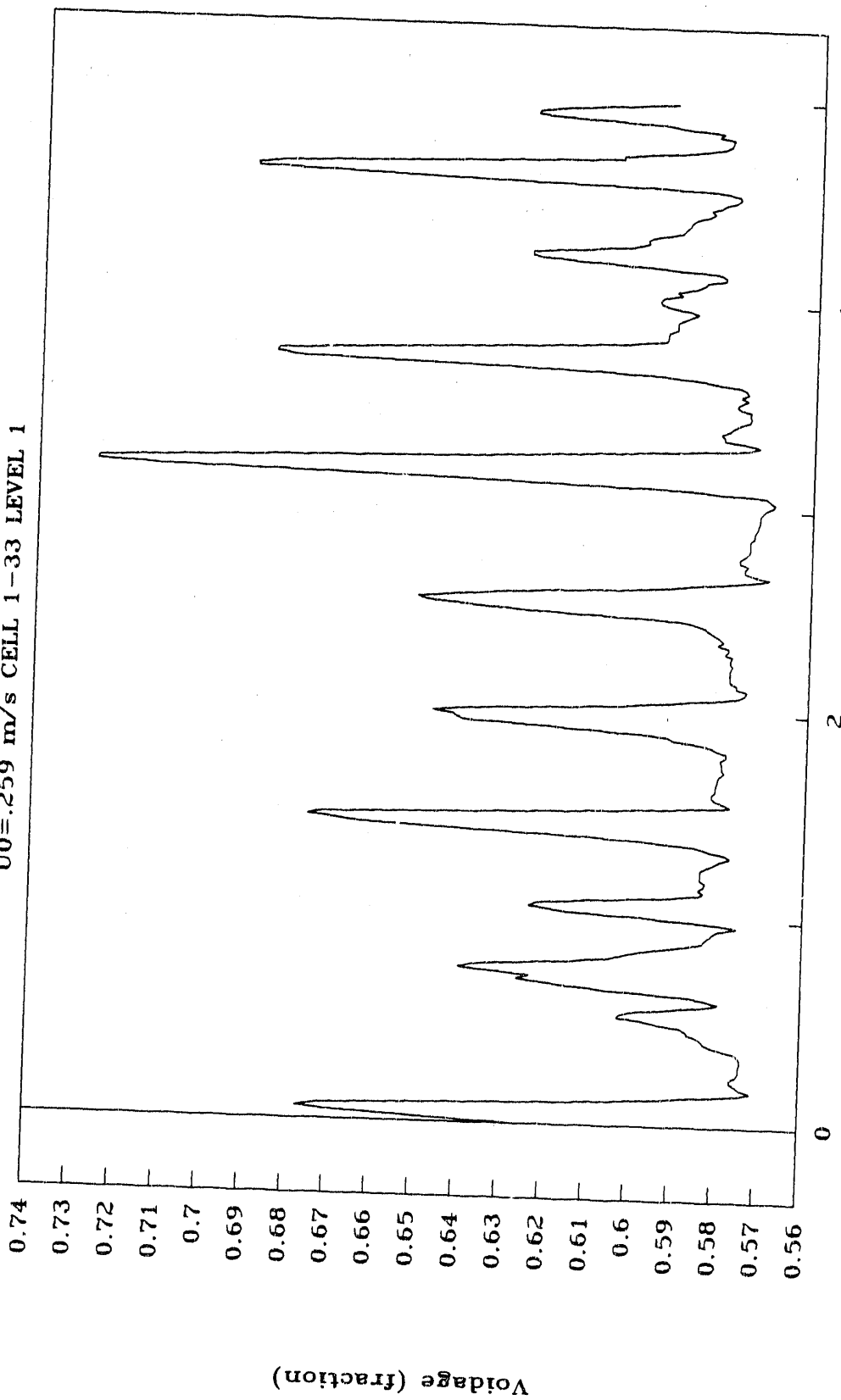


Figure 63. Local voidage versus Time ($U_0 = .259$, cell 1-33, level 1)

LOCAL VOIDAGE VERSUS TIME

$U_0 = .259 \text{ m/s}$ CELL 1-33 LEVEL 2

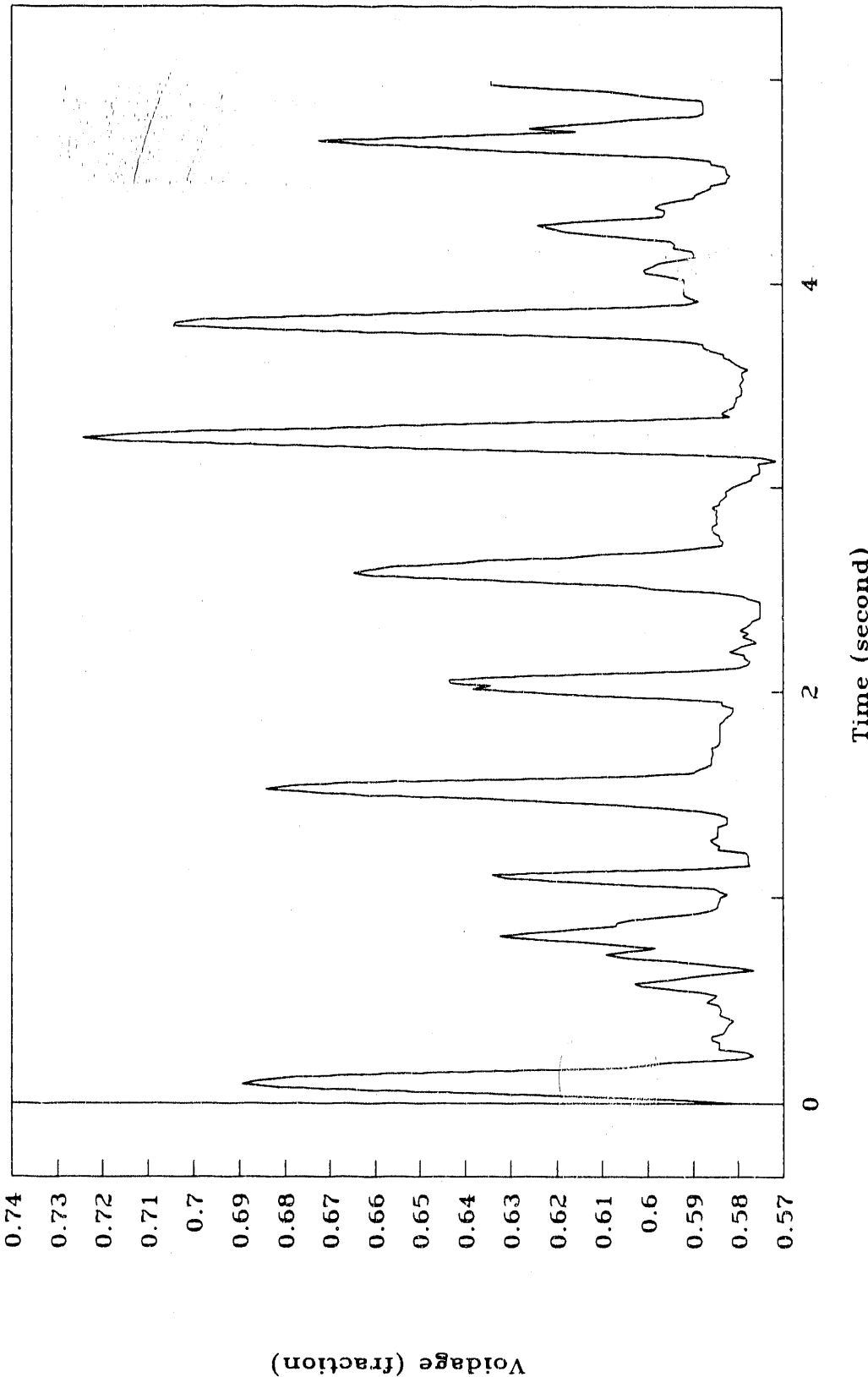


Figure 64. Local voidage versus time ($U_0 = .259$, cell 1-33, level 2)

LOCAL VOIDAGE VERSUS TIME

$U_0 = .259 \text{ m/s}$ CELL 1-33 LEVEL 3

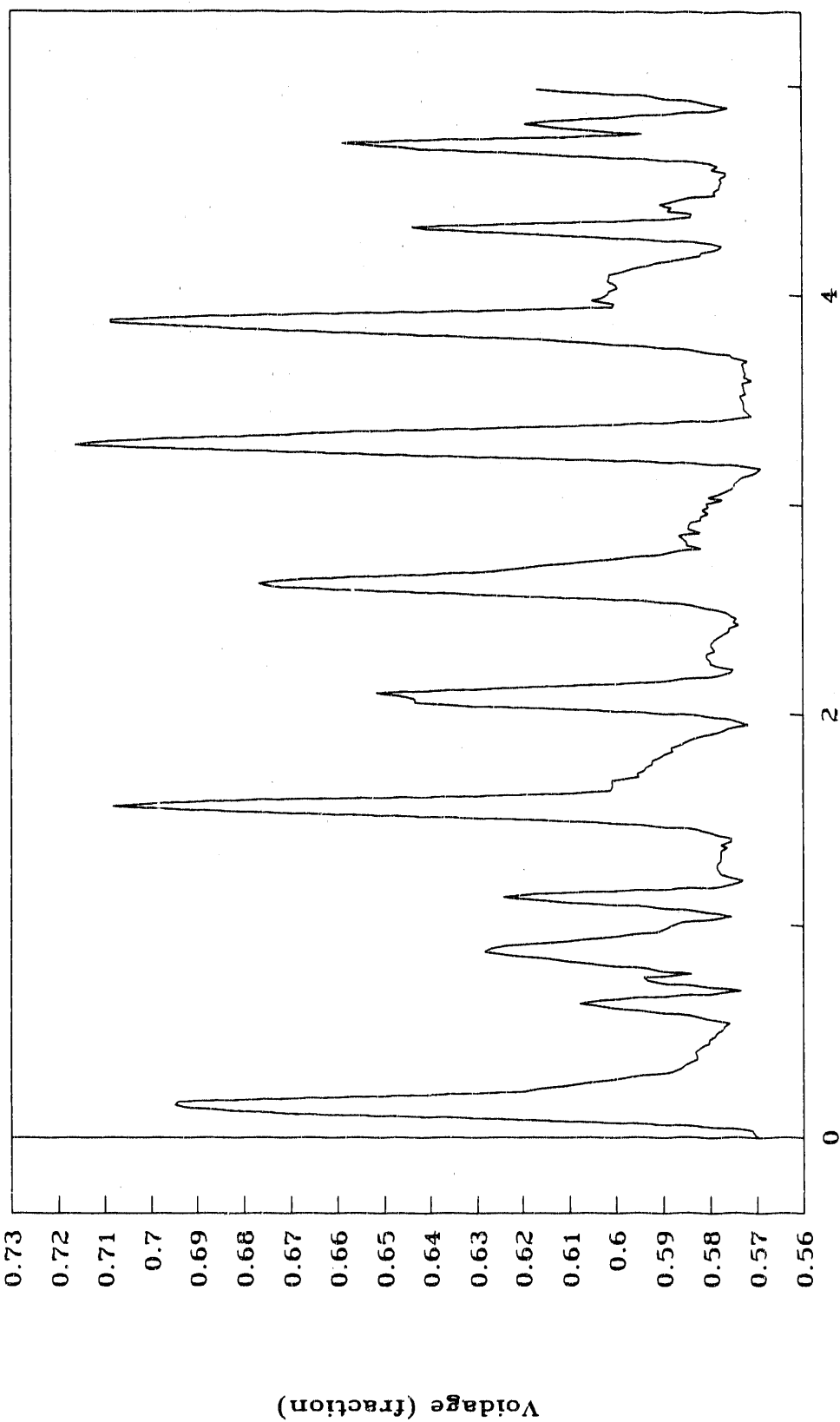


Figure 65. Local Voidage versus Time ($U_0 = .259$, cell 1-33, level 3)

LOCAL VOIDAGE VERSUS TIME

$U_0 = .259 \text{ m/s}$ CELL 1-33 LEVEL 4

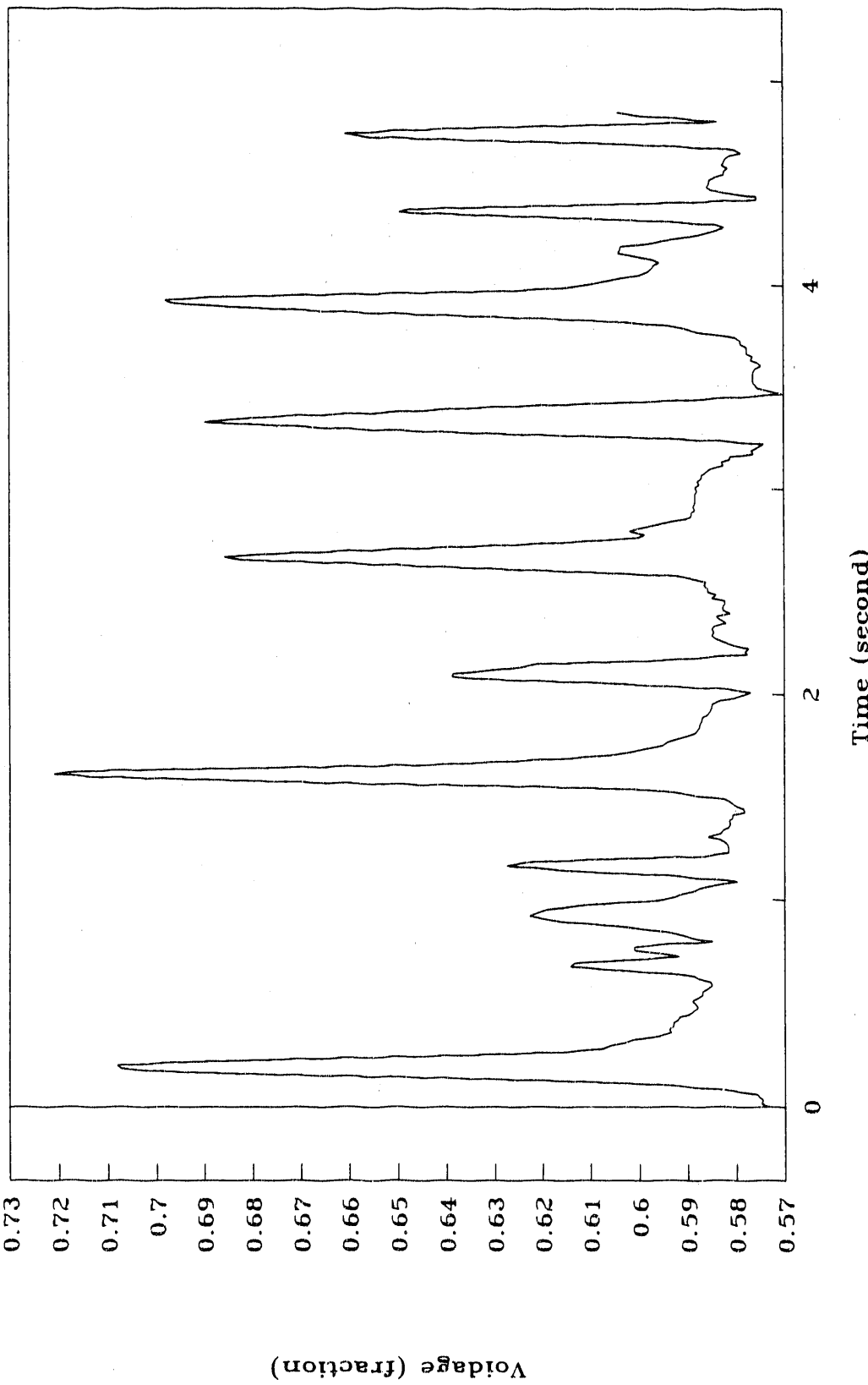


Figure 66. Local voidage versus time ($U_0 = .259$, cell 1-33, level 4)

LOCAL VOIDAGE VERSUS TIME

$U_0 = .316 \text{ m/s}$ CELL 1-33 LEVEL 1

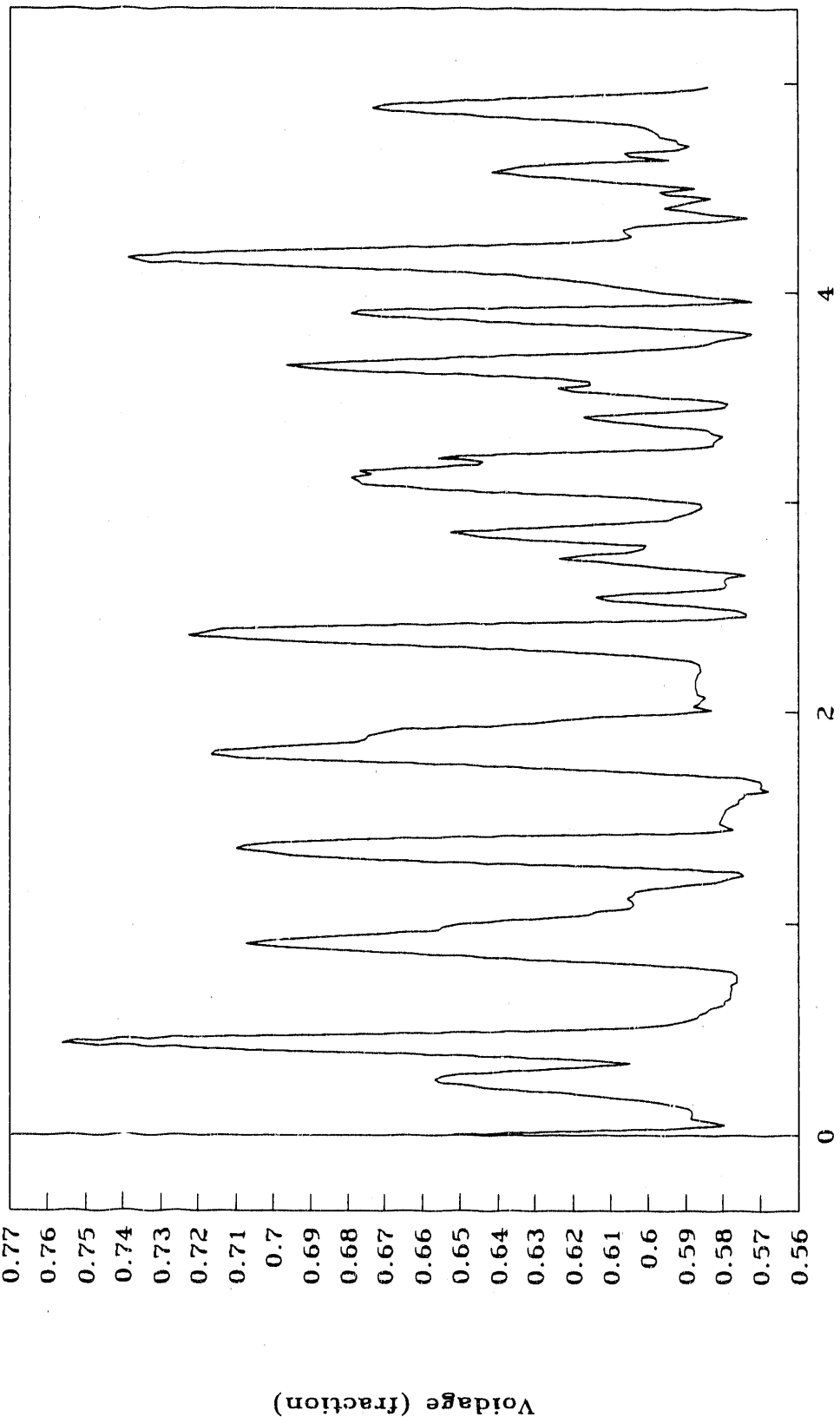


Figure 67. Local voidage versus Time ($U_0 = .316$, cell 1-33, level 1)

LOCAL VOIDAGE VERSUS TIME

$U_0 = .316 \text{ m/s}$ CELL 1-33 LEVEL 2

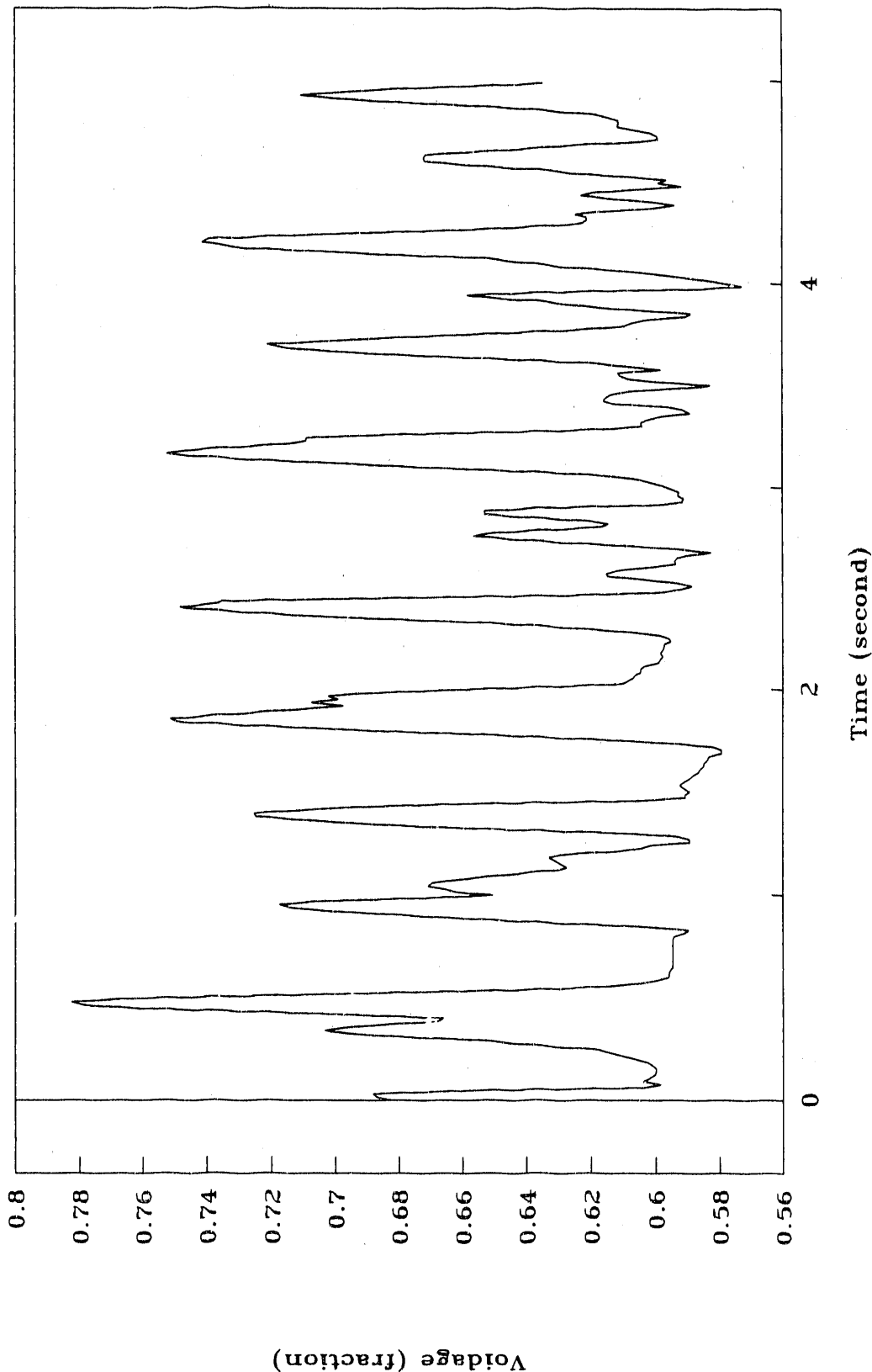


Figure 68. Local Voidage versus Time ($U_0 = .316$, cell 1-33, level 2)

LOCAL VOIDAGE VERSUS TIME

$U_0 = .316 \text{ m/s}$ CELL 1-33 LEVEL 3

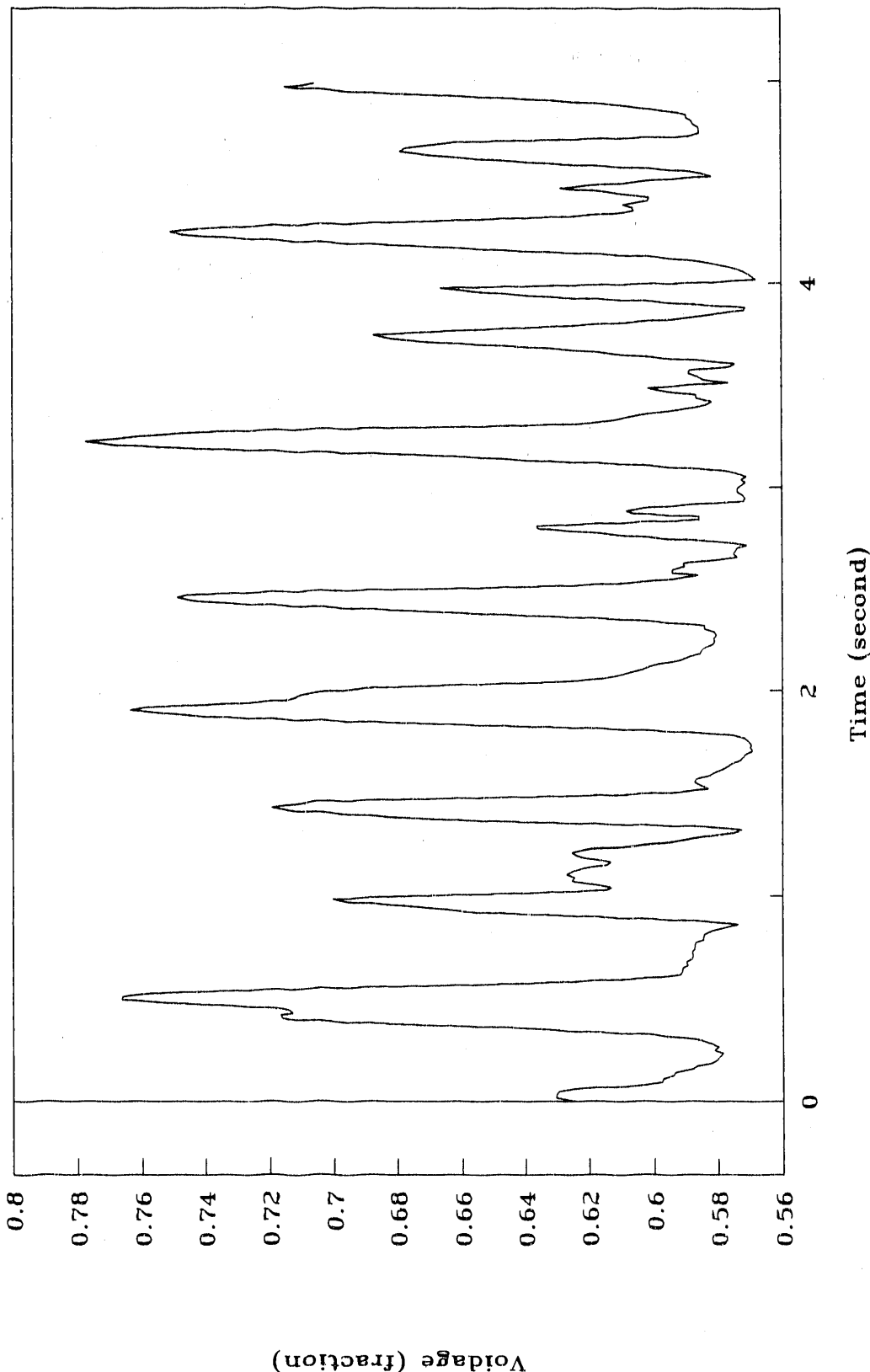


Figure 69. Local voidage versus Time ($U_0 = .316$, cell 1-33, level 3)

LOCAL VOIDAGE VERSUS TIME

$U_0 = .316 \text{ m/s}$ CELL 1-33 LEVEL 4

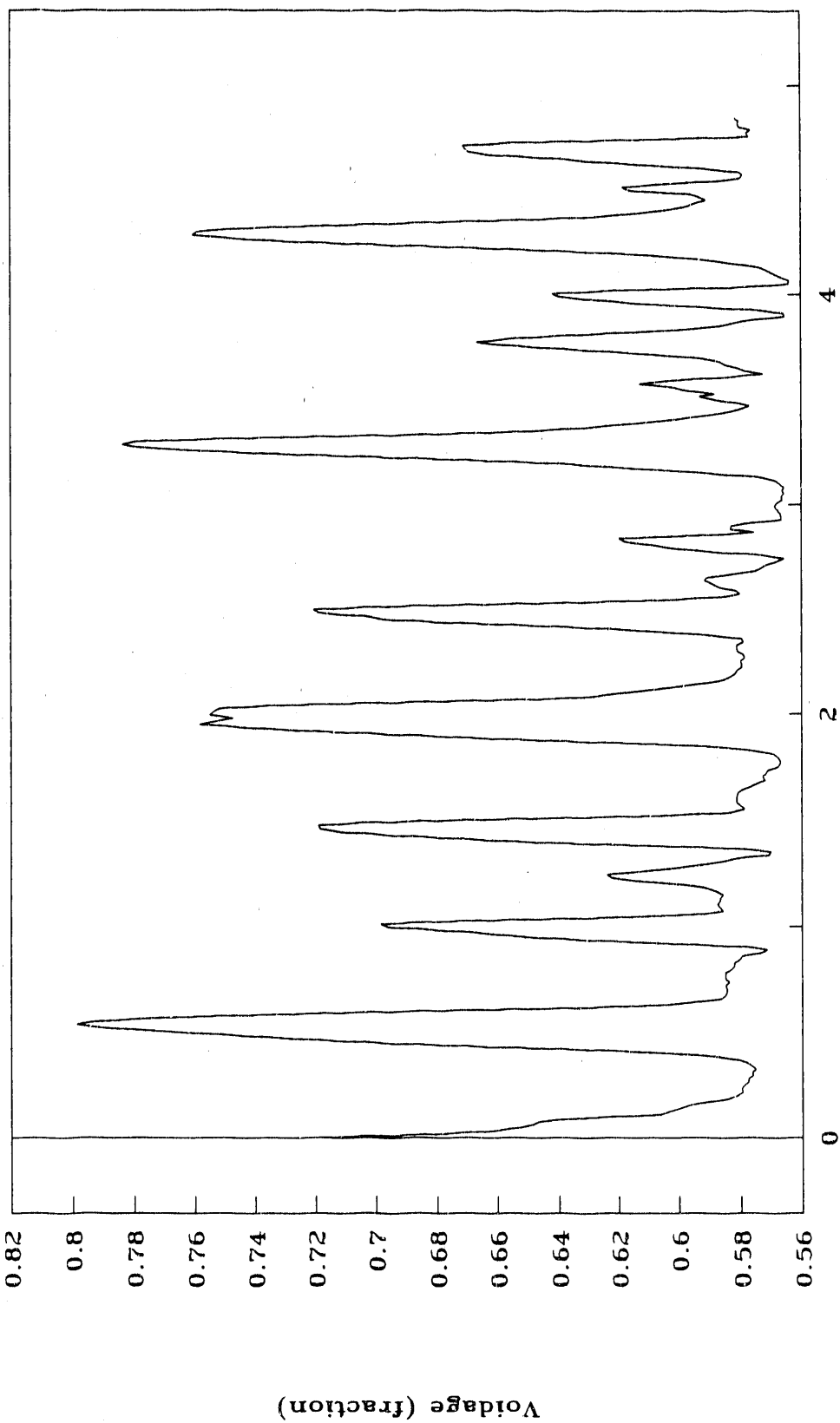


Figure 70. Local Voidage versus Time ($U_0 = .316$, cell 1-33, level 4)

LOCAL VOIDAGE VERSUS TIME

$U_0 = .361 \text{ m/s}$ CELL 1-33 LEVEL 1

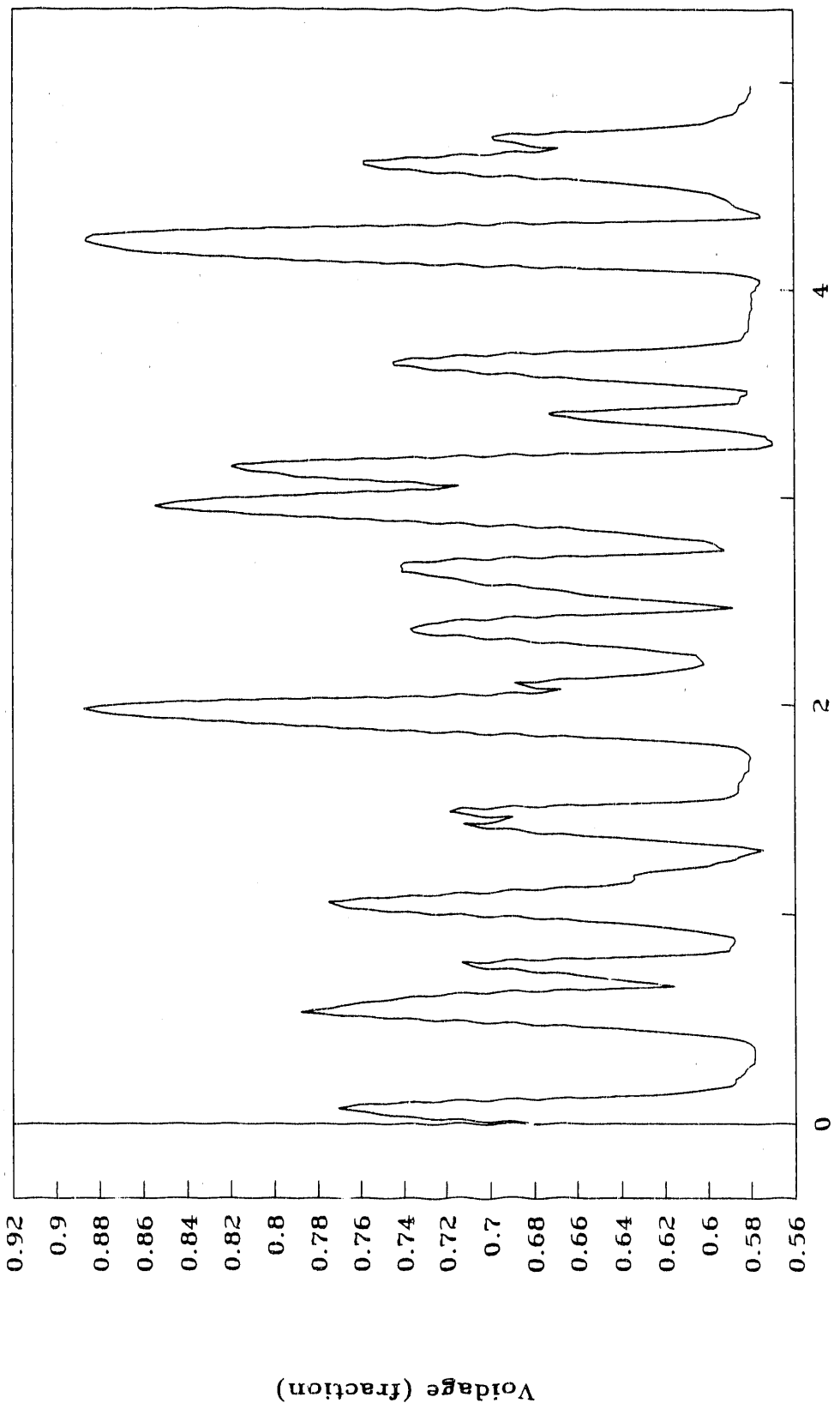


Figure 71. Local voidage versus time ($U_0 = .361$, cell 1-33, level 1)

LOCAL VOIDAGE VERSUS TIME

$U_0 = .361 \text{ m/s}$ CELL 1-33 LEVEL 2

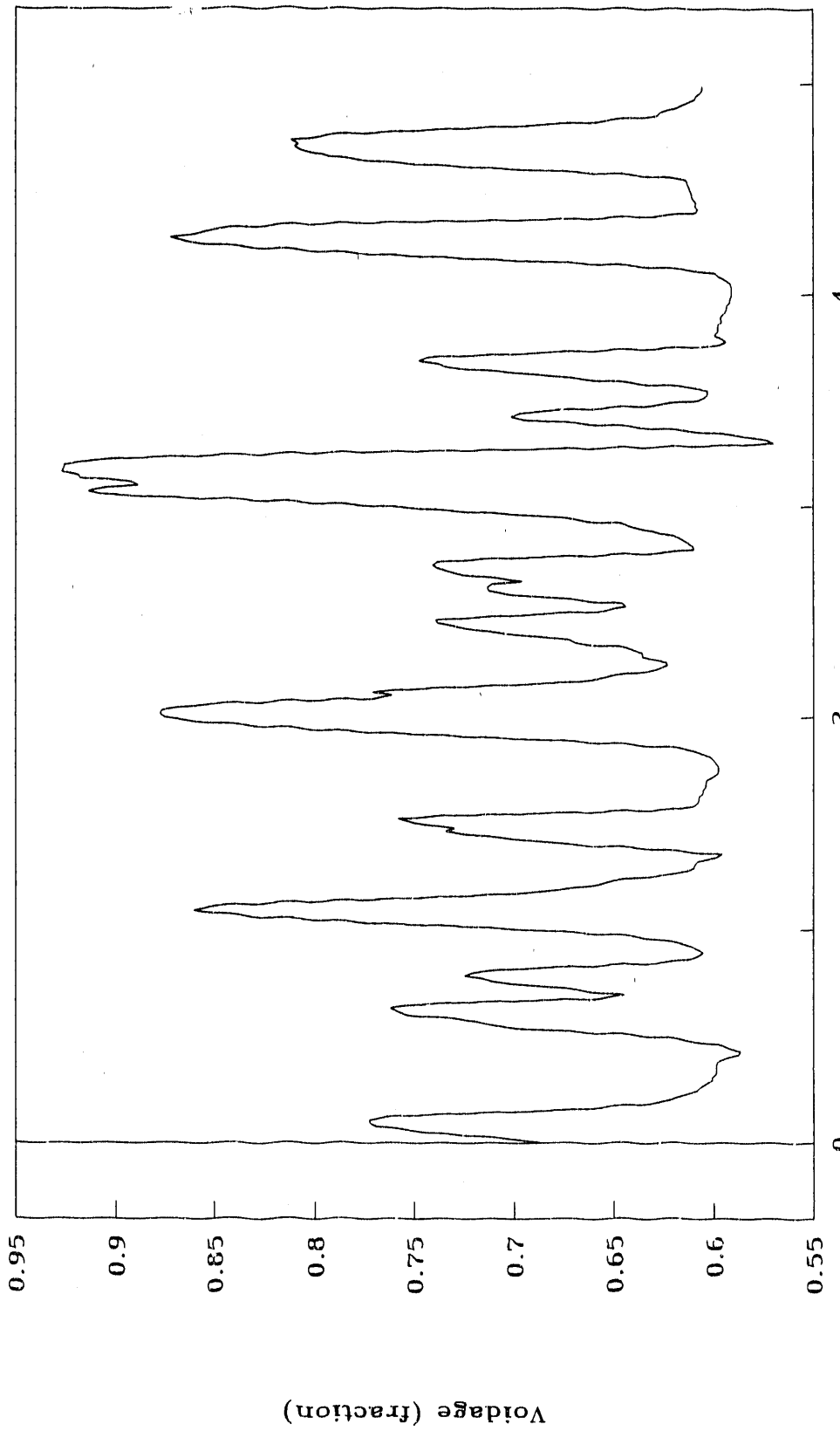


Figure 72. Local voidage versus time ($U_0 = .361$, cell 1-33, level 2)

LOCAL VOIDAGE VERSUS TIME

$U_0 = .361 \text{ m/s}$ CELL 1-33 LEVEL 3

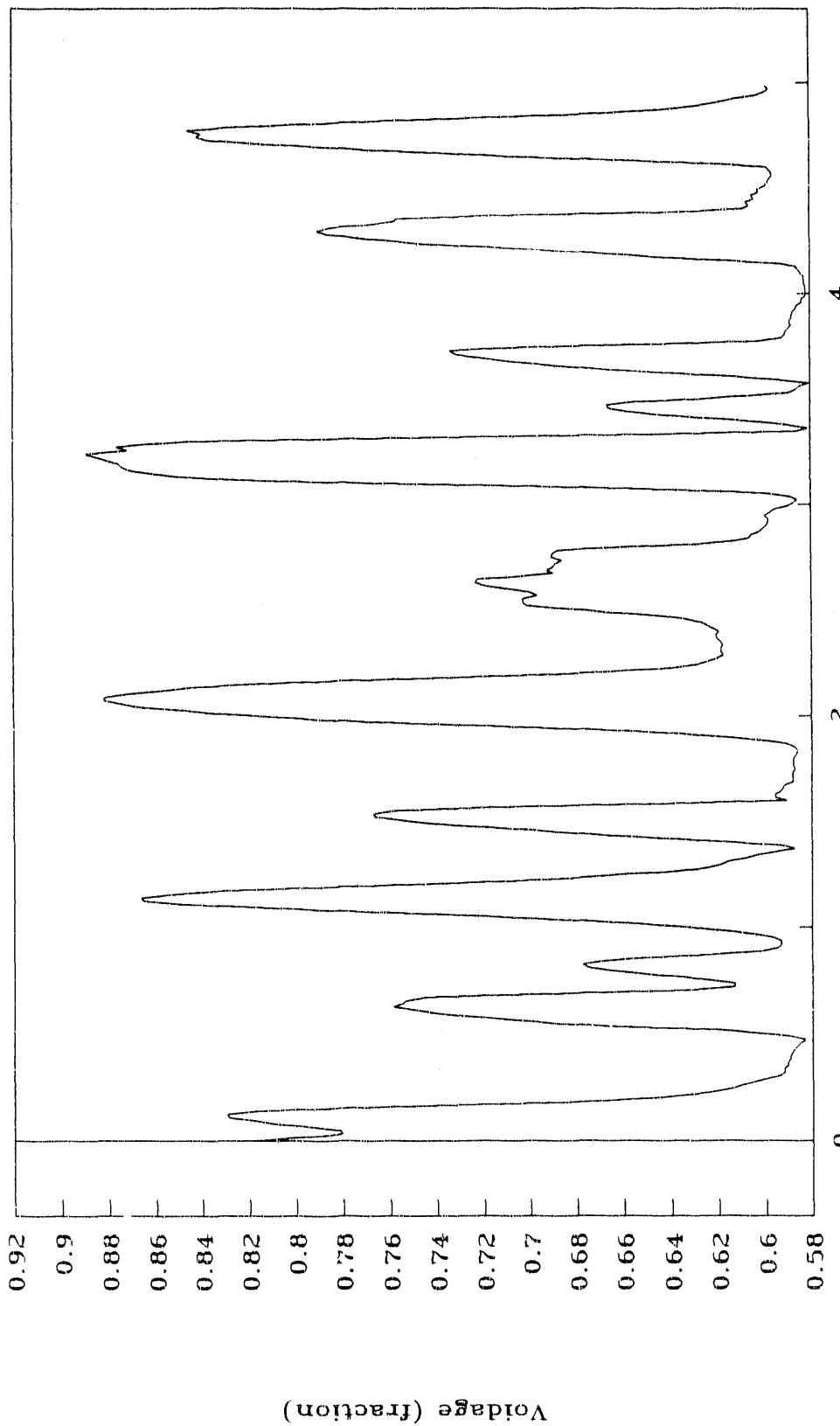


Figure 73. Local Voidage versus Time ($U_0 = .361$, cell 1-33, level 3)

LOCAL VOIDAGE VERSUS TIME
 $U_0 = .361 \text{ m/s}$ CELL 1-33 LEVEL 4

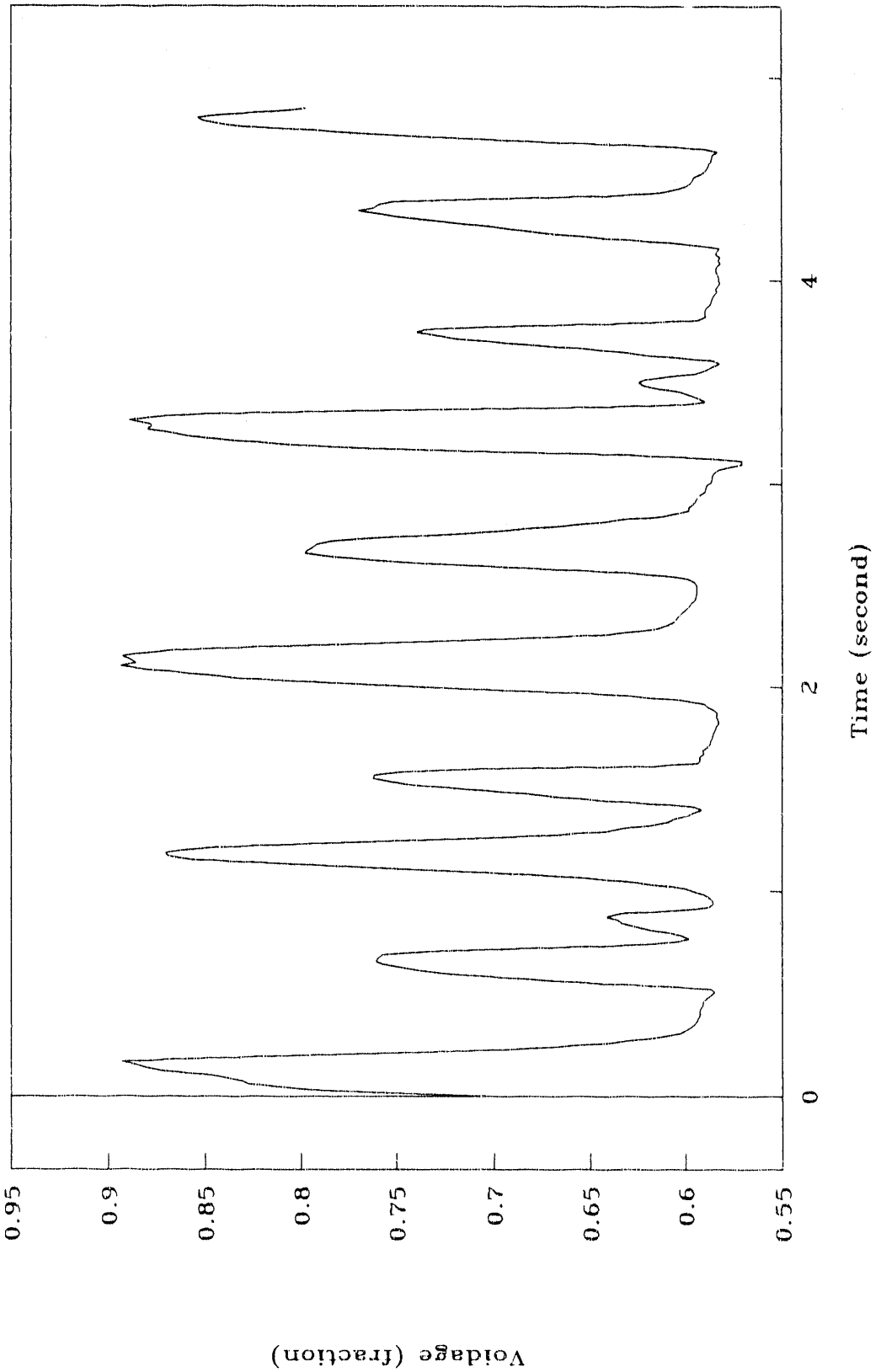


Figure 74. Local voidage versus time ($U_0 = .361$, cell 1-33, level 4)

LOCAL VOIDAGE VERSUS TIME

$U_0 = .220 \text{ m/s}$ CELL 1-33 LEVEL 1

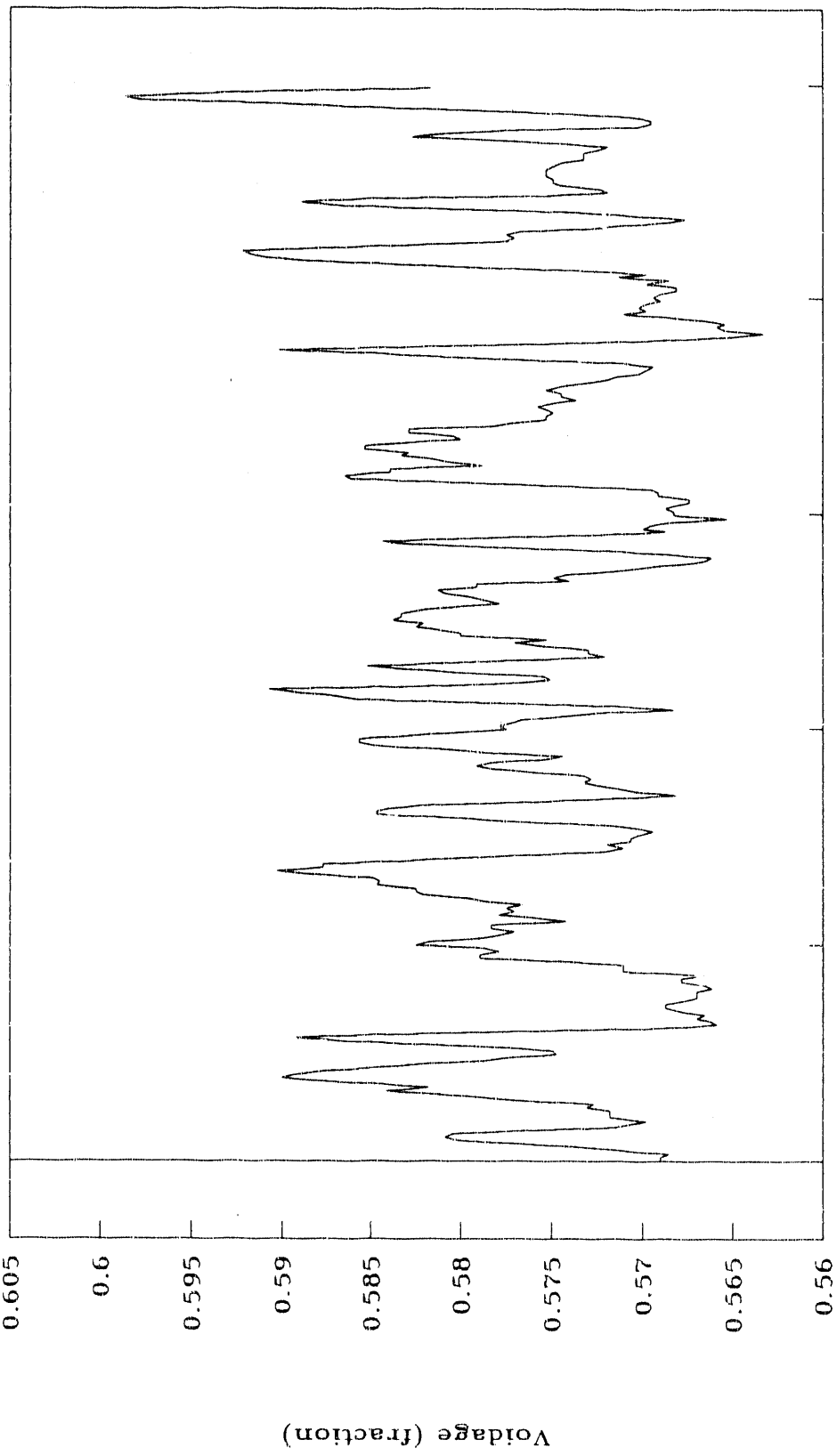


Figure 75. Local voidage versus time ($U_0 = .220$, cell 1-33, level 1)

LOCAL VOIDAGE VERSUS TIME

$U_0 = .220 \text{ m/s}$ CELL 1-33 LEVEL 2

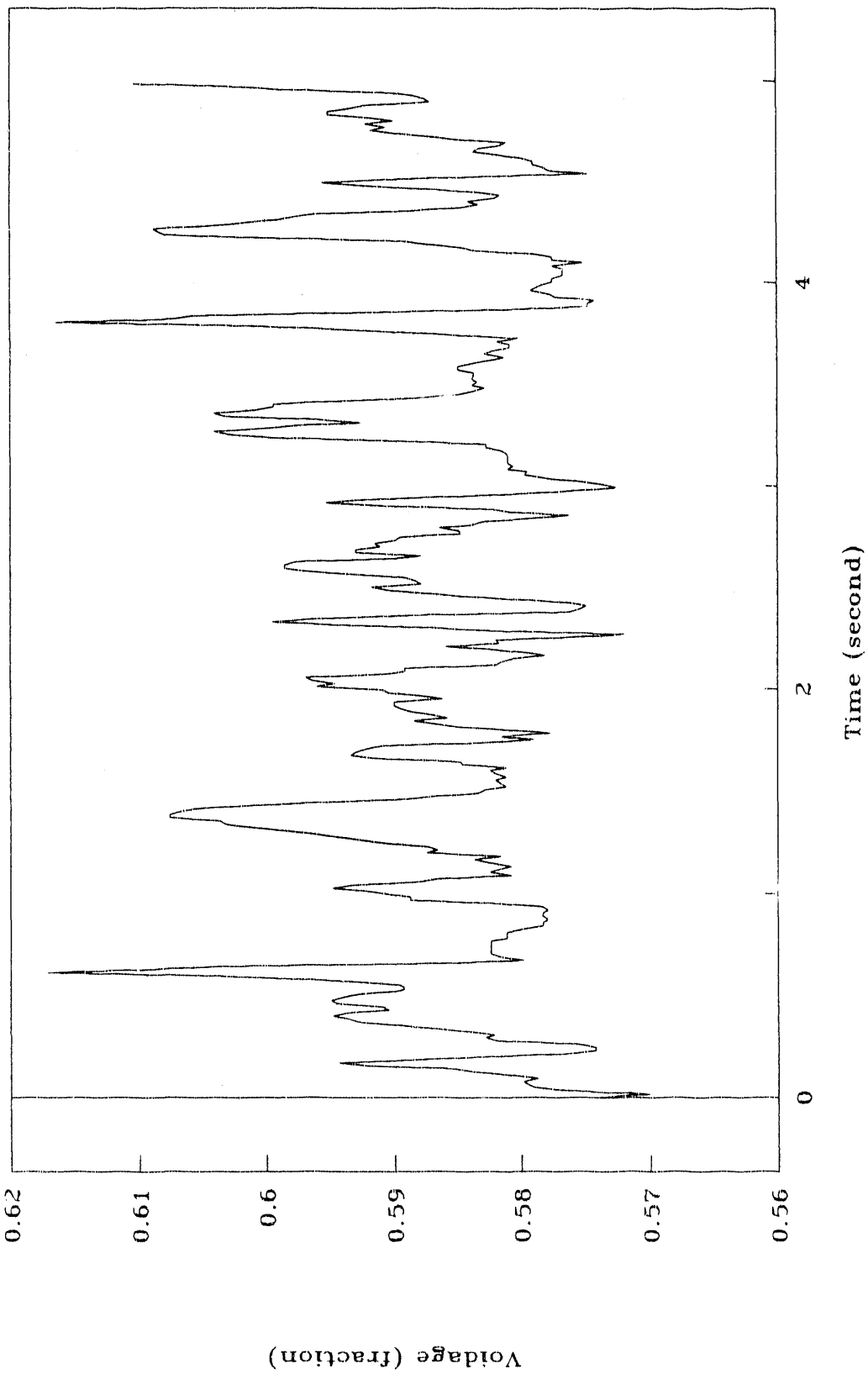


Figure 76. Local voidage versus time ($U_0 = .220$, cell 1-33, level 2)

LOCAL VOIDAGE VERSUS TIME

$U_0 = .220 \text{ m/s}$ CELL 1-33 LEVEL 3

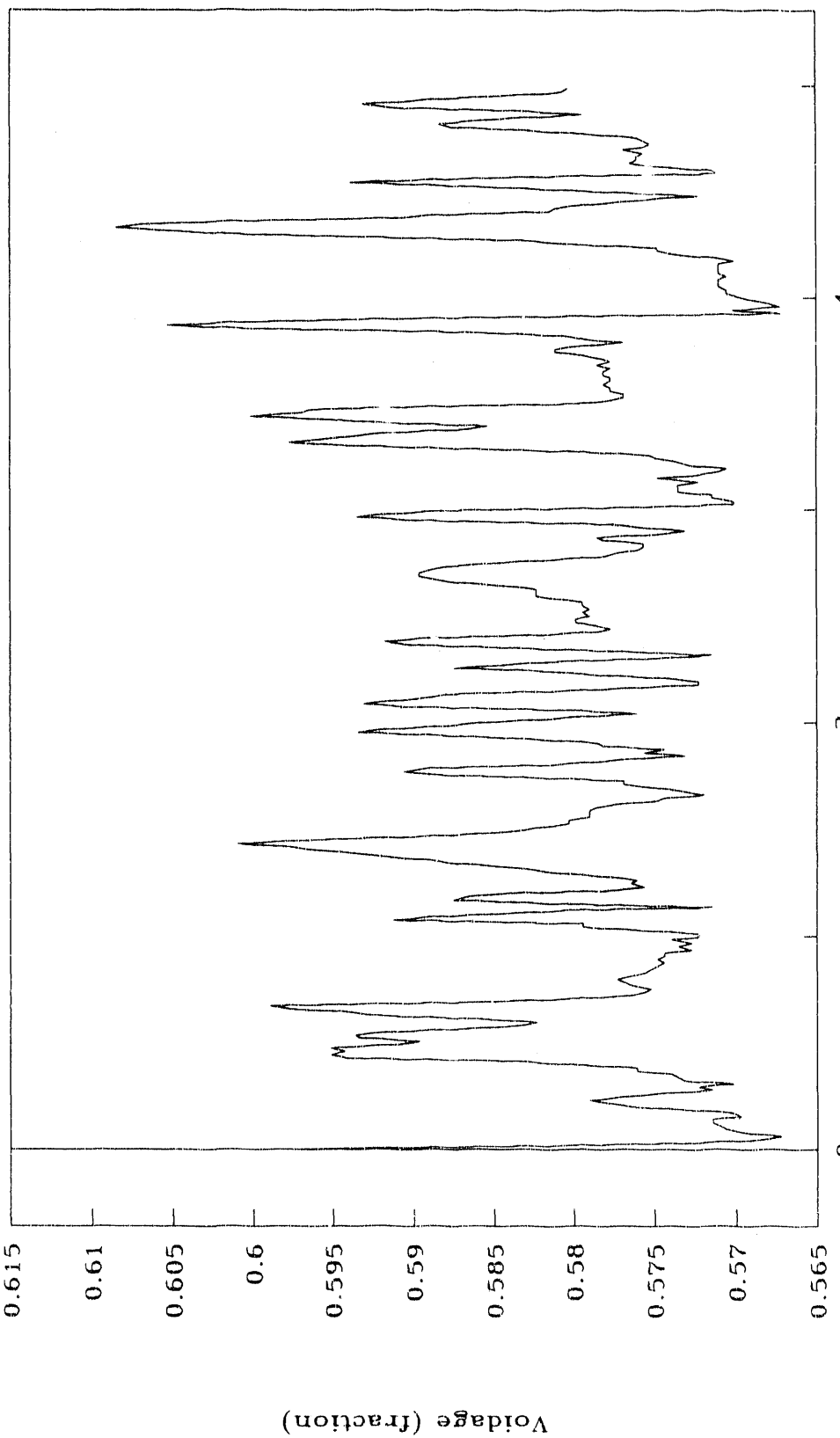


Figure 77. Local Voidage versus Time ($U_0 = .220$, cell 1-33, level 3)

LOCAL VOIDAGE VERSUS TIME

$U_0 = .220 \text{ m/s}$ CELL 1-33 LEVEL 4

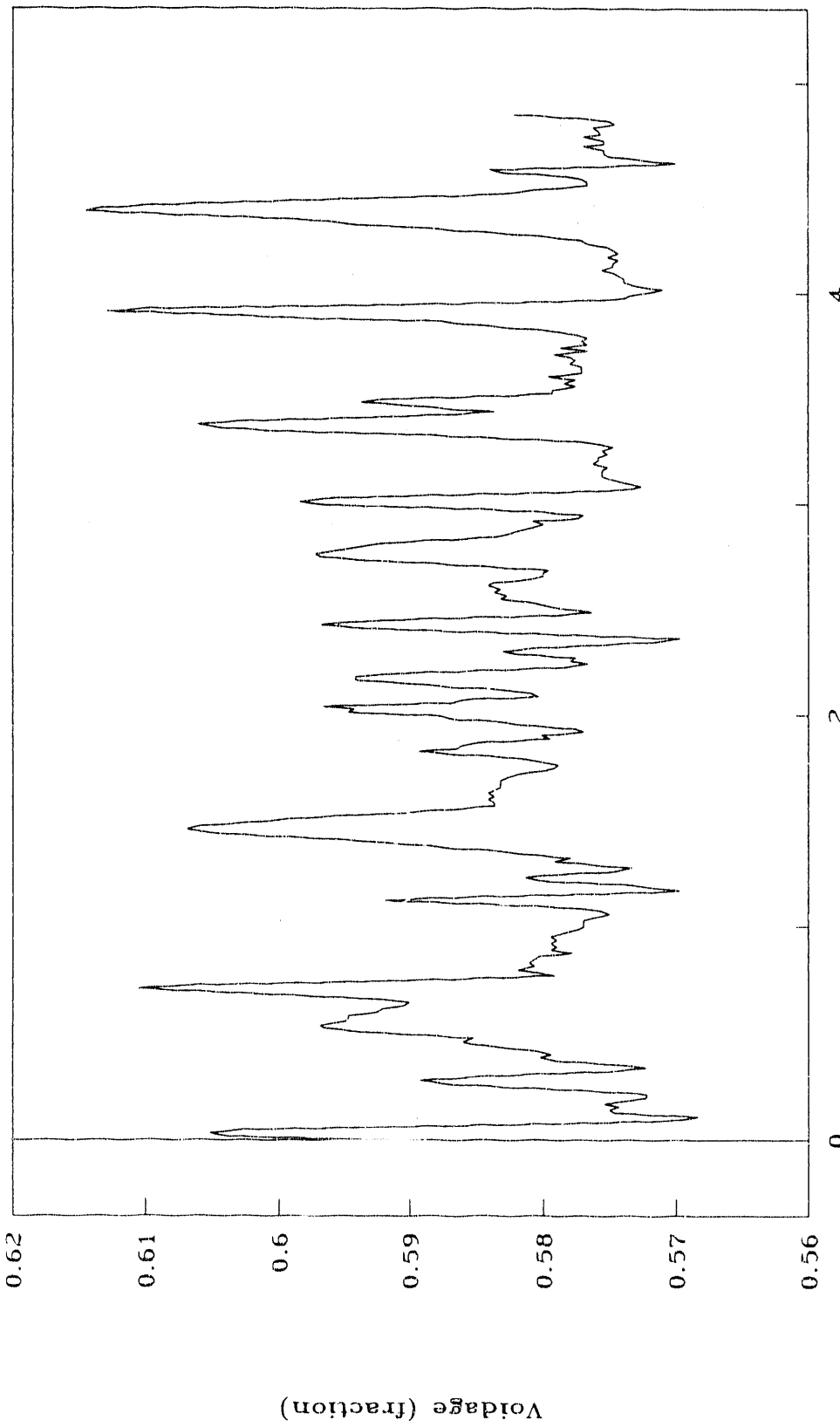


Figure 78. Local voidage versus time ($U_0 = .220$, cell 1-33, level 4)

PRESSURE FLUCTUATION VERSUS VOIDAGE
($U_0 = .259 \text{ m/s}$)

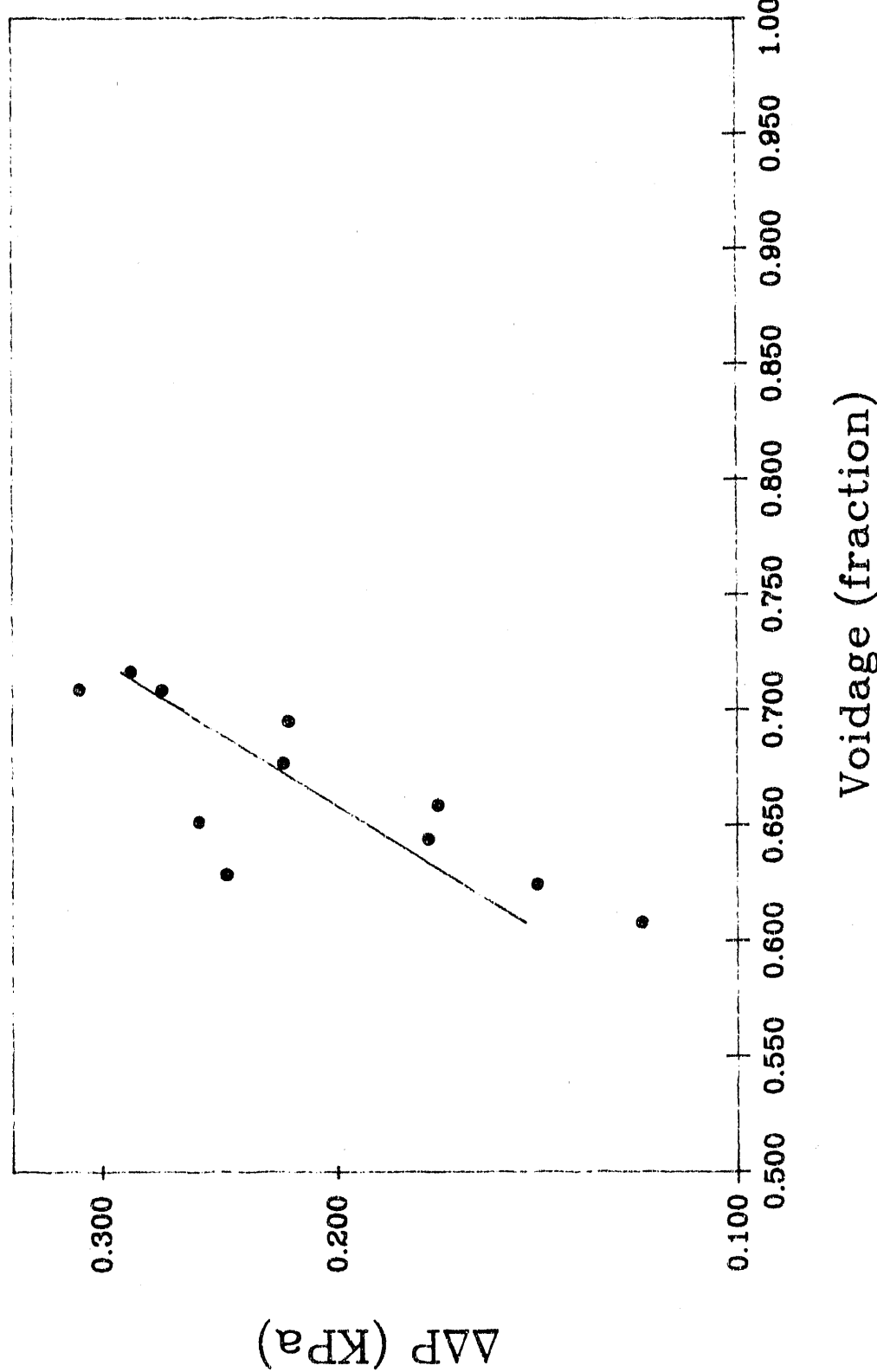


Figure 79. Pressure Fluctuation versus voidage ($U_0 = .259 \text{ m/s}$)

fluctuation may not be enough to quantify the behavior. It is recommended to increase the measurement point of gas phase pressure fluctuation. A more sophisticated, multi-correlation model should be better for explanation of the phenomena. These extended study will be included in our future work.

5. A NEW APPROACH FOR TRANSIENT GAS BUBBLE IMAGE - FORCE OF SOLID PARTICLES - GAS PRESSURE FLUCTUATION CORRELATION STUDY

Even though the fluidization condition in two and three dimensional fluidized beds is different from each other, the correlations between transient bubble image and transient force signals should be corresponding in both cases. As a supplementary study, we initiated an experimental work to correlate the transient force signals with the bubble images obtained by video in a two dimensional fluidized bed. We intend to correlate the transient forces of solid and gas directly to the bubble image in terms of video displays (not by indirectly using the voidage signals). A multiple data taking system was established, and three signals (displays) was synchronized by using trigger signals. This new approach provides an efficient way for a systematic study of transient gas bubble - force of solid particles - gas pressure fluctuation correlation.

5.1. Synchronize the Bubble Image with Transient Force of Solid Particles and Gas Pressure Fluctuation Signals

We successfully synchronized the transient force of solid particles and gas pressure fluctuation signals with the bubble image in video displays. The transient force and gas pressure signals are obtained by a computer system, and the video images are recorded by a video recorder. A timer is associated with the video display. A trigger signal starts the timer, and simultaneously sets a starting point for the computer data acquisition system. By doing so, we are able to obtain the video picture in every 0.0333 seconds, together with the synchronized transient solid force and gas pressure data. The schematic diagram of the experiment setting is shown in Figure 80.

5.2. Recognition of Bubble Behavior

The bubble motion in video display shows a great discrepancy against the classical theory. Bubble size is not at all constant, the direction of bubble movement changes frequently, and bubbles are shedding, twisting, splitting and coalescing. These phenomena indicate a complicated mechanism of transient bubble behavior.

Photographs 1 through 7 show how two bubbles coalesced and then split into several small pieces. This procedure happened within 0.2 seconds. Look at bubbles in the right bottom corner of the photographs 1 through 7. A small bubble expands, catches up a big

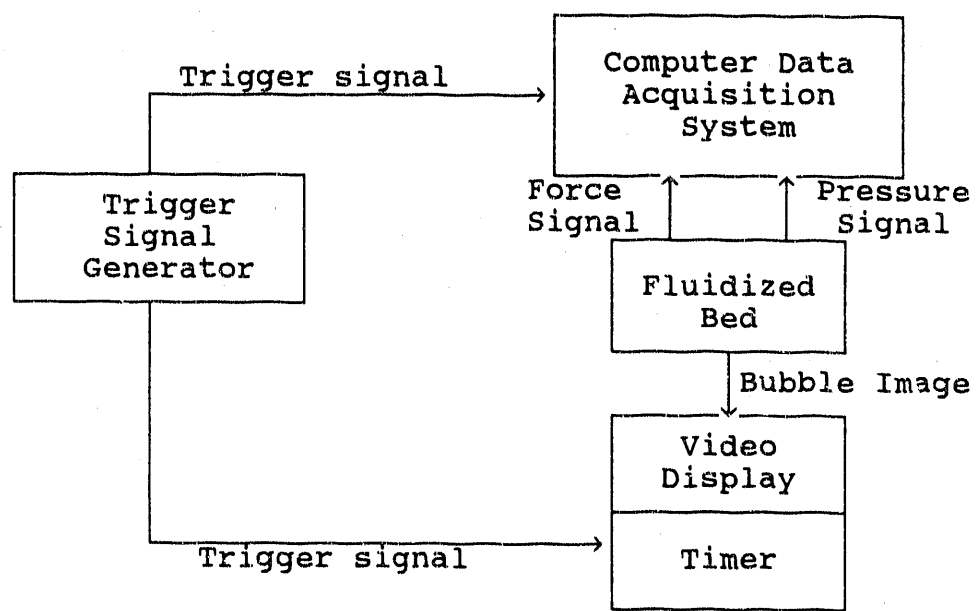


Figure 80. Schematic Diagram of the Experiment Setting



Photograph 1. Video Display at Time 15.44



Photograph 2. Video Display at Time 15.47



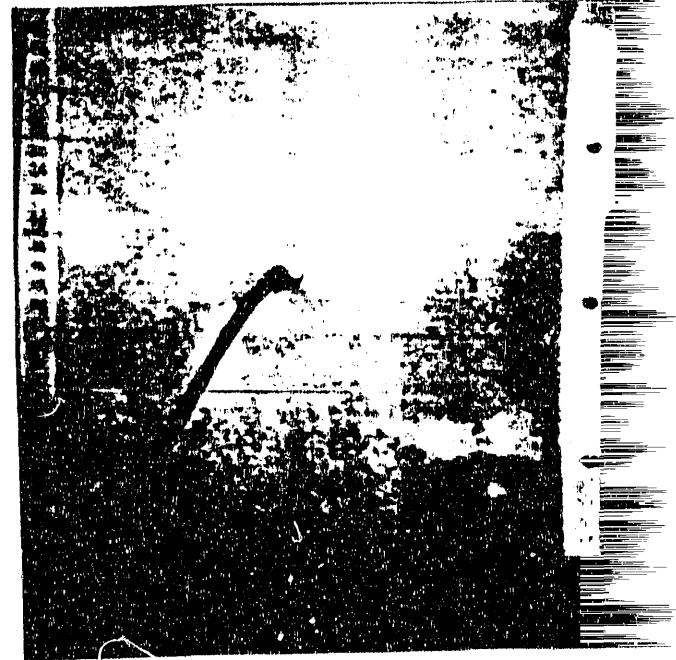
Photograph 3. Video Display at Time 15.50



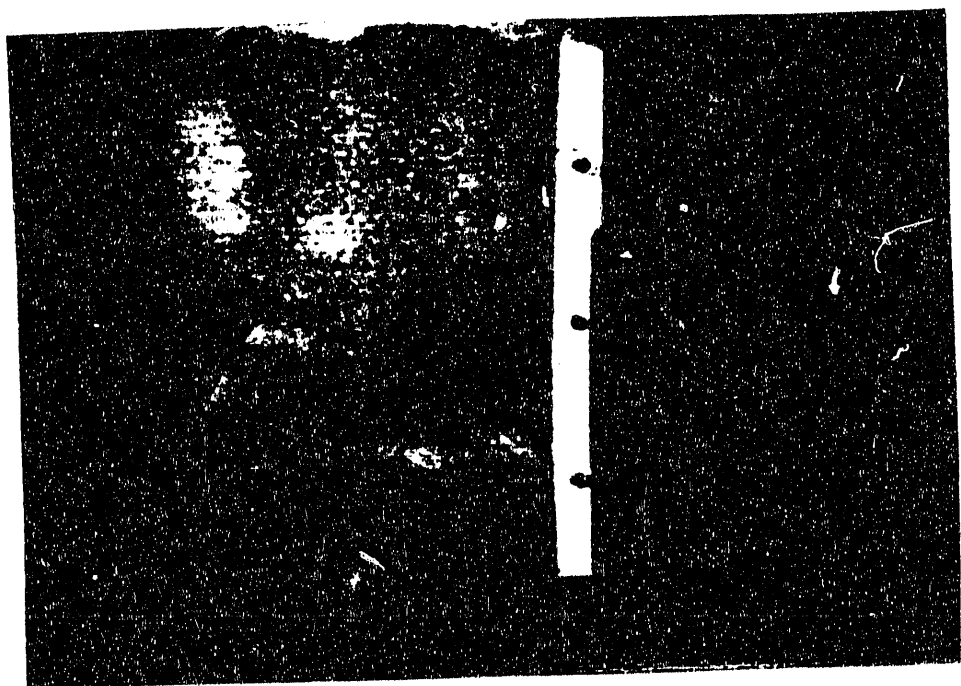
Photograph 4. Video Display at Time 15.54



Photograph 5. Video Display at 1000



Photograph 6. Video Display at 1000



Photograph 7. Video Display at Time 15.64

one. Two bubbles coalesces to form a signal bubble (Photographs 1 through 3). The bubble changes its shape and becomes flat (Photographs 4 and 5). Finally, it splits again to form three small pieces (Photograph 7).

From the above picture series we can also observe several bubbles reaching and passing through the measurement point, where the transient force signals are being measured. These pictures provided us with good information on transient bubble behavior. This preliminary work can serve as a base for systematic study on bubble - force - pressure correlation.

5.3. Correlation between Transient Bubble Image and Transient Force of Solid Particles - Gas Pressure Fluctuation Measurements

Transient forces of solid particles and gas phase pressure fluctuation were measured simultaneously, together with the video images. In an preliminary experiment, three types of signals (images) were obtained. Photographs 8 through 12 shows a series of pictures, which describe how a bubble passes through a measurement point. Figure 81 and 82 show how pressure and force fluctuate accordingly.

Pictures were taken in the time interval of 0.033 seconds. At time 22.94 a bubble arrived at the measurement point (Photograph 8), after 0.033 second, it passed through that point (Photograph 9). At time 23.00 the bubble turned its direction to the right (Photograph 10) and then at time 23.04 it left the measurement point (Photograph 11), changed its shape and went away (time 23.07, see Photograph 12).

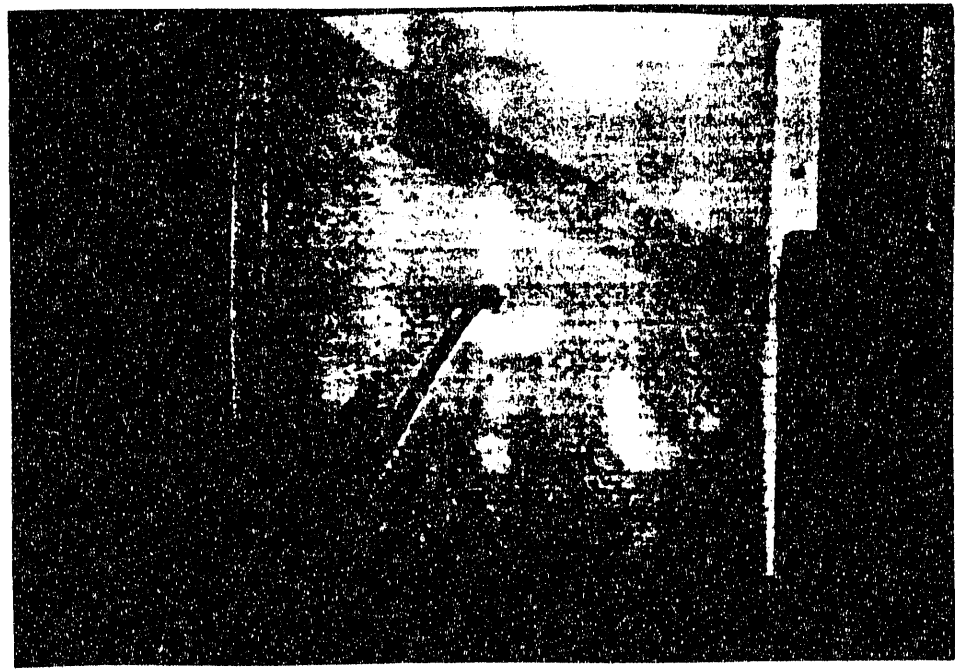
Figure 81 gives the pressure fluctuation from time 21.00 to 24.00. From the figure we can easily identify that at time interval 22.94 - 23.07, pressure was dropping and reached the locally minimum value. This means that energy releases when a bubble passing through.

Figure 82 shows the force fluctuation from time 21.00 to 24.00. Force signals are much more complex because Many small peaks are imbedded in big peaks. From a general trend we can also clearly observe a force drop process in corresponding time interval.

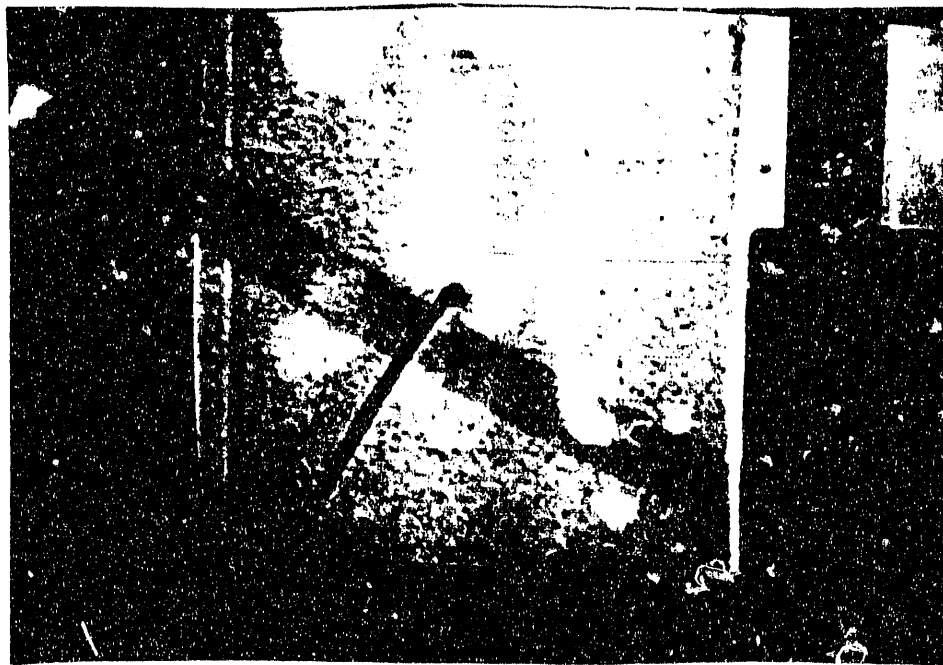
With the accumulation of data and video pictures, systematic study will be carried out to explore the bubble - force - pressure relationship.



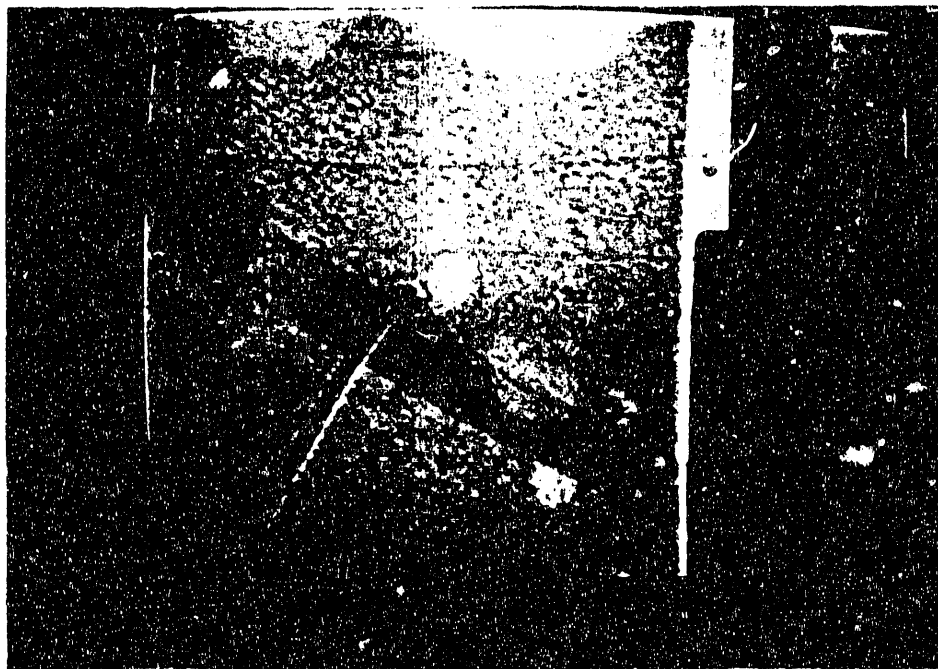
Photograph 8. Video Display at Time 22.93



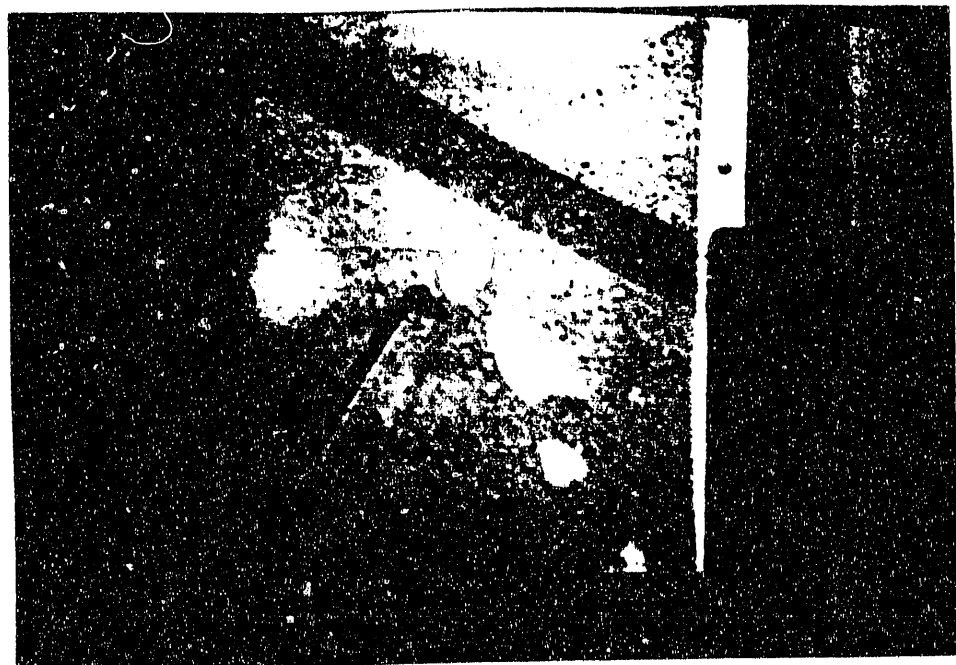
Photograph 9. Video Display at Time 22.97



Photograph 10. Video Display at Time 23.00

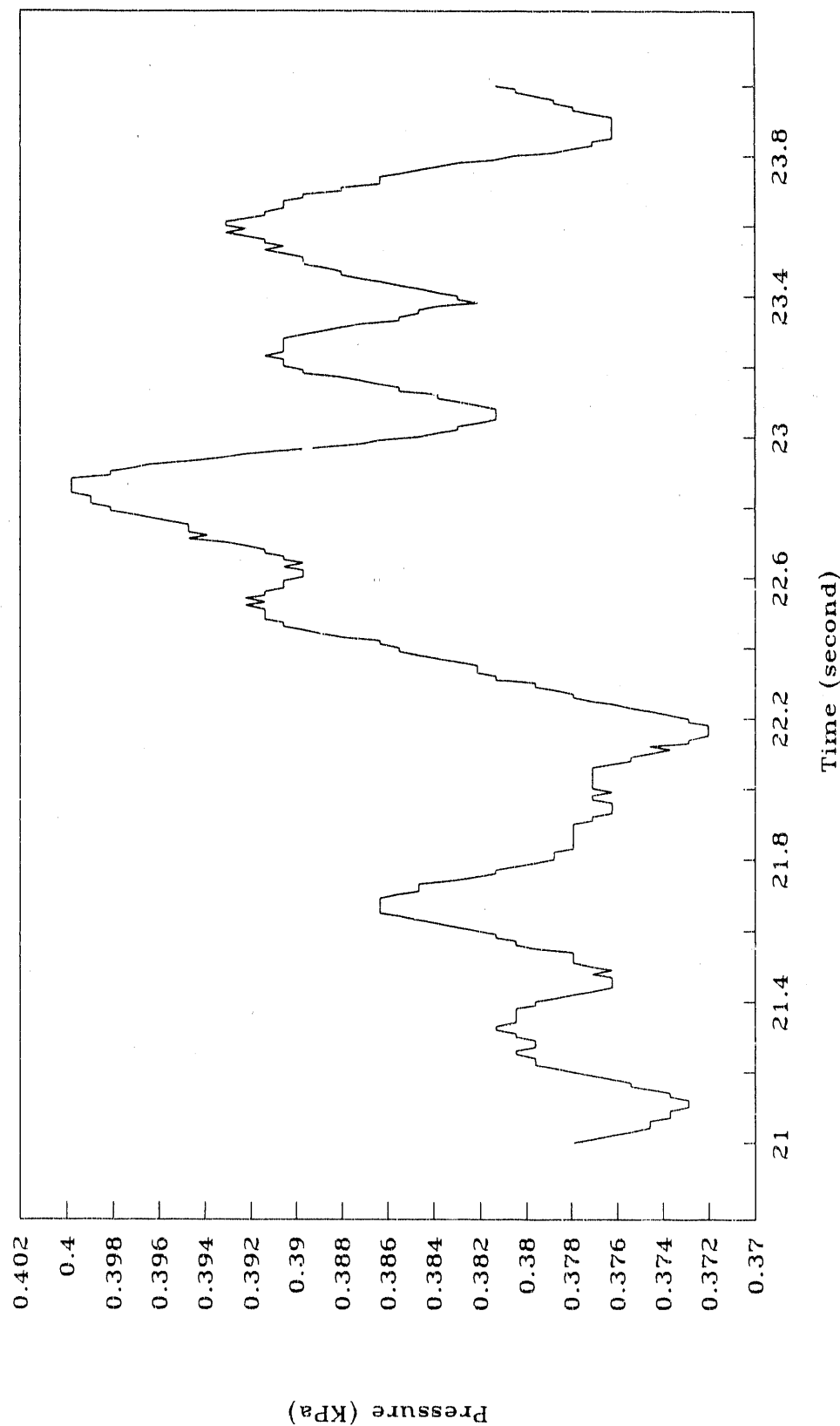


Photograph 11. Video Display at Time 23.04



Photograph 12. Video Display at Time 23.07

PRESSURE FLUCTUATION



Pressure (KPa)

Figure 81. Pressure Fluctuation in synchronized Experiment

TRANSIENT PARTICLE FORCE

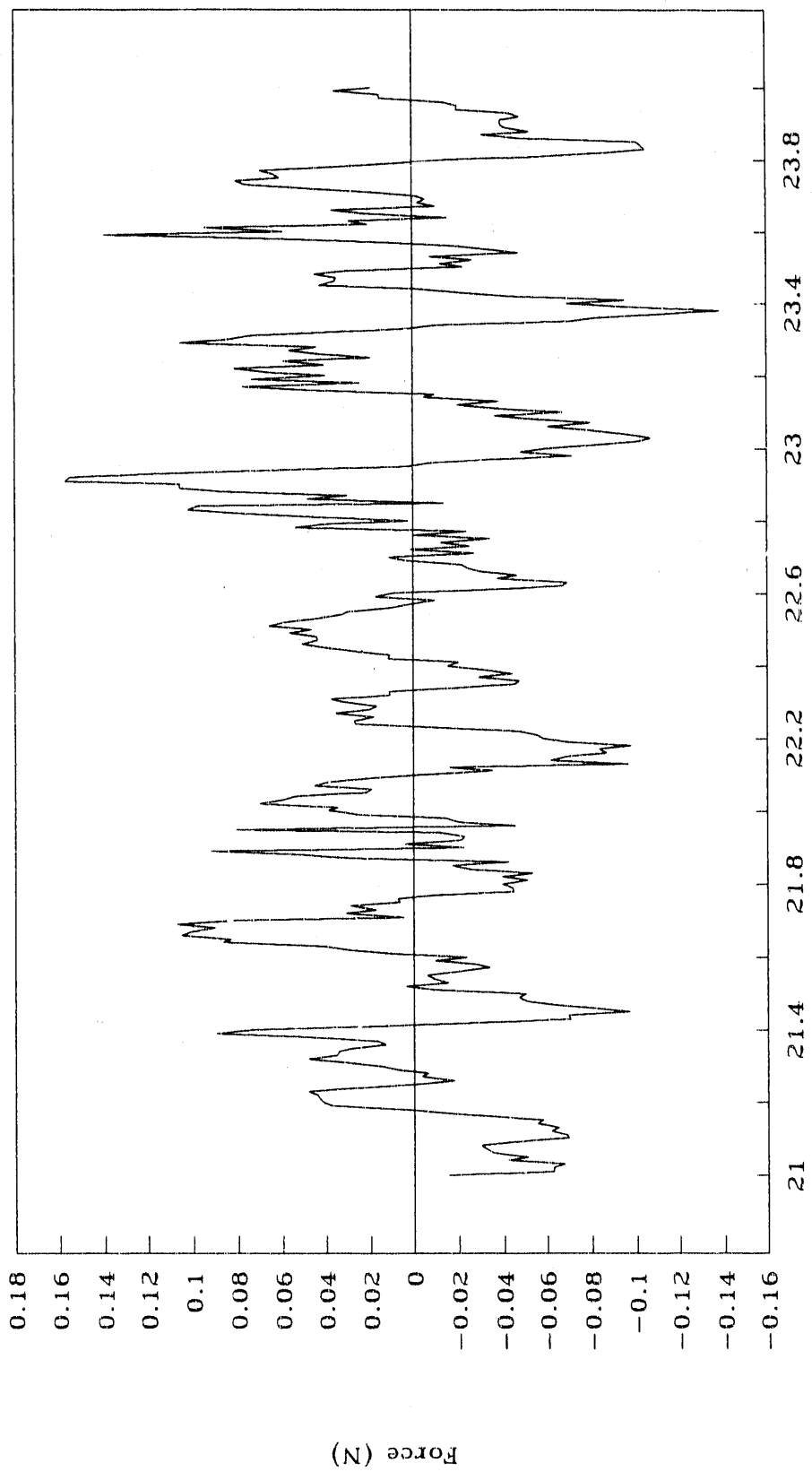


Figure 82. Transient Forces in Synchronized Experiment

6. CONCLUSIONS

To characterize and interpret the signals of transient motion of bubbles (slugs) in fluidized beds, the transient forces of solid particles were measured in an identical equipment simultaneously. Since bubble motion and solid particles are both transient, the two measurements have been synchronized by using TTL signal method for computer data processing.

These experiments were accomplished by using 6" I.D. fluidized bed located in METC.

As a sensor of measuring the transient forces of solid particles, the gas phase pressure fluctuation method was used, which can correlate with other measurement methods developed by Kono et al (1987, 1988, 1989, 1990).

The signals of transient forces of solid particles were correlated to the signals of transient bubble images. Results show that transient bubble image can correspond to the transient force of solid particles.

Based on the results of transient force signals, the appropriate data taking condition for transient bubble motion seems to be validated.

In view of transient force signal analysis, the data taking time of 5s seems not satisfactory, instead, it should be at least 30s. As for data taking rate, 100 1/s seems adequate but lower rate may be tested to minimize the total number of data. These appropriate data taking conditions were found to depend on the fluidization conditions.

A simultaneous study of video bubble display, transient force and pressure signals was initiated in a two dimensional fluidized beds. The preliminary results not only support the current research, but also provide an efficient way to a fundamental, systematic study.

7. NOMENCLATURE

d_p	Diameter of fluidized particle
D_t	Diameter of fluidized beds
F_T	Maximum force measured by fracture sensitive sensor
F_p	Maximum force measured by piezoresistive strain-gauge method
g	Gravitational constant
H	Loosely packed bed height
M	Mass of solid particle in a fluidized bed
$\Delta\Delta P$	Maximum gas phase pressure fluctuation
U_{mf}	Minimum fluidization velocity
U_o	Superficial gas velocity
V	Voidage when it reaches the peak point
e	The base of the natural logarithm function

8. BIBLIOGRAPHY

Davidson, J. F. et al , "Fluidized Particles", Cambridge University Press, p.50, 1963.

Hallow, J. S. et al, "Preliminary Capacitance Imaging Experiments of a Fluidized Bed", A. I. ChE Annual Meeting, San Francisco, 1989.

Kono, H. O. et al, "Kinetic Forces of Solid Particles in Coarse Particle Fluidized Beds", *Powder Technology*, 52, 49, 1987.

Kono, H. O. et al, "Kinetic Behavior of Solid Particles in Fluidized Beds", Annual Report DEAC-21-86MC23249, submitted in 1988.

Kono, H. O. et al, "Kinetic Behavior of Solid Particles in Fluidized Beds", Annual Report DEAC-21-86MC23249, submitted in 1989.

Kono, H. O. et al, :Kinetic Behavior of Solid Particles in Fluidized Beds", Quarterly Report DEAC-21-86MC23249, submitted in Jan 1990.

Rowe, P. N. et al, "Bubble in Fluidized Beds", *Nature*, London, 195, 278, 1962.

END

DATE
FILMED

12 / 8 / 92

